Chapter 7

EFFECT OF LBE AND LEAD ON MECHANICAL PROPERTIES OF STRUCTURAL MATERIALS*

7.1 Introduction

The use of heavy liquid metals, and especially of lead-bismuth eutectic (LBE) or lead for accelerator-driven systems (ADS) and lead-cooled (Pb) or lead-alloy-cooled (primarily Pb-Bi) fast reactor (FR) concepts of Generation IV requires an assessment of their compatibility with structural materials. Their deployment requires that the materials compatibility issue will be resolved, with and without irradiation, either under the mixed proton-neutron spectrum typical of the spallation source of an ADS in the one case, or under the fast neutron spectrum typical of an FR in the other case. The irradiation effects on structural materials in contact with HLM are the subject of a dedicated chapter.

One should not forget the experience gained with liquid metal-cooled FRs in industrialised countries. However, practically all these reactors have used sodium as their coolant, excepting the Russia. Moreover, the expertise on compatibility of stainless steels with sodium is not transferable to lead and lead alloys, due to the significant differences in their physics and metallurgic properties[1] [Gorse, 2006].

Certainly, the older literature dedicated to the mechanical properties of steels, from carbon steels to high Cr steels, in contact with lead and lead alloys is essentially of Russian origin: the research on HLMs technology will soon cover one century, early oriented toward developing a fundamental understanding of the LME mechanisms since the Rebinder discovery [Rebinder, 1928], then largely R&D oriented at the beginning of the fifties with the development of submarine propulsion reactors in parallel with two full scale ground test reactor facilities, using LBE as a coolant [Gromov, 1997].

In a European country like France, that early opted for the sodium-cooled FR concept with Rapsodie, Phénix, then Superphénix, the R&D continued in parallel on other reactor concepts, like for example the molten salt reactor (MSR) concept between 1970 and 1983, using a cooling system operating by direct contact between the salt and the molten lead. In this context, a harmful effect of reducing lead[2] on the tensile properties of Chromesco 3 and EM12 ferritic steels was noticed between 300 and 350°C [Broc, 1983], corroborating an earlier Japanese study [Tanaka, 1969]. The possible influence of lead on the fatigue strength of these steels remained unknown. In the US, a Pb-Bi cooled reactor was considered in the early fifties, and then abandoned in favour of sodium cooling [Manly, 1954]. In Japan, as in Europe and in the US, the sodium-cooled FR option was selected, with the related R&D for JOYO and MONJU. In Japan, as in many other countries, one finds also in the

---

* *Chapter lead: Dominique Gorse (CNRS, France). For additional contributors, please see the List of Contributors included at the end of this work. Thanks are expressed to J-B. Vogt (CNRS-LMPGM), T. Auger (CNRS-CECM) and V. Ghetta (CNRS-LPSC) for interesting and fruitful discussions.*

[1] Omitting voluntarily the difference in the nuclear (activation) and neutronic properties between Na and Pb or LBE, which is well outside the scope of the present chapter.

[2] Lead made reducing by introduction of a deoxidising agent (Zr, Ti…) and bubbling of an Ar-5%H_2 mixture, since the OCS technology developed in USSR was not yet redeveloped in Europe.

literature some studies dedicated to specific solid/liquid model systems [Mae, 1991] to the aim of improving the understanding of liquid metal embrittlement (LME), or to the aim of solving some industrial problems.[3] The Japanese literature on mechanical resistance of materials in contact with LMs is thus varied, going from basic papers aimed at understanding LME [Ina, 2004] to patents related to materials resistant to LME [Kanetani, 1992], to the evaluation of the resistance to embrittlement of metals in the environment [Funaki, 1993].

It is a fact that, in R&D devoted to nuclear systems using corrosive lead or LBE as a coolant, compatibility is generally associated to little or controlled corrosiveness [Loewen, 2003]. Lead or LBE induced corrosion is unacceptable to insure long-term safe operation of a future reactor.

In this context, the present chapter presents a review of the published works on the effect of LBE or lead on the mechanical behaviour of the 316L austenitic stainless steel and the T91 martensitic steel pre-selected for the design of a future European transmutation facility (EFIT, XT-ADS[4]), in the framework of the EUROTRANS[5] programme of FP6.

To provide as complete information as possible on ferritic/martensitic steels in contact with lead or lead alloys, the results of some studies carried out as part of the fusion programmes, on related steel grades like MANET, OPTIFER, 1.4914 in contact with Pb-17Li or even lithium, and also in contact with LBE are also included when available. Since information on 316L in contact with lead or LBE is lacking in some areas, the results of some studies conducted either as part of liquid metal fast breeder reactor (LMFBR) programmes on type 316 steel in contact with sodium, or as part of the spallation neutron source projects on type 316 steel in contact with mercury, and if possible on 316 type steel in contact with lead or LBE, are also included when available.

In this chapter, the tensile behaviour, then the fatigue and creep-fatigue behaviour, and finally some creep properties are presented and discussed. The fracture properties are just mentioned but not discussed, in absence of available data. The focus will be on T91 steels and 316L stainless steels in contact with LBE or lead. This chapter is organised as follows:

- Section 7.2 focuses on liquid metal embrittlement (LME). It is subdivided into two parts. Section 7.2.1 is dedicated to wetting, which is one of the two main requirements for occurrence of LME, and today the only one for which there is some data available on *real* systems, in addition to an abundant theoretical literature. Section 7.2.2 is devoted to the definition of LME, the criteria of occurrence of this phenomenon and presents the simplest analysis of the LME failure.
- Section 7.3 is dedicated to a closely related phenomenon, environment-assisted cracking (EAC), which permits an interpretation of the results of some tensile tests conducted on T91 or 316L steel in lead or LBE environment.
- The effect of lead or LBE on the tensile properties of T91 is well documented, thanks to the European TECLA and MEGAPIE-TEST[6] programmes of FP5. The results are summarised in Section 7.4. The tensile behaviour of 316 type stainless steel in contact with LBE or lead is less documented.

[3] For steel makers, LME studies are conducted to improve the machinability of steels, to understand the crack failure of hot-dip galvanised steel structures, or to develop weldability of metallic alloys.

[4] EFIT: European Facility for Industrial Transmutation; XT-ADS: eXperimental demonstration of the technical feasibility of Transmutation in an Accelerator Driven sub-critical System.

[5] EUROTRANS: EUROpean Research Programme for TRANSmutation of High-level Nuclear Waste in an Accelerator-driven System; Contract No.: FI6W-CT-2004-516520.

[6] TECLA: Technology, Thermohydraulics for Lead Alloys, European programme granted by the EU 5th Framework Programme.

- Today, and in spite of a lack of quantitative results on fatigue and fracture, based on an analysis of the data collected on the tensile behaviour, shown in Tables 7.4.1 to 7.4.8 and on the fatigue behaviour, shown in Tables 7.5.1 and 7.5.2, the question of the susceptibility to LME of T91 in contact with LBE and how to proceed from the metallurgical and chemical points of view to promote or hinder LME effects can be addressed. This is the subject of Sections 7.4.3 and 7.4.4.
- The effect of LBE and lead on the fatigue behaviour of T91 steel is reported in Section 7.5. As concerns 316L, limited results in LBE are shown. Studies of fatigue crack growth for both T91 and MANET II in LBE are summarised in Section 7.5.5.
- The effect of lead or LBE on the creep properties of both T91 and 316L are extremely limited. Data published from the fusion or LMFBR programmes represent the total data set available. A short paragraph, Section 7.6.4, will be dedicated to the phenomenon of liquid metal accelerated creep (LMAC), which includes the results of four-point bending tests carried out on T91 in contact with lead around 525°C in Section 7.6.5.
- Information on fracture mechanics, from fracture toughness to crack growth behaviour in contact with LBE does not exist: in Section 7.7 are summarised the actions defined by the EU partners of the EUROTRANS programme for future work.
- Section 7.8 is dedicated to recommendations for testing procedures.

A short conclusion terminates this chapter.

7.2 Liquid metal embrittlement

Liquid metal embrittlement (LME) is a physico-chemical and mechanical process, the interpretation of which is largely based on the wetting concept. For this reason a discussion of the wetting process is presented first in Section 7.2.1. Section 7.2.2 deals with the definition of LME, the criteria for occurrence of LME and presents a widely accepted explanation of the brittle LME failure.

7.2.1 Wetting: From ideal to real metallic systems

The study of the wetting, i.e. of the spreading of a liquid on a solid was first reported at the beginning of the 19th century with Laplace and Young [Young, 1805]. From the theoretical point of view, a renewal of interest was initiated by de Gennes in the early 80s [Leger, 1992], [de Gennes, 2002]. From the practical point of view, there are a number of applications,[7] which largely benefit from an improved understanding of the wetting phenomena, allowing for predictions of the interface reactions when a liquid is put into contact with a solid phase.

While the theoretical understanding improved since Young, it is worth emphasising that *real* solid/liquid (S/L) metal systems still remain too complex to allow for predictions of the spreading of one oxidisable metal alloy onto another metal alloy of different electronic and physicochemical properties, exhibiting thus differing oxidation properties (see Chapters 2, 3 and 4). Consequently, in most cases, experimental work is required in conditions that mimic the *real* situation of interest.

In the following, we shall consider first ideal S/L systems, second non-interacting metal-metal systems, then interacting S/L systems, including ceramic-metal systems. Finally we conclude with a discussion of the wettability of steels by HLMs.

[7] Such a paints, lubrication, gluing, cosmetology, without forgetting metallurgical processes like hot dip coating [Ebrill, 2000].

Ideal solid/liquid systems

Ideally, for a homogeneous and smooth surface, only partially wetted by a "simple" liquid, a liquid drop, small enough to neglect the gravity effects, does not spread and retains a spherical shape characterised by the contact angle between the liquid-vapour interface and the solid-liquid interface at the contact line where these two interfaces merge. The equilibrium contact angle θ_E is determined by the values of the surface tensions between the three phases. Each of these surface tensions is a force per unit length of the contact line, tangential to the interface, tending to retract the interface. At mechanical equilibrium, the horizontal components of these forces balance (Figure 7.2.1, left). This is the Young law:

$$\cos \theta_E = (\gamma_{sv} - \gamma_{sl})/\gamma_{lv} \tag{7.1}$$

with γ_{sv}, γ_{sl}, γ_{lv} being respectively the solid-gas, solid-liquid and liquid-gas surface tensions. Eq. (7.1) can be rewritten in terms of the spreading coefficient $S = \gamma_{sv} - (\gamma_{sl} + \gamma_{lv})$, as:

$$S = \gamma_{lv} (\cos \theta_E - 1) \tag{7.2}$$

showing that θ_E can be defined only in case of partial wetting with $S < 0$.

Figure 7.2.1. *Left*: The mechanical equilibrium of the solid-liquid-vapour triple line determines the value of θ_E. *Right*: Liquid metal drop spreading completely on a solid substrate ($S > 0$) or not ($S < 0$) until attainment of the equilibrium contact angle θ_E.

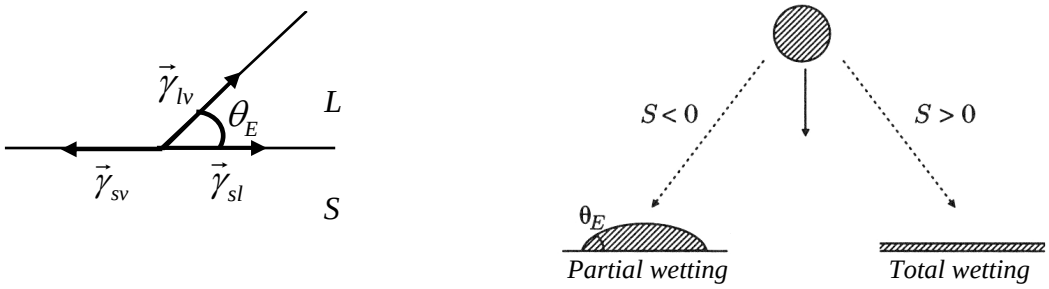

Total wetting is characterised by $S > 0$ with the drop spontaneously spreading and tending to cover the solid surface (Figure 7.2.1, *right*).

In less ideal situations, taking into account the heterogeneities, the chemical contamination and the roughness of the solid surface, one does not measure the equilibrium contact angle θ_E of the Young law, but at best a steady state contact angle depending on the history of the system. If the liquid-vapour interface has been obtained by advancing the liquid (after spreading of a drop), the contact angle has a value θ_A larger than the equilibrium value θ_E. The advancing contact angle θ_A is defined as the threshold value beyond which the contact line begins to move when the liquid advances (Figure 7.2.2). If, on the contrary, the liquid-vapour interface has been obtained by receding the liquid (by aspiration or retraction of the drop), the measured contact angle θ_R is smaller than the equilibrium contact angle θ_E. θ_R is defined as the limit value without moving the contact line by aspiration of the drop (Figure 7.2.2). Intuitively, the advancing contact angle θ_A is larger than the equilibrium contact angle θ_E, which is again larger than the receding contact angle θ_R: $\theta_R < \theta_E < \theta_A$.

Figure 7.2.2. Advancing θ_A and receding θ_R contact angles

The difference $\theta_A - \theta_R$ (> 0) informs on how far from ideal is the surface state. The hysteresis $|\theta_A - \theta_R|$ can reach tens of degrees depending on the surface conditions, whether it is contamination or roughness. The prediction of the wetting hysteresis of a randomly rough *real* surface will always be difficult due to the lack of determination of the relevant size of defects on/in the surface. Note that one knows today that the triple line can stick at very small defects of micrometric size [de Jonghe, 1995]. This suggests that if one wants to classify the wettability of *real* surfaces by a given liquid, the experimental procedure must be extremely rigorous [de Gennes, 2002].

Non-interacting metal-metal systems

This condition is idealised by ignoring the potential influence of impurities and especially oxygen at the interface, *after* de Gennes [de Gennes, 2002]. The spreading coefficient *S* is determined by the respective Van der Waals interactions in both phases in contact and at the interface. *S* can thus be re-written as:

$$S = V_{sl} - V_{ll} \tag{7.3}$$

with V_{sl} and V_{ll} being respectively the Van der Waals energy at the S/L interface and in the liquid phase. Wetting will be generally good and even total if the liquid is less polarisable than the solid. Note that Eq. (7.3) describes a situation where there is no electronic and ionic charge transfer at the S/L interface. At the macroscopic scale, this means no mass transfer between two immiscible phases (no oxidation, no corrosion reactions).

For interacting S/L systems (e.g. ceramic-metal)

In this case, so-called reactive wetting occurs by successive stages accompanied by interfacial reactions, changing *de facto* the nature of the interface. Dynamic non-equilibrium wetting occurs with the spreading rate of the initially non-interacting system, determination of a first quasi-equilibrium contact angle, followed by a modification of the spreading rate due to interfacial reactions, until attainment of an equilibrium contact angle at the interface between new phases of *a priori* different composition, structure and properties [Nakae, 1992]. In case of reactive wetting, the contact angle obeys the empirical law:

$$\cos\theta_{\min} = \cos\theta - \frac{\Delta\gamma_r}{\gamma_{lv}} - \frac{\Delta G_r}{\gamma_{lv}} \tag{7.4}$$

with $\Delta\gamma_r$ and ΔG_r being respectively the change of interfacial energy brought about by the interfacial reaction(s) and the change in free energy per unit area released by the reaction of the material contained in the immediate vicinity of the metal substrate interface [Espié, 1994]. It has been proposed that spreading occurs because ΔG_r is at least partially transformed to interfacial energy [Naidich, 1981]. Note that until now there is no generally accepted theory capable of describing reactive wetting satisfactorily. As noted above, experimental work is necessary for each interacting S/L system of interest. However, as far as ceramic-metal model systems are concerned, equilibrium phase diagrams are available and help perhaps not to predict the wetting behaviour but at least to explain the observed wetting behaviour.

Interacting steel/HLM systems

For interacting steel/HLM systems, like T91-LBE and T91-lead, or 316L-LBE and 316L-lead couples, the following points are immediately noticeable:

1) It is very difficult to predict the wettability of a Cr-containing steel (like T91, 316L…) by molten HLMs (Pb, Pb-55Bi, Pb-17Li, Hg…) and to verify *a posteriori* that a wetting angle, if measurable [Chatain, 1993], is acceptable, since research on the equilibrium phase diagrams for such multi-component systems is very new. The reader should read the studies on the Bi-Fe-Hg-O-Pb quinary systems or on the Bi_2O_3-Fe_2O_3 pseudo-binary system performed by A. Maitre, J-C. Gachon and co-workers during the last five years [Maitre, 2002, 2004, 2005]. To be more precise, today, it is impossible to predict whether lead and/or bismuth will form stable phases with one of the components of the T91 steel substrate (essentially Fe and/or Cr), if and how reactive wetting will occur. However, XPS analysis of the oxidised T91-lead interface has revealed the presence of lead at the steel/oxide interface [Gamaoun, 2003].
2) Being unpredictable, the wettability of steels (T91, 316L) by lead, LBE and other liquid metals must be determined in each experimental situation, as function of the composition and structure of the interfacial oxide film [Medina, 2006]. It is once again worth emphasising that a meaningful steady state contact angle will not be obtained if the surface state and overall experimental procedure are not rigorously controlled, according to the recommendations of Section 7.8.[8]
3) It is generally observed that an oxidised metal or metal alloy is at most partially wetted ($\theta_E < 90°$) or poorly wetted ($90° \leq \theta_E \leq 130°$) by a liquid metal. The tendency to spreading can be estimated if one knows the value of the liquid-vapour surface tension of the LM of interest in contact with the steel surface. Several measured values for the surface tension of liquid metals are listed in Table 7.2.1.

   For example, considering T91 steel or, more specifically, some Russian steels grades with a significant Si content (from 0.4 to 1.3 wt.%), a plausible hypothesis is that for some temperatures and oxygen activities, the uppermost surface layers of the oxidised steel will be essentially a silicon oxide. Considering that the surface tension of SiO_2 should be of the order of 150 mN/m, no wetting of the steel by Bi, Pb or Hg is expected based on the high values of surface tensions reported in Table 7.2.1.
4) As of this date, there are few reliable studies concerning the wetting of lead or LBE on T91 steel. On a diamond-polished T91 steel specimen, a contact angle of $126 \pm 5°$ was found at 380°C with 99.9999% pure lead by using a sessile drop setup installed in a ultra high vacuum (UHV) chamber [Lesueur, 2002]. This contact angle did not change whatever the annealing time and volume of the lead drop. This result is consistent with the presence of a $FeCr_2O_4$ oxide film onto the T91 steel surface. These results have been corroborated by other works performed on the T91-lead system at 450°C by V. Ghetta, *et al.* [Ghetta, 2001] (see Figure 7.2.3).

As shown above, the oxidised T91 steel is poorly wetted by lead in the 380-450°C range. Certainly, wetting studies of T91 and 316L steel in either "reducing" or "oxidising" lead and LBE, covering the 450-600°C temperature range would be of interest in the future.

Long-term aging in flowing and even stagnant HLM may modify the surface state, with successive phases of stability/instability of the surface oxide. Correlatively a non-wetting $\rightarrow$ wetting "transition" could occur, with consequences on the potential damages due to the HLMs.

[8] See, for example, the influence of microscopic defects on the pinning of the triple line [Leger, 1992].

Table 7.2.1. Surface tension of some liquid metals at the melting point or just above in vacuum or under rare gas (He, Ar…), with exception of Pb-55%Bi for which the temperature of the measurement is indicated. The surface tension is given in mN/m (= dyne/cm).

Potassium	118	[Passerone, 1998]
Sodium	$191 \leq \gamma_{Na} \leq 205$	[Handbook, 1966]
Bismuth	$376 \leq \gamma_{Bi} \leq 390$	[Handbook, 1966]
Bismuth	$370 \leq \gamma_{Bi} \leq 410$	[Novakovic, 2002]
Bismuth	389	[Passerone, 1998]
Lithium	399	[Passerone, 1998]
Lead	$450 \leq \gamma_{Pb} \leq 480$	[Handbook, 1966]
Lead	471	[Passerone, 1998]
Lead	$443 \leq \gamma_{Pb} \leq 480$	[Novakovic, 2002]
Lead-55%Bismuth	406 at 350°C	[Novakovic, 2002]
Lead-55%Bismuth	391 at 500°C	[Pokrovskii, 1969]
Mercury	$435 \leq \gamma_{Hg} \leq 485$	[Handbook, 1966]
Mercury	498	[Passerone, 1998]
Magnesium	577	[Passerone, 1998]

Figure 7.2.3. Lead drops on T91 steel after 15 days exposure to a reducing stagnant lead bath under OCS at 450°C; note that the contact angles θ_E are larger than 90°, and approach 130°

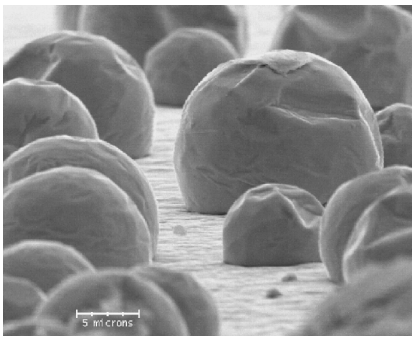

7.2.2 Definition and criteria of occurrence of LME

Slight differences between the definitions of LME can be found in the literature. The reader should return to the review papers on LME by Rostoker [Rostoker, 1960], Westwood [Westwood, 1963], Kamdar [Kamdar, 1973], Nicholas [Nicholas, 1979], Gordon [Gordon, 1982], to the recent models review by B. Joseph [Joseph, 1999], to the point of view of E.E. Glickman in 2000 [Glickman, 2000]. The very important former USSR literature was stimulated by Academician P.A. Rebinder, since its discovery in 1928 [Rebinder, 1928]. A new field of research, referred to as "physico-chemical mechanics", headed by Rebinder, started in 1954 and lasted until the end of the twentieth century… [Likhtman, 1954, 1958, 1962], [Shchukin, 1977, 1999].

The following definition is proposed: LME is the reduction in ductility and strength that can occur when normally ductile metals or metallic alloys are stressed whilst in contact with liquid wetting metals.

LME is considered as a special case of brittle fracture, intergranular (IG) or transgranular (TG) by cleavage, that occurs in absence of an inert environment and at low temperature.[9] Last, LME is accompanied by little or no penetration of the embrittling atomic species into the solid metal [Kamdar, 1973]. In other words, strictly speaking, a time and temperature dependent fracture process will not be considered as a manifestation of LME.

In this line, corrosion or diffusion-controlled grain boundary penetration of a solid metal by a liquid metal, that occurs under tensile stress tending to zero or even stress independent,[10] which characterise a limited number of well-known metallic couples like Al-Ga or Zn-Hg… is considered as a liquid metal induced damage, irrelevant in the present chapter.

LME failure occurs by nucleation of a crack at the wetted surface of a solid and its subsequent propagation into the bulk until ultimate failure. Work is still strongly needed to clarify this very old and tricky problem in physical metallurgy. Single crystals can be susceptible to LME [Likhtman, 1962]. In this case, a model including all physico-chemical and metallurgical aspects, from initiation to intermittent crack growth [Goryunov, 1978] until final rupture, is still strongly missing. This is also the case of *real* materials, in spite of the potentially pre-existing crack embryos. Today, for *real* materials prone to LME, the main issue is why and how some micrometric or nanometric cracks will remain stable whereas others (at least one), made unstable, will develop under the influence of the embrittling metal atoms filling the crack until the crack tip [Clegg, 2001], [Ina, 2004]. In some cases, crack propagation is also found spasmodic in polycrystals.[11] A crucial issue is why and how the presence of embrittling metal atoms accelerates the crack kinetics [Glickman, 2000]. Note that the embrittling metal phase, often considered as a macroscopic liquid controlling the crack propagation [Robertson, 1966] is also sometimes considered as a "quasi-liquid" with approaching the crack tip area [Rabkin, 2000]. In short, this means that, in the future, a multi-scale modelling approach will be necessary to account for all LME failures. This is not the scope of this chapter. However, this had to be underlined in this Chapter of which one target will be to examine the susceptibility to LME of some new systems with respect to the today available literature reviews [Nicholas, 1979, 1981, 1982]…

The prerequisites for LME are listed below:

1) Intimate or direct contact at the atomic scale between the solid and liquid metal phases, a concept classically interpreted as wetting.
2) Applied stress sufficient to produce plastic deformation, even if the required deformation may be produced, on a microscopic scale, at stresses much below the engineering yield point.
3) The existence of stress concentrators or pre-existing obstacles to the dislocations motion. This requirement is a matter of controversy, and is not considered as important as the two already mentioned criteria.

In the discussion, we shall come back to the concept of wetting, in general considered macroscopically and thermodynamically. It will appear that the behaviour of structural materials in contact with liquid metals can be rationalised only if one discriminates properly non reactive from reactive wetting. Most often, assumptions will be made to produce consistency between the various literature sources.

[9] We do not consider here high-temperature liquid metal embrittlement.
[10] And the related macroscopic phenomenon of grain separation and decohesion.
[11] For example, spasmodic crack propagation was observed with a Russian ferritic/martensitic steel in contact with lead [Abramov, 1994]. See Table 7.4.10 in the annex to this chapter.

A widely accepted explanation of the LME failure is based on the Griffith criterion establishing the fracture stress σ_F for crack propagation [Griffith, 1920], modified to take into account the Rebinder effect, i.e. the reduction of the surface free energy, γ_{sl}, by adsorption of a liquid metal with respect to an inert environment [Rebinder, 1928]. σ_F is written as follows:

$$\sigma_F = \sqrt{\frac{E\gamma_{sl}}{2c}} \tag{7.5}$$

where E is the Young modulus, and c is the crack dimension or its radius in case of an internal flaw as shown in Figure 7.2.4. [Griffith, 1920]. Eq. (7.5) supposes that the change in stored elastic strain energy is entirely used in the fracture process to create fresh fracture surfaces.

Figure 7.2.4. Flat crack, of length 2c and width 2r, in a sheet, subject to a tensile stress σ, perpendicular to the crack length

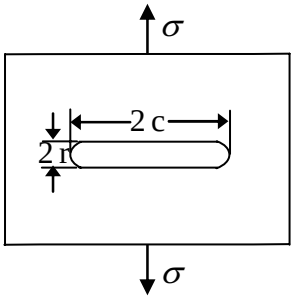

In *real* situations, rupture does not proceed as a result of the development of an elastic microcrack since a crack cannot be stable in an ideal lattice; as soon as it appears, it will develop at a rate of the order of the sound velocity throughout the whole crystal, if there is no barrier to its development. Assuming that a stable crack serves as a stress concentrator, this crack already exists in the deformed lattice. Thus plastic deformation first occurs, and only after a stable crack may appear and survive at the so-called subcritical stage, so long as the stress intensity factor K, written $K=Y\sigma\sqrt{\pi c}$ with Y being a geometric correction factor and c the crack length, does not attain the threshold $K_{C,LME}$.

In *real* situations, Rebinder and Shchukin [Rebinder, 1972] proposed to include the plastic deformation of the material accompanying crack growth, and to write a critical fracture stress as:

$$\sigma_c = \mu\left(E/c\right)^{1/2}\left(\gamma_p+\gamma_{sl}\right)^{1/2} \tag{7.6}$$

where μ, E, γ_p and γ_{sl} are respectively a proportionality coefficient, the Young modulus, a contribution to the plastic deformation and the solid-liquid interfacial free energy defined above. This expression is still the central point of all Russian models of LME. The correctness of Eq. (7.6) was already questioned by Popovich [Popovich, 1979]. At this point it is worth recalling that, until now, in the literature, there is no analytical expression of the fracture stress, accounting for the energy to create a new fresh surface wetted by a liquid metal and the plastic energy to form the plastic zone around the crack tip.

The consequences of metal adsorption on softening or strengthening of the surface layers is still a matter of discussion in metallurgy in the absence of a universal modelling of dislocation-atomic impurities interactions and consequences on plastic flow.

At this point, it is worth mentioning that the necessary condition of "intimate contact at the atomic scale between the solid and liquid metal phases" for occurrence of LME, which can be reformulated as the metal adsorption condition due to Rebinder, implicates various physico-chemical macroscopic processes that include: 1) dissolution and formation of dealloyed layers possibly brittle (as in SCC modelling) in the case of corrosive LM; 2) inter-atomic mixing and formation of surface alloys whose consequences depend on the SM/LM system in case of limited solubility between the two metallic phases, a concept that may be interpreted diversely; 3) no exchange, at the atomic scale, between the two solid and liquid phases, considered immiscible, which is rigorously impossible to prove experimentally.

7.3 Environment-assisted cracking

7.3.1 Definition of EAC

Environmentally-assisted cracking refers to the premature and catastrophic failure of a material in the simultaneous presence of a tensile stress and an even possibly only mildly corrosive environment.

7.3.2 Phenomenological criteria of occurrence of EAC

The prerequisites for EAC are the following:

1) Liquid-metal-induced corrosion (LMC), that may be localised, intergranular or uniform, or to the contrary that may lead to the growth of an oxide film at the solid metal surface, is considered as a main requirement for occurrence of EAC. As indicated above, the corrosiveness of the LM may be very limited, affecting only the superficial solid layers.
2) Plastic deformation, interacting with corrosion, characterises EAC at all stages of the process.

It is worth recalling that corrosion and consequently EAC are time-dependent. Therefore a liquid metal induced degradation of the mechanical properties that will be indubitably function of the ageing time in the LM will be considered as a case of EAC in the following discussion of the data in Section 7.4. Let us note that the crack velocity in EAC never attains the values reported in LME, which may attain 10^{-1} m/s for some embrittling couples [Glickman, 2000].

Nevertheless, so long as LME and EAC are not better understood, which is the situation today, so long as the wetting concept intervening in LME is defined macroscopically, and in case there is some doubt about the fracture surface, corroded or not, wetted or not, it may happen that the fracture of a material in contact with a liquid metal will be considered as a manifestation of LME or EAC depending on the author.

In order to discriminate properly between these two related phenomena, EAC and LME, it is essential to properly characterise the surface state in contact with the LM phase, at the appropriate scale. Once passed this crucial phase, the metallurgical and mechanical parameters for either LME or EAC failure could be better defined [Glickman, 2000], [Gorse, 2000].

7.4 Tensile behaviour of austenitic and ferritic/martensitic steels in contact with lead, LBE and other liquid metals

7.4.1 Definitions

The tensile test consists of the application of an increasing load on a specimen, which will progressively deform and fracture it. Typically the data are presented as load as a function of specimen elongation. Tensile tests are usually displacement controlled, but they can be also load controlled. The uniaxial tension specimen with a circular cylindrical gage-length represents an extremely useful and convenient test-geometry for studying the constitutive behaviour of materials. An ongoing application of tensile tests is the study of fracture processes in metals. They are used in Sections 7.4.2, 7.4.3, 7.4.4 and 7.4.5 to assess the susceptibility to LME and EAC of the T91-LBE or T91-lead couples.

From the recording of the engineering stress-strain curve (load divided by the initial section area versus elongation normalised by the initial length L_0), the following data can be obtained: 1) yield strength ($R_{p(x\%)}$ or $\sigma_{0.2}$) at a specific value of the engineering stress for a given value of the plastic strain, conventionally 0.2%; 2) ultimate tensile strength (UTS) (R_m or σ_{TS}), the maximum value of engineering stress during the test (F_m/S_0); 3) the effective yield strength (σ_Y), average of the 0.2% yield and the ultimate tensile strength; 4) the total elongation (A%), $100 \times (L_f - L_0)/L_0$ elongation of the specimen at fracture, where L_f is the length of the gage length after fracture and the total elongation is the sum of the uniform elongation and of the post necking elongation; 5) the reduction of area $Z\% = 100 \times (S_0 - S_u)/S_0$ where S_u is the section area after fracture (usually elliptical, due to anisotropy).

7.4.2 Tensile behaviour of smooth, rough and notched martensitic steel specimens in HLMs

The experimental results are collected in Tables 7.4.1 to 7.4.8 in the annex to this chapter. The chemical compositions of the studied steels are reported in Table 7.4.9 below and in the annex to this chapter.

7.4.2.1 Tensile behaviour of smooth and rough T91 steel specimens in lead, LBE and tin

The first tests were conducted on electro-polished specimens at 350°C in oxygen-saturated lead, and resulted in a ductile fracture of T91 [Legris, 2000, 2002], [Verleene, 2006]. No change was found after 1 hour of tempering at 500°C. Combining the effect of a notch and of a hardening thermal treatment was apparently required to obtain a brittle failure, not only in Pb at 350°C, but also in LBE and Sn at 260°C [Nicaise, 2001], [Legris, 2002]. A ductility trough was estimated in between 350 and 425°C for T91 in oxygen-saturated lead [Vogt, 2002].

In Table 7.4.2, the tensile data for notched T91 in contact with stagnant LBE are presented. The specimens are in the standard metallurgical state: normalised at 1050°C (1 h), then air cooled, followed by tempering at 750°C (1 h) and final air cooling. A preliminary study had revealed that it was possible to make LBE locally adherent onto T91 after 12 hours at 600°C or 650°C in an environment consisting of flowing He-4%H_2 [Pastol, 2002]. In same environment (LBE under flowing hydrogenated helium) but at much lower temperatures of 200, 300°C, it was also shown that a thin oxide layer has grown after 12 h of exposure and that the as-formed oxide is easily spalling off without roughening the steel surface, to which LBE could possibly adhere. For these conditions, a deleterious effect of LBE has been shown [Pastol, 2002], [Guérin, 2003].

In Table 7.4.3, the tensile data of smooth specimens, diamond polished [Pastol, 2002] or electro-polished so as to remove the flaws unintentionally produced during the specimens preparation [Dai, 2006] are shown. For these conditions, oxygen-saturated LBE under vacuum, the steel specimens are rather well protected by an oxide film, certainly more efficiently after electropolishing than after diamond polishing and there is no effect on the tensile properties. Indeed, any LBE effect would be unlikely, due to the fact that the liquid metal cannot make contact with the oxidised steel surface, except in case where the oxide film would be intrinsically brittle, which is unexpected in this case.

Table 7.4.3 also presents the results of tensile tests performed on rough (unpolished) specimens, with the surface state resulting from coarse mechanical grinding [Sapundjiev, 2006]. No significant effect of LBE is found, in spite of the fact that the chemistry of the LM phase was carefully controlled. The absence of LBE-induced damage is consistent with the fact that the LM cannot wet the T91 steel with this surface condition.

7.4.2.2 Tensile behaviour of T91 steel specimens in LBE, in the presence of flaws

Table 7.4.4 is devoted to the deleterious effect of flaws on the tensile behaviour. These defects were unintentionally produced during the preparation of the tensile specimens [Dai, 2006b], [Glasbrenner, 2003]. Considering the set of data collected in [Dai, 2006b], for tests conducted between 250 and 425°C, a temperature effect was also evident. Such an effect can be rationalised if one considers that the penetration of the LM in the cracks is competing with the oxidation of the crack walls and the crack tip.

7.4.2.3 Tensile behaviour of MANET II and T91 steels after pre-exposure to LBE

In Table 7.4.5, the influence of pre-exposure to LBE for short or long durations (up to thousands of hours) in forced circulation (LiSoR, LECOR) loops, in either oxidising [Glasbrenner, 2003] or reducing [Fazio, 2003], [Aiello, 2004] conditions is reported. A loss of ductility was found for MANET II at 250 and 300°C in oxidising LBE [Glasbrenner, 2003], and for T91 at 400°C after exposure to reducing LBE [Aiello, 2004]. To the contrary, only a slight detrimental effect of 4000 h ageing in stagnant LBE was found on T91 at 450°C after tensile testing in LBE under hydrogenated argon [Sapundjiev, 2006]. This result is certainly due to the preparation procedure of the tensile specimens, coarse mechanical grinding not allowing for wetting by LBE, which explains the absence of embrittling effect (see Section 7.2.1). Traces of zinc in the LBE probably caused the brittle fracture of T91 steel at 380°C [Gamaoun, 2002, 2003] after at least one month preliminary ageing in pure LBE under the oxygen control system (OCS) adapted by V. Ghetta, *et al.* [Ghetta, 2001, 2002].

7.4.2.4 Tensile behaviour of T91 in air, at room temperature after pre-exposure to LBE

The results of Table 7.4.6 show that, whatever the surface state, with oxide formed during exposure at 650°C, with Pb-Bi locally adherent onto the steel surface (at $T \geq 600$°C) or not ($T < 300$°C), the ductility of T91 steel is unaffected so long as the tensile tests are conducted at room temperature. The current conclusion is thus that solidified LBE is not embrittling, for the experimental conditions for which data exists. The effect of HLMs, liquid at or near room temperature, like mercury on the tensile behaviour of T91, was very recently investigated, and revealed that both the T91-Hg and 316L-Hg couples are embrittling [Medina, 2006].

7.4.2.5 Tensile behaviour of T91 in conditions of direct contact with Pb-Bi

Table 7.4.7 is devoted to the effect of Pb-Bi on the tensile behaviour of T91 in conditions of direct contact with the steel surface, in absence of interfacial oxide. Surface physics techniques were used to deoxidise the gage length of the cylindrical diamond-polished tensile specimens, and to deposit Pb-Bi layers [Auger, 2004, 2005]. These results clearly revealed a susceptibility of T91 to embrittlement by Pb-Bi.

7.4.2.6 Tensile behaviour and embrittlement of martensitic steels in contact with Li and Pb-17Li

The results of selected studies are reported in Table 7.4.8. Li causes (intergranular) corrosive attack of 1.4914 steel grade and a net degradation of the tensile properties for tests conducted in lithium, with and without preliminary exposure to Li [Borgstedt, 1986]. To the contrary, it is noticeable that pre-exposure to Pb-17Li in very different experimental conditions did not affect the mechanical properties (here tensile) of HT9, F82H-mod, OPTIFER IVb… In some cases, a pre-wetting treatment is mentioned, but a complete description of the surface state before and after the tensile test is often missing whereas, on the contrary, the chemistry of the melt is clearly described.

The study conducted on EUROFER 97 in the LIFUS loop is worth mentioning [Benamati, 2002]: the analysis of the surface state reveals that Pb-17Li is in direct contact with the steel surface as a result of long term ageing in the LIFUS loop. However, the tensile tests conducted on Pb-17Li wetted EUROFER 97 specimens under argon did not revealed any change in the tensile behaviour.

Table 7.4.9. Chemical compositions of the above mentioned steels (wt.%, balance Fe)

	Cr	W	Ni	Mn	V	Nb	Mo	Ta	Ti	Al	Cu	C	N	P	S	B	Si	Ref.
Chromesco 3	2.09	–	–	0.50	–	–	1.09					0.085					0.30	[Sannier, 1982]
EM 12	9.65	–	–	1.03	0.32	0.46	2.04					0.105					0.37	[Sannier, 1982]
T91	8.26		0.13	0.38	0.2	0.08	0.95			0.024	0.08	0.105	0.055	0.009	0.003		0.43	[*]
MANET	10.37	–	0.657	0.76	0.21	0.16	0.5B	–	–	0.007	0.01	0.10	0.032	0.004	0.005	0.0075	0.18	[Glasbrenner, 2003]
1.4914	10.6		0.82	0.54	0.24	0.19	0.49	–	–	0.05	0.01	0.172		0.005	0.005	0.002	0.34	[Borgstedt, 1986]
HT9	11.8	0.52	0.51	0.50	0.33	–	1.03	–	–	–	–	0.21	–	–	–	–	0.21	[Chopra, 1986]
F82H-mod	7.66	2.0	–	0.16	0.16	–	–	0.02	–	–		0.09	0.005				0.11	[Sample, 2000]
OPTFER IVb	8.3	1.4	–	0.34	0.22	–	–	0.06	–	–		0.12	0.03					[Sample, 2000]
EUROFER 97	8.8	1.15	–	0.44	0.2	0.002	0.003	–	–	–		0.10	–				0.05	[Benamati, 2002]

[*] = [Legris, 2000, 2002], [Nicaise, 2001], [Vogt, 2002], [Pastol, 2002], [Gamaoun, 2002, 2003], [Guérin, 2003], [Auger, 2004, 2005], [Verleene, 2006], since the T91 steel whose composition is reported above was supplied by Creusot Loire Industrie in the frame work of the French GEDEON programme on structural materials for ADS.

7.4.3 Experimental results that may be interpreted as LME effects: Case of T91 in contact with LBE or lead

When the French, European (TECLA, MEGAPIE-TEST…) and international (MEGAPIE…) programmes on ADS began, there was little information about the compatibility of 9-12%Cr containing steels with lead and lead-bismuth alloys. The publications in Russian journals dedicated to the compatibility of structural materials with liquid lead or lead alloys were largely unknown, un-translated or poorly translated. This is for example the case of all studies dealing with the liquid metal induced failure of steels before 1955, which was the subject of a monograph of Ya.M. Potak [Potak, 1955b]. It would have been also interesting to know the works related to the mechanical properties of austenitic and ferritic/martensitic steels in contact with lead which were proposed for the

main components of the BREST-OD-300 reactor, and especially that liquid lead has practically no effect on the tensile properties of austenitic steels between 420 and 550°C or that the lead effect on the tensile properties of the selected 9Cr ferritic/martensitic steels simply consists in a decrease of elongation near the melting point at 350°C, and disappears at higher temperatures [Abramov, 2003]. It would have been also interesting to know that researches to optimise the composition and structure of steels for Pb-cooled, Pb-Bi-cooled reactors were done in Russia [Gorynin, 2000], [Solonin, 2001]. In this line, all information on the influence of HLMs on the mechanical properties of steels obtained to design and build the Russian reactor facilities by a very active scientific community was fully missing at the beginning of the EU, US and Asia programmes on ADS and LMFBRs.

Last, it would have been of primary importance to know that V.V. Popovich already noted in 1978 that wetting of iron and iron base alloys by lead or bismuth is not so easily achieved [Popovich, 1978], even when using the efficient method of the soldering fluxes and, consequently, that Pb or Bi should not be strong embrittlers of steels.

Thus, initially, T91 was pre-selected as a structural material for the European ADS project and for the MEGAPIE spallation target, due to its excellent mechanical properties under irradiation by fast neutrons. As mentioned above, it was a challenge to prove that contact with molten lead or LBE could produce LME effects. Now, after more than four years, it is known that T91 can be embrittled by LBE and it is possible to make a review, at least partial, of the metallurgical conditions producing LME effects. It is also possible to propose solutions to protect T91 steel against LME.

Let us keep in mind that, until now, the answer to the question of the susceptibility to LME of both the T91-LBE and T91-lead couples is only qualitative: it is based on an analysis of tensile tests reported in Tables 7.4.1 to 7.4.8 (see annex). A rigorously quantitative answer requires fatigue and fracture mechanics tests conducted in strictly controlled environmental conditions, such as the ones planned in the framework of the DEMETRA programme of FP6.[12]

In the following, we consider successively the role of the different parameters, which demonstrate a LME effect.

7.4.3.1 Role of the bulk metallurgical state

Application of a hardening heat treatment to smooth cylindrical specimens of T91 steel was not sufficient to produce an embrittling effect in contact with stagnant lead under air at 350°C, after J.B. Vogt and co-workers [Legris, 2000], [Nicaise, 2001]. The presence of a stress concentrator, like a notch machined in the hardened T91 steel smooth specimen, leads to brittle fracture in contact with not only liquid lead [Legris, 2000], [Nicaise, 2001] and LBE [Legris, 2002], but also with tin [Legris, 2002], over the temperature range from 260 to 350°C. The corresponding experimental load-elongation curves and fractography are reproduced in Figure 7.4.1.

Tensile tests on hardened notched T91 specimens, prepared as above, were also conducted in Hg (under air) and in air for comparison at 20°C [Legris, 2002]. Since a brittle fracture was found in both cases, with and without mercury, these results must be considered cautiously.

[12] DEMETRA: DEvelopment and assessment of structural materials and heavy liquid MEtal technologies for TRAnsmutation systems, is one of five technical domains of the EUROTRANS programme granted by PF6.

Figure 7.4.1. a) Tensile test results of notched specimens obtained at 260°C in liquid Sn (full squares), in LBE (full circles), in air (open triangles) and at 350°C in liquid lead (full diamonds) and in air (open squares); b) SEM micrograph of the fracture surface obtained in LBE at 260°C.

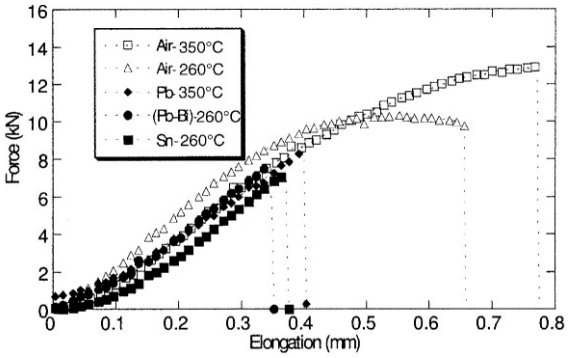

a)

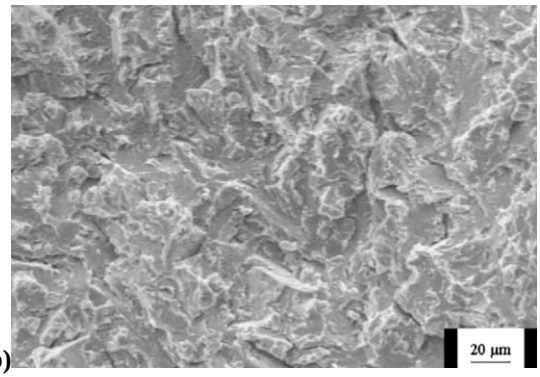

b)

For the T91-Pb couple, a ductility trough was found to extend from about 350 to 425°C. It is noticeable that the tests were all conducted in oxygen-saturated lead, with fully oxidised specimen surfaces, unwetted. This suggests that crack initiation required, at the same time, oxide film breakdown accompanying some localised plasticity. Otherwise, the fracture would intervene at identical stress level, independently of the liquid metal phase, which is not the case.

To conclude this paragraph, so long as the mechanical tests are carried out on oxidised T91, in oxygen-saturated HLM (Pb, Pb-55Bi, Sn, Hg), the combination of a hardening heat treatment and of a notch machined in the tensile T91 specimens is required to produce LME effects.

These results were later confirmed by H. Glasbrenner and F. Gröschel [Glasbrenner, 2004] on U-bent T91 specimens, hardened by means of the hardening heat treatment applied above by J-B. Vogt and co-workers (one hour tempering at 500°C, air cooling). Deep cracks, filled with LM, were found on the bent regions of the specimens exposed for 1000 hours to bismuth or Pb-17Li at 300°C. No such effect was found after 1000 hours exposure to LBE at 300°C, these results suggesting the existence of a stable and protective superficial oxide film. No oxygen control system (OCS) was in place in the system at 300°C. Improvements of the OCS allowing for reliable measurements at temperatures in the range of 350°C and below are recent [Ghetta, 2001, 2002], [Courouau, 2002, 2004]. The fact that Pb-Bi is less corrosive than bismuth and less reducing than Pb-Li does not justify the obtained results, which cannot be interpreted today. The authors suggest that the harmful effect of LBE could be just delayed. However, as recalled above in the definition of LME, a fracture process that is a function of the environmental conditions and more precisely time and temperature dependent cannot be, strictly speaking, considered as a pure manifestation of LME.

7.4.3.2 Role of wetting

T91 steel is highly oxidisable and passivatable, due to its 9% chromium content. As a result, its native oxide film is stabilised after a few hours of ageing in the laboratory environment. It has been shown that the native oxide film on T91 does not dissolve in high purity (99.9999%) lead at 380°C after prolonged ageing [Lesueur, 2002]. At the same time, it has also been shown that T91 is poorly wetted by lead over the 380-450°C range, even in presence of active OCS in the melt.

Indirect contact via an oxide film

First, the hypothesis was made that short ageing in LBE, which is more corrosive than pure lead, would allow for removing gently and at least partially the thin oxide film grown after 12 hours in LBE, avoiding surface roughening and permitting some (localised) wetting of T91 by LBE:

- As long as un-notched specimens were tested, no effect of LBE was detected over the 200-450°C temperature range, neither under vacuum, nor under hydrogenated helium.
- When notched specimens were tensile tested, after standard heat treatment and careful surface preparation (cf. Section 7.8), a damaging effect of LBE was found, strongly dependent on the liquid and gas phases in contact as is shown in Figure 7.4.2. The reduction in strength and ductility, undetectable at 200°C, passes through a maximum at 350°C before beginning ductility recovery at 400°C. The effect of LBE, maximised under He-4%H_2, was shown in ductility and energy to rupture, with a clear dependence on the deformation rate against oxidation rate [Guérin, 2003].

Figure 7.4.2. Load versus cross-head displacement curves obtained with notched T91 specimens, after standard heat treatment, at 350°C for a cross-head displacement rate of 6.7 10^{-4} mm/s, showing the environmental effects: vacuum (V), LBE under vacuum (V+LBE), He-4%H_2, LBE under He-4%H_2 (He-4%H_2 + LBE)

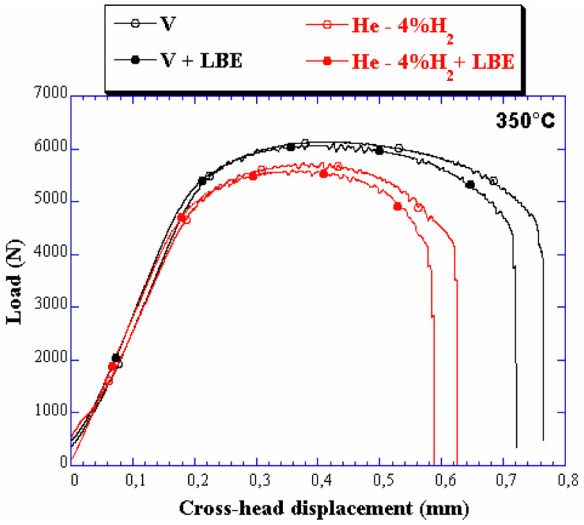

However, in the above experiment [Guérin, 2003], the surface state was not rigorously controlled, smooth at submicroscopic scale and wetted, by comparison with the experiment that will be described now [Auger, 2004].

In order to remove the oxide film so as to wet the T91 steel and check whether the T91-LBE couple is embrittling, there are different methods of surface preparation. We focus on the more efficient ones.

Direct contact via physical vapour deposition

To deoxidise the T91 steel, without roughening, corroding and contaminating the steel surface, it is necessary to proceed under UHV. The oxide film is removed by argon ion sputtering in an UHV chamber, followed by physical vapour deposition of Pb-Bi layers of thickness of order of a few hundred of nanometers. After tensile testing at 340°C under helium at a strain rate of 10^{-4} s^{-1}, brittle

fracture is observed with a number of small cracks on the gauge length of the T91 specimen as shown in Figure 7.4.3, after T. Auger, *et al*. [Auger, 2004 and 2005]. The fracture process is controlled by the reservoir of embrittling atoms at the specimen surface.

Figure 7.4.3. *Top:* In case of direct T91-LBE contact obtained by ion beam sputtering in an UHV chamber prior to deposition of Pb-Bi by PVD, LME effects are produced at 340°C under He. *Bottom left:* SEM micrograph (SE2) of the multi-cracked gauge length of the T91 specimen. *Right:* SEM micrograph (SE2) of an initiation site close to the surface showing a quasi cleavage fracture surface.

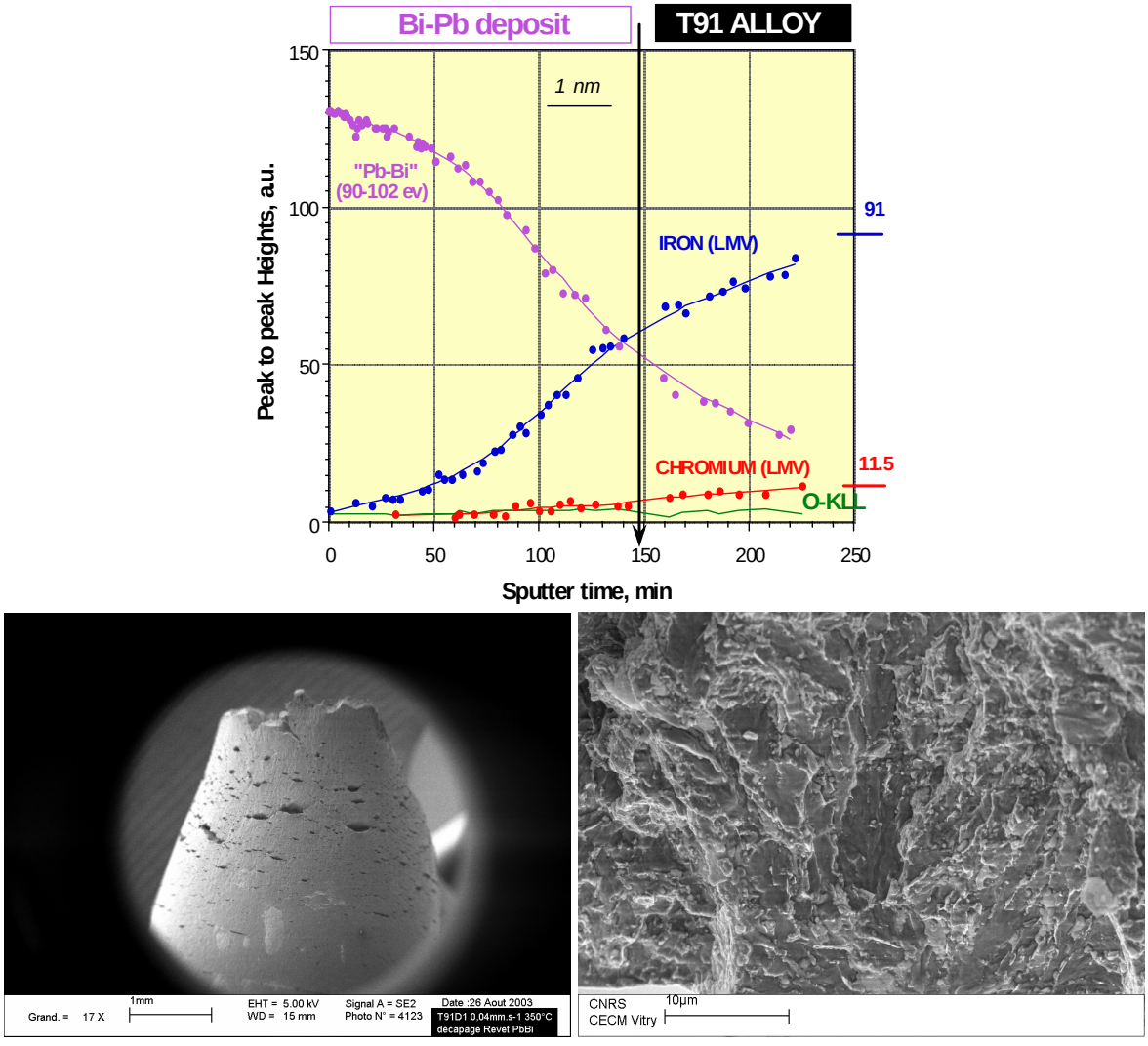

Intimate contact by means of chemical fluxes

This method was largely employed in the former USSR In almost all reported works [Abramov, 1994], [Antipenkov, 1991], [Balandin, 1970], [Bichuya, 1969], [Chaevskii, 1962, 1969], [Dmukhovs'ka, 1993], [Gorynin, 1999], [Nikolin, 1968], [Popovich, 1978, 1979, 1983], [Soldatchenkova, 1972], the intimate contact between Armco iron or other Russian steel grades and a potentially embrittling metal (Cd, Ga, Bi, Pb, Sn… or their alloys) is forced by using the method of the soldering fluxes.

De facto, the hypothesis is made that the flux does not perturb the experiment with residual impurities at the steel/LM interface. This drawback, inherent to the method, was minimised by the Russian scientists. For pre-tinning steels specimens with LBE, the employed soldering flux contains zinc, known as a strong embrittler. Balandin tested the mechanical properties of steel specimens in liquid Pb-Bi containing 0.05 to 0.1% Zn and found results comparable to those obtained with pre-tinned specimens tested in pure Pb-Bi [Balandin, 1970]. This does not constitute a proof that Zn does not affect the results of the mechanical tests.

Wetting of T91 steel by LBE has also been achieved by the method of the soldering fluxes. However, the LME effects obtained under these conditions are not reproduced here, because of the embrittling influence of the chemical impurities, and especially zinc, at the steel-LBE interface. In fact, brittle failure of T91 in stagnant LBE containing traces of zinc was observed by F. Gamaoun [Gamaoun, 2003]. To give another example in a different context, a harmful effect of zinc as an impurity in flowing sodium on the creep life of a type 304 SS at 550°C was noted by Huthmann [Huthmann, 1980].

Once again, it appears that the surface preparation is a crucial phase to determine the susceptibility to LME of a given solid-liquid couple.

Last, let us note that dewetting of Armco iron (0.37%C), initially coated with Pb, Bi or LBE by the method of soldering fluxes, may occur due to interfacial oxidation caused by atmospheric oxygen inward diffusion, throughout the embrittling metal layers [Popovich, 1978]. At this point, it could be mentioned that the inward diffusion of oxygen toward the interface could affect the results of the mechanical tests before that dewetting becomes macroscopically observable. However, the remarkable efficiency of the method of the soldering fluxes was proved by Yu.F. Balandin in a study of a 12 KhM pearlitic steel in contact with LBE: the author has shown that, after exposure to oxygen saturated LBE for durations going from 2.5 hours to 25 hours at 500°C, re-tinning with LBE restores its embrittling effect [Balandin, 1970].

7.4.3.3 Role of surface flaws

At the microscopic scale, cracks formed over the whole surface of the tensile specimen invariably promote premature brittle fracture of T91 steel when in contact with LBE. This was shown by different authors, in different environmental conditions [Vogt, 2002], [Dai, 2006], [Fazio, 2003].

Specimen preparation by EDM cutting, even followed by mechanical polishing, results in micro-cracks, randomly distributed over the whole specimen surface, which act as incipient cracks susceptible to propagate rapidly in contact with LMs, and produce LME effects. Moreover, the stress-strain state due to EDM cutting is also unknown. The detrimental effect of EDM-cutting was observed recently by Y. Dai, on flat tensile specimens over a wide temperature range extending from 300 to 425°C, in oxygen saturated LBE under argon, as illustrated in Figure 7.4.4 at 325 and 375°C [Dai, 2006]. Some scattering in the results (particularly the elongation to rupture) is unavoidable with an uncontrolled distribution of micro-cracks, filled or not by LBE, which is absolutely unpredictable. Moreover, the advance of the cracks filled with LBE is always competing with the oxide film formation on crack walls and at crack tip, which is also unpredictable.

The potentially embrittling effect of sharp micro-cracks generated in the cold worked area that forms in the notch during its mechanical machining has been observed [Vogt, 2002]. During loading of hardened and notched T91 steel specimens, the micro-cracks in the notched zone will propagate under the influence of the liquid metal.

Figure 7.4.4. *Top:* Microcracks due to EDM-cutting. Before (*left*) and after (*right*) tensile testing in LBE; note that all pre-cracks are not filled by LBE. *Bottom*: Tensile test results of mechanically polished EDM-cut specimens obtained. At 325°C in oxygen-saturated LBE under argon (*left*) and at 375°C in oxygen-saturated LBE under argon (*right*).

The exposure time to LBE prior testing is indicated. The propagation of the micro-cracks filled by LBE is revealed during tensile testing.

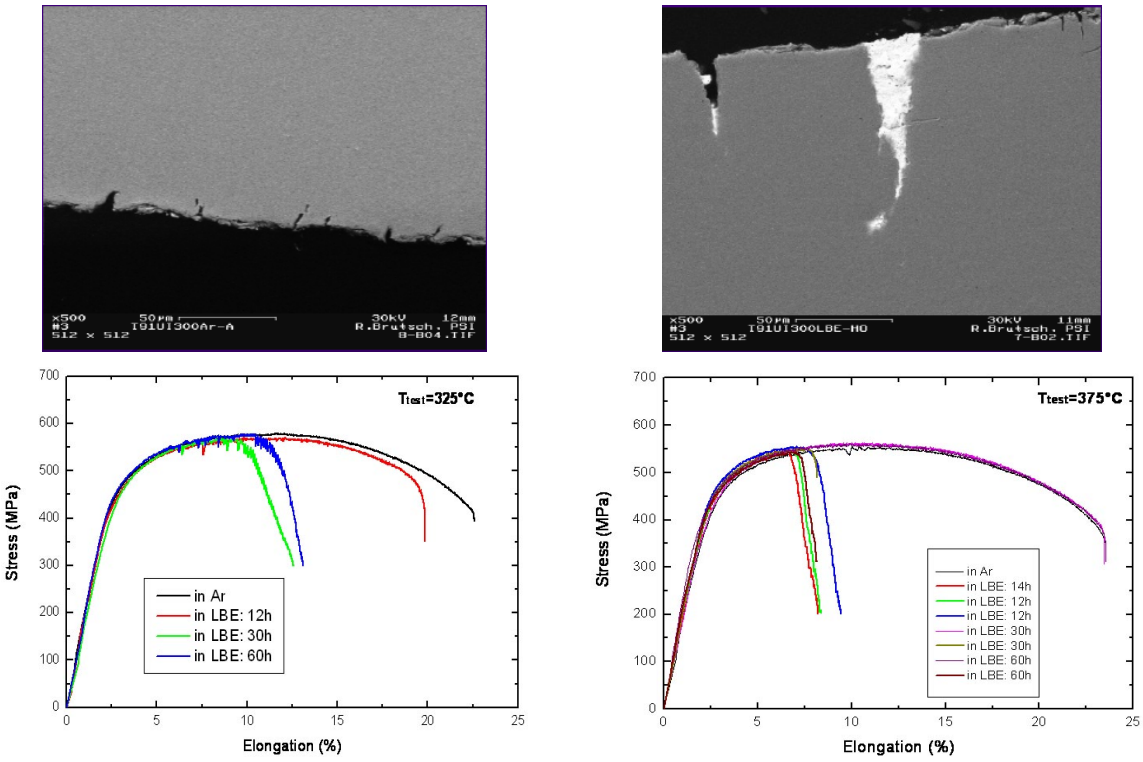

H. Glasbrenner, *et al.* performed tensile tests during the commissioning phase of the LiSoR loop, using flat specimens of MANET II, at a strain rate of 10^{-4} mm s^{-1} [Glasbrenner, 2003]. Ductile behaviour was observed under argon over the whole temperature range tested (T_{room} to 250°C), whereas some embrittling effect is apparently observed in flowing (1 m s^{-1}) oxygen-saturated or at least "close to saturation" LBE, once reached 250 and 300°C. The results of these tests are shown in Figure 7.4.5.

Figure 7.4.5. a) Comparison of stress-strain curves obtained in argon and in oxygen-saturated LBE (no OCS) in LiSoR loop at 250 and 300°C. b) SEM micrograph showing the mixed fracture surface obtained with MANET II after tensile testing at 300°C in LBE.

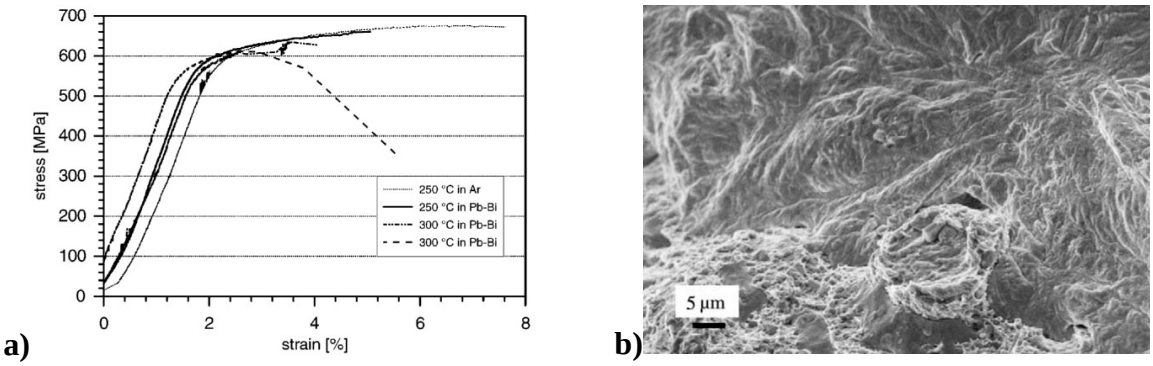

Under the LiSoR loop conditions, a mixed fracture surface was obtained with both flat and ductile areas. The final surface preparation of the tensile specimen was not specified. However, the presence of small cracks initially present onto the specimen surface, propagating under the influence of liquid Pb-Bi, and more specifically bismuth as indicated by the Authors, is a plausible hypothesis, possibly more plausible than the suggestion that the specimens of MANET II could be wetted by LBE under these conditions at 250 or 300°C after two hours pre-exposure to oxidising LBE before tensile testing. Note that ductile failure was always obtained for MANET II in LBE at the lower temperatures tested of 180 and 200°C.

7.4.3.4 Role of traces of impurities

An example of the embrittling effect of zinc, even at trace levels, was shown by F. Gamaoun during his PhD thesis [Gamaoun, 2003]. Cylindrical smooth specimens of T91, diamond polished, were first exposed for one month at 525°C in reducing LBE. The specimens were then submitted to a relaxation test in LBE at 380°C for a few days, and finally ruptured by tensile testing at the same temperature. The main characteristics of the test results were: 1) a significant reduction of the elongation to rupture; 2) a brittle fracture; 3) a surface completely covered with LBE, adherent over the whole gauge length.

A reasonable assumption is that the so obtained surface state and the brittle failure obtained during tensile testing were promoted by traces of zinc in the liquid LBE, as already mentioned above.

The embrittling effect of zinc, antimony and tin, alloyed to lead, was emphasised by W.R. Warke, K.L. Johnson and N.N. Breyer in a review paper of 1970 [Warke, 1970]. However these authors were considering their role as alloying elements, and not at the level of trace elements…as is the case here. Note that the influence of trace elements on mechanical properties in metallurgy remains today a matter of debate.

7.4.4 Main requirements to prevent LME effects

The following conditions must be fulfilled to prevent LME effects:

1) Excellent surface finish of the steel surface, which must be free of surface defects such as pre-cracks, scratches as a result of the surface preparation, and also free of inclusions or precipitates which could act as stress concentrators and initiate cracks in service conditions.
2) The presence of a protective oxide film on to the steel surface prior and during contact with the liquid metal, and self-healing in service conditions. This can be achieved by implementation of an OCS in the system. However, no OCS is required in the case of oxygen-saturated HLM during the entire life of the installation of interest.
3) No specific recommendation on the oxide film thickness, provided that the film remains adherent to the steel surface, with sufficient plasticity. This supposes an adapted oxide film composition and structure, which must be determined and controlled over the test duration, in each experimental situation of interest [Bichuya, 1969].
4) The temperature must be chosen outside the ductility trough, above the upper temperature limit, which means, for example:
   - $T \geq 425$°C for T91, after hardening heat treatment and using notched specimens in oxygen-saturated lead [Nicaise, 2001], [Vogt, 2002];
   - $T \geq 400$°C for T91, after standard heat treatment, and using notched specimens in oxygen-saturated LBE [Guérin, 2003].

There is no rigorous proof that the range of the lower temperature limit, close to the melting point or below the melting point of the embrittling metal, must be avoided. However, besides LME, solid-metal-induced embrittlement (SMIE) is a well-known phenomenon. Some manifestations of SMIE are famous in the literature [Gordon, 1982], which strongly suggests that one keeps the system above the upper limit of the ductility trough. This supposes a systematic study of the influence of the temperature and strain rate to determine the ductility trough of each new steel-HLM system, if no reliable data are available. This supposes also that the metallurgical state of the steel and the chemistry of the HLM be controlled over the entire testing procedure.

5) Control of the presence of impurities: attention must be paid to metallic embrittling impurities like zinc, antimony, tin, and to metalloid impurities and also to chloride and fluoride species not only in the liquid metal phase but also at all stages of the specimen preparation, especially if one uses the method of the soldering fluxes to wet the steel under study. Their presence, even as trace elements, may affect significantly the mechanical properties [Huthmann, 1980].

7.4.5 Experimental results that may be interpreted as EAC effects

We comment briefly on the tensile tests performed on pre-corroded 1.4514 steel grade, HT9, F82H-mod, OPTIFER IVb and EUROFER 97 in contact with Li or Pb-17Li, all reported in Table 7.4.8. Then we come back to the tensile properties of pre-corroded T91 in contact with LBE collected in Table 7.4.5 (see Annex).

7.4.5.1 Case of some ferritic/martensitic steels in contact with Li and Pb-17Li

H.U. Borgstedt, *et al*. [Borgstedt, 1986] observed that corrosive attack, superficial and at pre-cracks, induced by prolonged pre-exposure of 1.4914 steel to pure stagnant lithium at 500°C does not influence the stress-strain curves obtained during tensile tests conducted in air. To justify these results, it was reasonably argued that only the surface but not the bulk properties are affected during aging in contact with lithium. However, when the specimens pre-exposed to lithium were tensile tested in lithium at 250°C, the fracture behaviour changed, exhibiting both brittle and ductile fracture areas, but the specimens always retained some amount of plastic strain at rupture.

O.K. Chopra and D.L. Smith [Chopra, 1986] did not observe any influence of flowing Pb-17Li at temperatures between 273 and 454°C on the tensile behaviour of normalised and tempered HT9, that was preliminary exposed to flowing Pb-17Li at 427°C for 18 hours in order to wet the HT9 specimens by Pb-17Li.

T. Sample and H. Kolbe [Sample, 2000] confirmed those findings in a study of two low activation steels – F82H-mod and OPTIFER IVb – in the fully tempered martensitic state. After a pre-wetting treatment of 15 hours at 500°C in Pb-17Li under argon, the tensile properties were found unchanged in Pb-17Li at 250 and 400°C. After 1500 to 4500 hours exposure to Pb-17Li at 480°C in the LIFUS II loop, G. Benamati, *et al*. did not observe any degradation of the tensile properties of EUROFER 97 during testing under argon at 480°C, whereas the specimen surface was largely corroded by Pb-17Li, and poorly adherent corrosion layers were present on the steel surface [Benamati, 2002].

It is worth remembering that lithium and Pb-17Li are both reported to be reducing and corrosive media. Exposure to Li or Pb-17Li at high temperature (from 427°C [Chopra, 1986] to 480 [Benamati, 2002] and 500°C [Sample, 2000]) invariably corrodes and roughens the steel surface, less for the ferritic/martensitic steel here considered than for an austenitic steel, but this is not the point.

Consequently, assuming that complete wetting can be achieved by pre-heating at high temperature from tens to hundreds of hours depending on the authors, this is not the wetting between two metals with negligible mutual solubility, in other words the wetting required for occurrence of LME, after Kamdar. Therefore, the consequences of such reactive wetting on the mechanical properties remain today totally unpredictable. They will depend on the corrosion processes occurring prior to or under mechanical loading. In all cases, we consider that the degradation of the mechanical properties of martensitic steels caused by contact with Pb-17Li is a manifestation of EAC.

7.4.5.2 Case of T91 steel in contact with LBE

In the framework of the TECLA and MEGAPIE-TEST programmes, G. Benamati, C. Fazio, *et al*. studied the T91-LBE couple using the above described experimental procedure (see Table 7.4.5): long-term exposure of T91 to flowing and reducing Pb-55Bi at 400°C in the LECOR loop (1500-4500 h) followed by tensile test under argon at same temperature [Fazio, 2003], [Aiello, 2004].

The oxygen level in the melt, ranging from $3\ 10^{-10}$ to 10^{-7} wt.ppm was lowered by addition of Mg and bubbling under pure H_2. The results are: i) a net reduction of the elongation to rupture, ii) a decrease of the ultimate tensile strength, iii) with mixed ductile (at the centre) and brittle (at the periphery) fracture surfaces (Figure 7.4.6).

These results tend to demonstrate that the surface state obtained after such long-term ageing in Pb-55Bi is the one required to produce embrittlement. Today, with all that we know about EAC and LME phenomena, these results could be interpreted as a manifestation of either EAC or LME.

Very recently, a detrimental effect of long-term exposure to LBE on the tensile properties of T91 was also observed by D. Sapundjiev, *et al*. [Sapundjiev, 2006]. This work also shows an effect of the ageing temperature, clear at 450°C but undetectable at 300°C (Figure 7.4.7). The results of this study are not in so good agreement with the ones described from the beginning of this chapter. This could be explained by the conditions of specimen preparation (mechanical grinding not followed by any surface treatment to minimise the roughness of the tensile specimens) and testing procedure, differing from the ones applied in the other quoted works.

In all cases, a systematic analysis of the composition and structure of the interface with the liquid phase is lacking, and also of the transport properties of metal ions elements throughout the interface. A better knowledge of the composition, structure and transport at the S/L interface would permit interpretation without ambiguity the obtained results.

7.5 Fatigue behaviour of austenitic steel of type 316 and ferritic/martensitic steel of type T91 in contact with lead and LBE

7.5.1 Definition

Among the different definitions for the term “fatigue”, the most appropriate for the materials of concern in this chapter is as follows: Fatigue is the progressive, localised and permanent change that occurs in a material subjected to conditions that produce fluctuating stress and strain at some points and that may culminate in cracks or complete fracture after a certain number of fluctuations.

Figure 7.4.6. a) Stress-strain curves obtained at 400°C in argon at strain rate of 3 10^{-3} s^{-1} after long term exposure of T91 to LBE at 400°C in LECOR loop. b) Morphology of T91 specimens after 4500 h in LECOR loop at 400°C followed by tensile testing in argon at 400°C. c) SEM micrograph showing a zone at the periphery of the fracture surface of the T91 tensile specimen [Aiello, 2004].

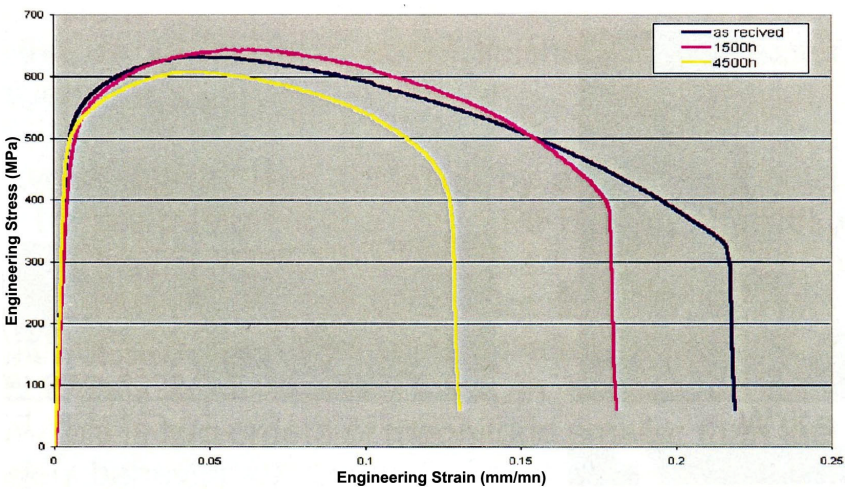

b)

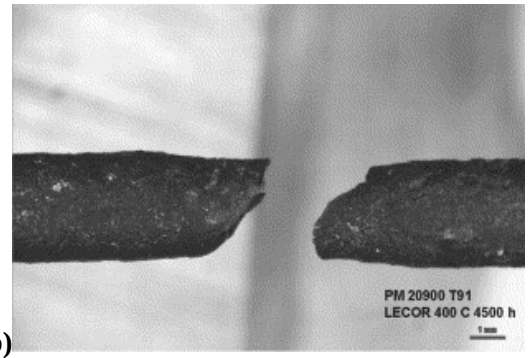

c)

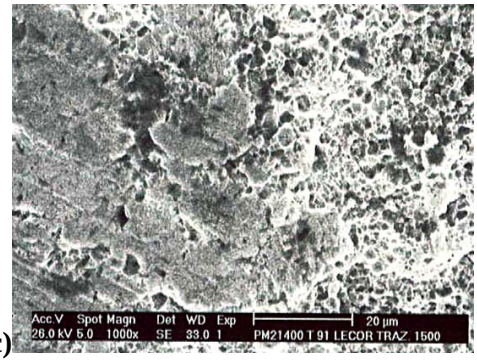

Figure 7.4.7. Engineering stress-strain curves obtained with T91 specimens, after standard heat treatment, after 4000 h pre-exposure to LBE at 450°C, followed by tensile test at 300 and 450°C at a strain rate of 5. 10^{-5} s^{-1}

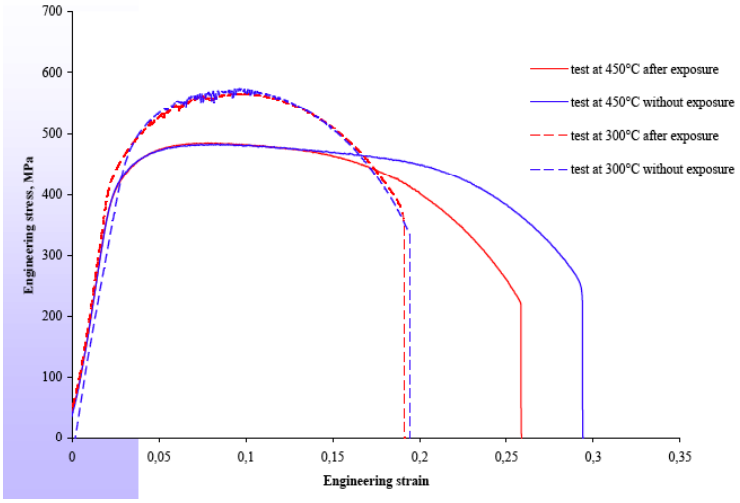

The procedures of “fatigue testing” can be classified into four groups:

- the stress life approach;
- the strain life approach;
- the fatigue crack propagation approach;
- the component test model approach.

Corrosion-fatigue is one of the environmentally-assisted cracking phenomena.

The strain life and fatigue crack propagation approaches have been investigated in the framework of the French GEDEPEON programme, TECLA and MEGAPIE-TEST European programmes on ADS by J-B. Vogt, *et al.* [Vogt, 2004, 2006], [Verleene, 2006]. This was motivated by the fact that information on the resistance to crack initiation, the behaviour of small cracks and the crack velocity under cyclic loading in contact with LBE were extremely sparse. Consequently, low-cycle fatigue (LCF) as well as fatigue crack propagation (FCP) tests in HLMS were developed:

- FCP tests inform about the velocity of long cracks. Pre-cracked specimens, of CT or four-point bend type, are used. The test is generally performed under load control and requires the measurement of the single crack advance that propagates through out the specimen. The results are compiled into a relationship of type $da/dN = f\Delta K)$ where da/dN is the crack velocity expressed in mm/cycle and ΔK the stress intensity factor range.
- LCF tests inform about the cyclic accommodation of a material and characterise the resistance to crack initiation under cyclic loading. It uses smooth specimens (cylindrical, or hourglass shape gage length, plates). LCF tests are conducted under total or plastic strain control, with $\Delta\varepsilon_t$ ranging from 0.4% to 2.5%, generally with a triangular waveform and constant strain rate (in the range of 10^{-2} to 10^{-4} s^{-1}). Stress-strain hysteresis loops are periodically recorded during cycling allowing for the measurement of the stress range $\Delta\sigma$. The LCF life is equal to the number of cycles required to initiate surface cracks, and the propagation of at least one of them to failure.

Fatigue testing began on T91 in contact with LBE in the framework of the MEGAPIE target project. There were at least two motivations. Design of the target window has to ensure that cyclic loading imposed to the target window by the beam trips is less than the critical load leading to crack initiation after about 10^4 load cycles, i.e. the expected lifetime foreseen for the LBE liquid metal target. Besides the beam trips, the structural materials of an ADS, especially the target container, will be subjected to a variety of loading conditions in service, thermo-mechanical or not.

When the French GEDEPEON and European programmes on ADS started, the information was extremely sparse about the effect of both lead and LBE on the fatigue behaviour of ferritic/martensitic steels like T91, MANET II... This is no longer the case [Kalkhof, 2003], [Vogt, 2004, 2006], [Verleene, 2006].

In some aspects, the situation is different as concerns the fatigue behaviour of 316 type austenitic stainless steels:

- In the framework of the fusion programme, the compatibility of 316L type SS with lithium or Pb-17Li, its corrosion and mechanical behaviour including low-cycle fatigue (LCF) have been extensively studied for decades [Borgstedt, 1991], [Chopra, 1983], [Benamati, 1994].

- In the framework of the LMFBR project, the fatigue behaviour of 316L type SS in contact with alkali metals, particularly sodium and lithium, was also thoroughly investigated for years now [Borgstedt, 1991], [Mishra, 1997], [Kalkhof, 2003].
- Recently, in the framework of the Japanese or US projects of spallation neutron sources, the compatibility of type 316LN stainless steel with mercury has been the subject of a number of works, since a type 316LN SS was selected for the vessel containing mercury [Strizak, 2001, 2003], [Tian, 2003].

However, to our knowledge, besides the former USSR literature concerning carbon steels and various Russian steel grades pre-tinned with LBE, tin or tin-lead eutectic [Bichuya, 1969], [Nikolin, 1968], [Chaevskii, 1969], [Popovich, 1979], [Dmukhovs'ka, 1995]…the effects of lead or LBE on the fatigue behaviour of 316 type SS are largely unknown. In the following, we briefly comment recent results [Kalkhof, 2003], [Vogt, 2004, 2006], [Verleene, 2006].

7.5.2 Low-cycle fatigue behaviour of ferritic/martensitic steels in contact with LBE

We first recall the conditions of the study due to D. Kalkhof and M. Grosse [Kalkhof, 2003]: Fully reversed (R = -1) strain controlled LCF tests were performed on a Schenck servo-hydraulic machine with a load capacity of 250 kN, at total strain amplitude (ε_{at}) varying from 0.2% to 1% (i.e. total strain range $\Delta\varepsilon_t$ varying from 0.4% to 2%) at 1 Hz cycle frequency, with some tests conducted at $\Delta\varepsilon_t$ = 0.3% and 0.1 Hz frequency. The environmental conditions are air or stagnant LBE at 260°C, with no indication of the oxidising or reducing power of LBE. Some tests were also carried out in air at room temperature.

The conditions of the study of J-B. Vogt, I. Serre, *et al*. are based on the ASTM standard E 606 (Annual book of ASTM standards – 1991, Section 3, Vol. 03.01) [Vogt, 2004, 2006], [Verleene, 2006]: LCF tests were carried out at 300°C in air and in oxygen-saturated LBE under air, using a hydraulic MTS closed loop servo-controlled machine with a load capacity of 100 kN. A cylindrical vessel containing the HLM surrounded the specimen. Tests were total axial strain controlled using a strain gage extensometer set outside the HLM vessel. They were conducted in a fully push pull mode (R = -1) at different imposed total strain ranges: $0.4\% \leq \Delta\varepsilon_t \leq 2.5\%$, using a triangular waveform and a control of the strain rate ($4.\ 10^{-3}\ s^{-1}$). Hence, the cyclic frequency ranged from 0.25 Hz to 0.08 Hz for the smallest and highest strain tests respectively. During cycling, hysteresis loops were periodically recorded allowing for the measurement of the stress variation $\Delta\sigma$ at each cycle. The fatigue life is defined as the number of cycles for which a 25% drop in the quasi stabilised tensile stress occurs.

In all cases, attention was paid to the surface state of the specimens, carefully manually polished [Kalkhof, 2003], or electro-polished [Vogt, 2004, 2006] depending on the authors.

The LCF behaviour of MANET II and T91 in contact with LBE or lead at $\Delta\varepsilon_t < 0.3\%$ is unknown.

7.5.2.1 Role of LBE on cyclic accommodation

Cyclic softening was observed for both MANET II [Kalkhof, 2003] and T91 [Vogt, 2004], independent of the environment, air or stagnant LBE, in the previously described experimental conditions. This point is illustrated for the T91-LBE couple in Figure 7.5.1. These results suggest that LBE affects only the surface but not the bulk properties.

Figure 7.5.1. Evolution of the stress amplitude with the number of cycles for tests carried out at $\Delta\varepsilon_t$ ranging from 0.4% to about 2.5% at 300°C in air and in LBE for the T91 steel

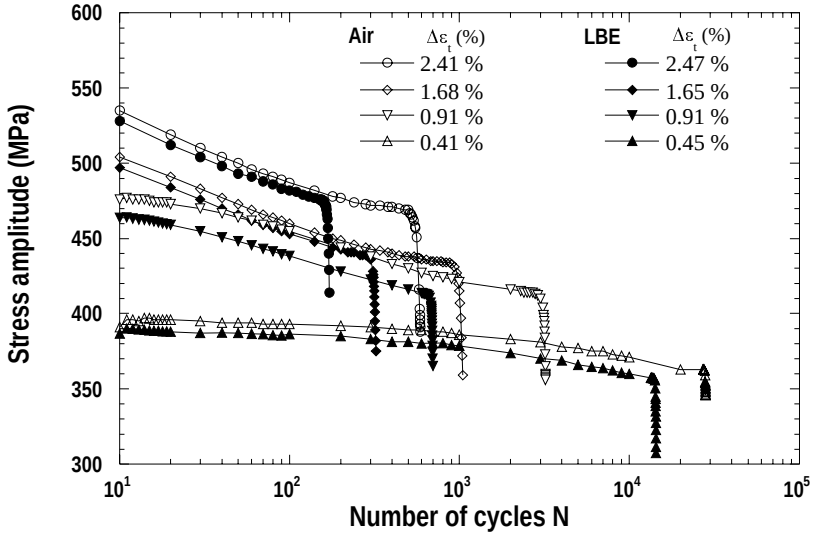

7.5.2.2 Role of LBE on fatigue resistance

For 316L [Kalkhof, 2003], the fatigue lives in LBE appeared to be similar when compared to the results in air especially at low strain amplitude where scatter in the fatigue lives was observed. At higher strain amplitudes (ε_{at} = 0.5, 0.6%), there was a little influence of LBE on the fatigue resistance as is shown in Figure 7.5.2.

This contrasts very much with the behaviour of both MANET II [Kalkhof, 2003] and T91 [Vogt, 2004], [Verleene, 2006] whose fatigue life is reduced in contact with LBE as shown in Figure 7.5.2. The effect is function of the total strain amplitude and cycle frequency. The main trend is a decrease of fatigue life, amplified with increasing $\Delta\varepsilon_t$ and decreasing cycle frequency.

Figure 7.5.2. Total strain amplitude vs. cycle number for crack initiation curves for 316L stainless steel in air and PbBi at 260°C, after Kalkhof and Grosse

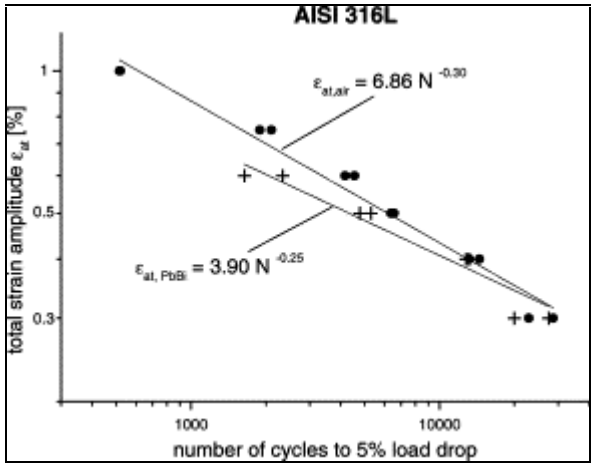

The oxygen activity in the LBE was not mentioned by Kalkhof. This information would have been of interest, since the surface state of the steel, either MANET II, T91 or 316L SS, is already largely modified by oxidation/corrosion at 260°C.

7.5.3 Influence of hold time on fatigue behaviour of T91 in LBE

Data as a function of hold time are presented in Figure 7.5.3 (Table 7.5.2 in annex and [Vogt, 2006]). The tests were performed under strain control, using a trapezoidal wave-form, with 10 min. tension hold time. The environmental conditions were 300°C in air or oxygen-saturated LBE.

Figure 7.5.3. Fatigue resistance of T91 in air and in LBE, with and without 10 min hold time in tension. As an example, for $\Delta\varepsilon_t$ = 0.7%, the fatigue life is reduced of a factor ~2 at 300°C in oxygen-saturated LBE and by a factor of ~4 if a hold time is introduced.

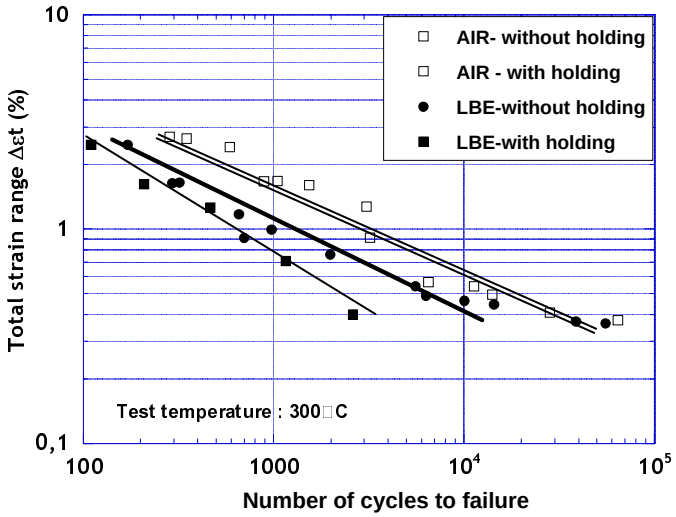

The stress response to strain cycling is unmodified by the introduction of a hold time, either in air or in LBE. No stress relaxation was recorded at this temperature. On the contrary, for all tests performed at imposed total strain ranges in between 0.4% and 2.5%, the fatigue life of T91 decreases with application of a hold time in tension, contributing to the modification of the surface state in contact with LBE at 300°C. A synergistic effect of the environment and the mechanical test conditions may explain this decrease of LCF life. No such effect was observed in air.

7.5.4 Influence of preliminary exposure to LBE on fatigue behaviour of T91

A first batch of specimens was exposed in a LBE loop for 613 h at 600°C in reducing conditions (oxygen content less than 10^{-10} wt.%). Another batch was exposed to oxygen-saturated LBE (air over-pressure of 200 mbar) at 470°C for 502 hours. They were then fatigued in LBE at 300°C with the mechanical testing conditions reported in Table 7.5.2: strain control, symmetrical triangular wave form (R = -1) [Vogt, 2006]. The stress responses to strain cycling of T91 steel in LBE at 300°C after pre-exposure to LBE in either oxidising or reducing conditions, under OCS, were similar to that of non-exposed specimens.

The results of LCF tests are shown in Figure 7.5.4. The following results were observed:

- Cyclic softening was unaffected by preliminary ageing in LBE, whatever the conditions.
- Fatigue life was significantly decreased by preliminary ageing in reducing LBE.
- Fatigue life was unmodified or slightly increased by preliminary ageing in oxidising LBE.

Figure 7.5.4. Influence of pre-exposure of T91 to LBE under reducing or oxidising conditions (under OCS, in collaboration with A. Terlain, CEA-Saclay) on the fatigue resistance at 300°C in LBE under air. Note that the fatigue life of T91 aged in oxidising LBE is similar to that of the reference in air (AIR_as received), but larger than the fatigue life of T91 aged in reducing LBE for $\Delta\varepsilon_t$ ~ 0.4%, the effect being less marked for $\Delta\varepsilon_t$ ~ 0.9%.

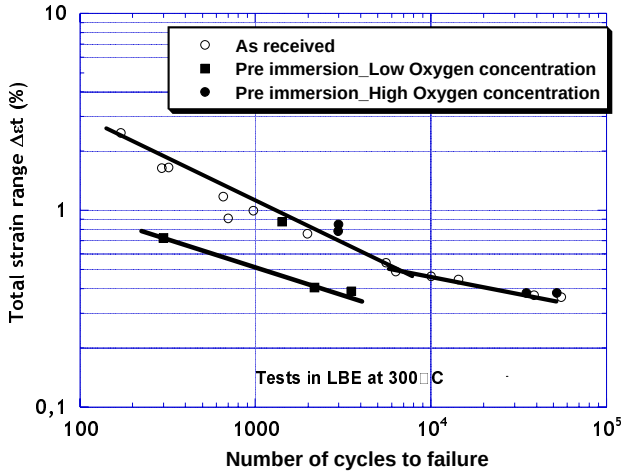

7.5.5 Influence of LBE on fatigue crack growth of T91 and MANET II

Strictly speaking, only fatigue crack growth rate tests using pre-cracked specimens can give quantitative information on the effect of LBE.

However, a qualitative behaviour or tendency can be obtained from LCF tests. Indeed, the final decrease of the stress amplitude (see Figure 7.5.1) is related to crack propagation in the bulk. It was found that the stress decrease was more abrupt in LBE than in air suggesting that the crack growth rate is accelerated by LBE for both 316L [Kalkhof, 2003] and T91 [Kalkhof, 2003], [Verleene, 2006].

Crack propagation is faster in LBE than in air for MANET II and T91, in roughly similar testing conditions (see Table 7.5.1).

This result will be corroborated by making use of a more quantitative approach [Verleene, 2006], based on a specific experimental procedure of the AFNOR standard A03.404 (1991). Tests were carried out using four-point bend specimens (10 mm × 10 mm × 55 mm) under load control. The crack opening displacement (COD) was measured using a strain gage extensometer. The COD was converted into crack length using a calibration procedure, which allowed the calculation of both the crack growth rate da/dN (mm/cycle) and the cyclic stress intensity factor ΔK (MPa.√m). Pre-cracking was performed in air at room temperature at 15 Hz using the step down procedure starting at 20 MPa.√m and decreasing load to attain about 5 MPa.√m. Then the FCG tests started from 5 MPa.√m at a frequency of 5 Hz and a stress ratio R = 0.5, at 300°C in air and in LBE.

The results shown in Figure 7.5.5 reveal a net increase in the fatigue crack growth rate for T91 in contact with LBE, in comparison with air, in agreement with the LCF results of Figures 7.5.1 and 7.5.2.

Figure 7.5.5. Fatigue crack growth curves for T91 at 300°C in air and in LBE (5 Hz, R = 0.5)

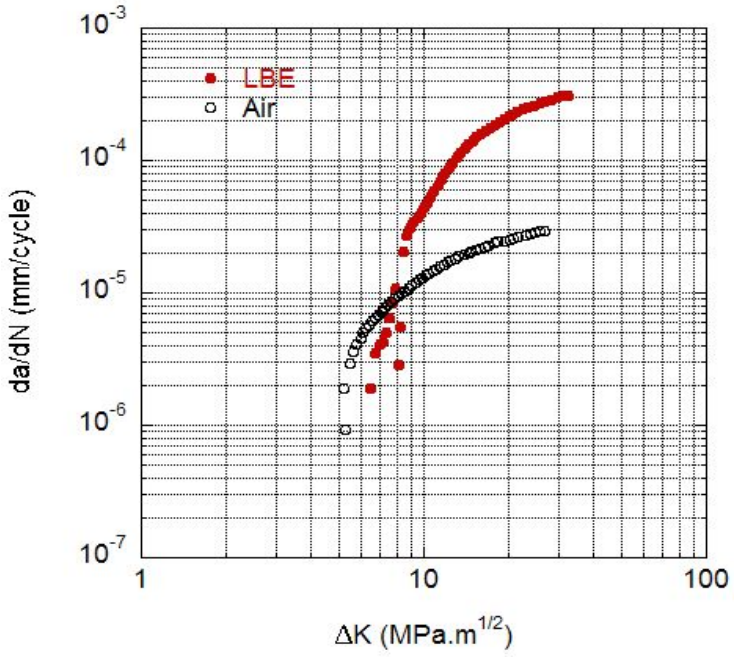

The above results are remarkable, owing to the common observation that LBE does not easily reach the crack tip. Intergranular penetration of the liquid metal is not a characteristic of the T91-LBE couple. In this system, crack opening is not immediately followed by filling with liquid metal, contrary to model systems like Cu-Bi or Ni-Bi [Wolski, 2002].

Moreover, for both studies devoted to FCG of MANET II and T91 in LBE, it is also worth remembering that the oxidising or reducing power of LBE was unknown in one case [Kalkhof, 2003], and that the LBE was oxidising in the other case [Verleene, 2006].

7.5.6 Influence of LBE on fatigue fracture surface morphology of T91

LBE influences the macroscopic fracture surface morphology and fracture mode as is illustrated in Figures 7.5.6 and 7.5.7. The following characteristics are observed:

- After LCF test of T91 in air [Figure 7.5.6(a)], the fracture surfaces are rather tortuous with a fracture surface at about 45° with respect to the loading axis. Multiple initiation sites, from which cracks propagated into the bulk, are observed. The fracture surface results from the junction of the various propagation planes, which entails a macroscopically inclined fracture.
- After LCF test of T91 in contact with LBE, without preliminary exposure to LBE, the fracture surface was rather flat with a unique crack initiation site [Figure 7.5.6(b)].
- After LCF test of T91 in contact with LBE, with preliminary exposure to LBE, the fracture surface was rather flat with several crack initiation sites.

Figure 7.5.6. Macroscopic view of typical fatigue fracture surfaces of T91 after LCF tests conducted (*left)* on specimens tested in air, and (*right*) on as-received specimens directly immersed in LBE for LCF testing

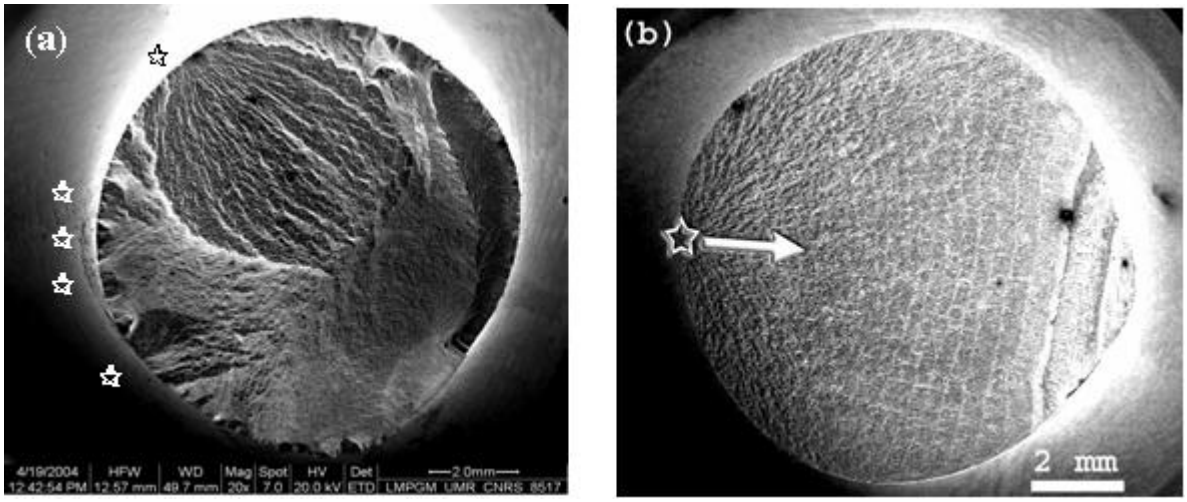

At microscopic scale, some differences could be noticed between fracture surfaces in air and in LBE. However, fretting of the surface during the test made the SEM examinations rather difficult. Nevertheless, fatigue striations, typical of fatigue failure were observed in some situations.

- The striations, visible after LCF fracture in air, are enlarged as a result of LCF testing in LBE: about a few μm in air and possibly attaining ~100 μm in LBE.
- A change in the fracture mode was observed in the FCGR specimens, with a transition from ductile striations with small distances between them in air [Figure 7.5.7(a)] to a mixed brittle inter- and transgranular fracture in LBE [Figure 7.5.7(b)].

These results are in agreement with the acceleration of the FCG rate induced by LBE, and illustrated with Figure 7.5.5.

Figure 7.5.7. SEM micrographs of typical fatigue fracture surfaces, as a result of FCP tests of T91 (*left*) in air, and (*right*) in LBE

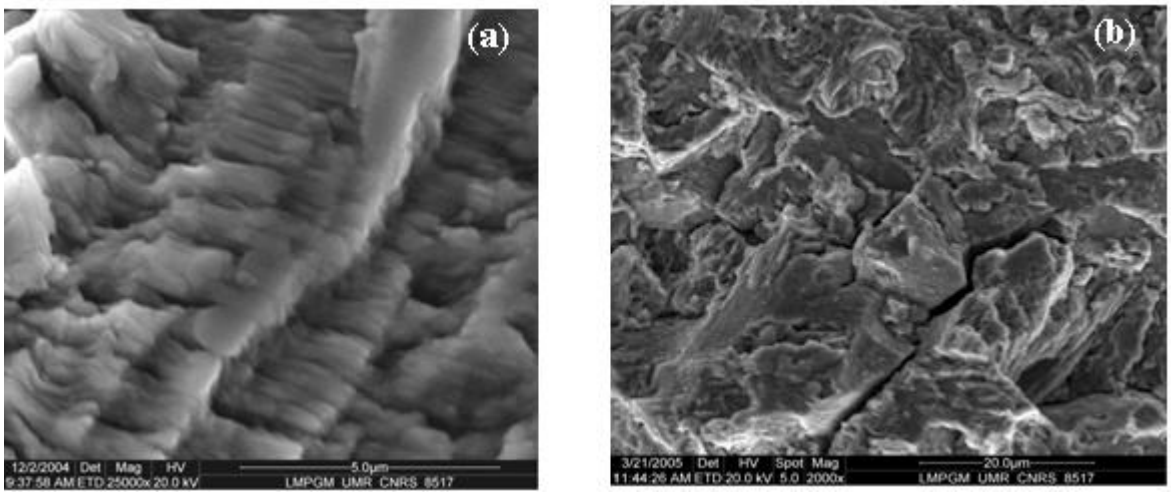

7.5.7 Influence of LBE on fatigue crack initiation in T91 and MANET II

For both MANET II and T91, the crack initiation mechanism is modified by contact with LBE, in comparison with air, as reported in [Kalkhof, 2003] and [Vogt, 2004], [Verleene, 2006].

For MANET II, a strong reduction in the number of cycles for fatigue crack initiation was observed at 260°C in LBE in comparison with air. This was discussed on the basis of metallographic observations.

The two crack initiation sites and cracks are shown in Figure 7.5.8. After LCF testing in air, a main crack and a number of short cracks coexist at the MANET II specimen surface, whereas one single crack remains in LBE, whose morphology contrasts with the one of the air-formed cracks. This main crack presents straight walls and lateral sub-cracks are filled with LBE.

Figure 7.5.8. Photomicrographs of MANET II specimens after LCF testing (*top*) in air and (*bottom*) in LBE. Note the fast crack propagation for MANET II in LBE compared to 316L in otherwise identical conditions.

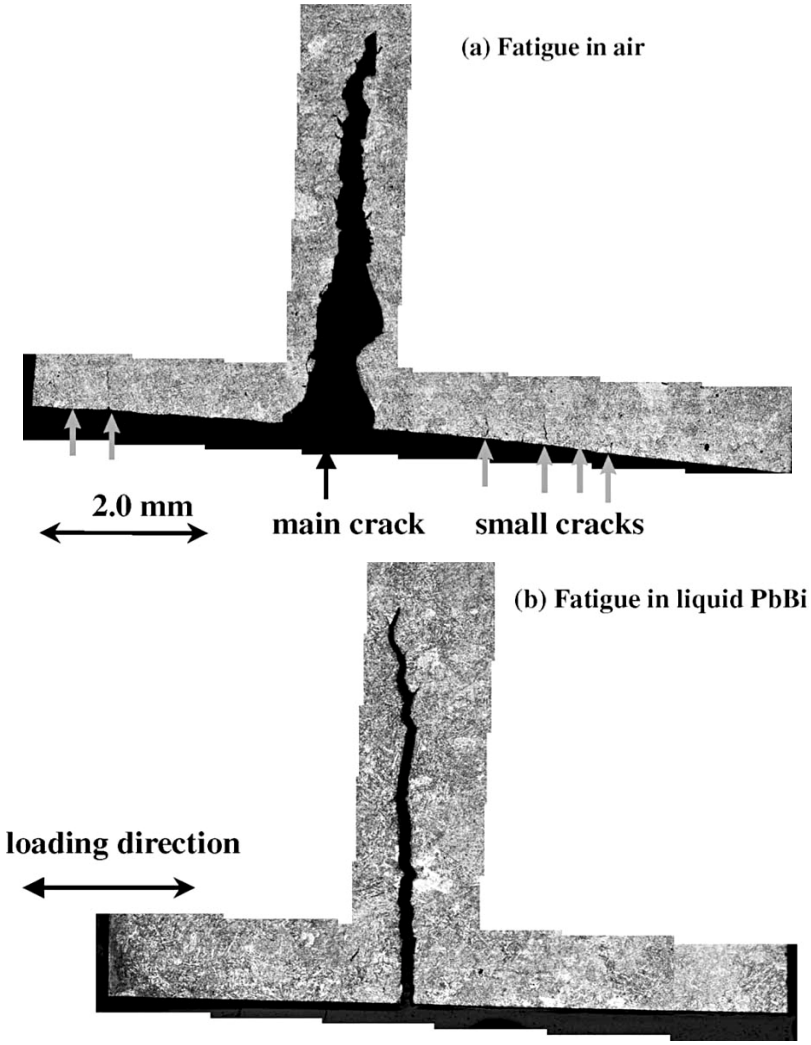

Complementary information on the crack initiation mechanism is given by J-B. Vogt, *et al*. [Vogt, 2006], [Verleene, 2006]. Crack initiation was found to be transgranular in air and LBE alike. Cracks grow through the grains, occasionally at grain boundaries in LBE. In addition, the cracks exhibited the following characteristics:

- In air, the short cracks are generated by a classical extrusion-intrusion process.
- In LBE, the evolution of the population of cracks initiated in T91 specimens is similar to that represented in Figure 7.5.8 for MANET II.
- Preliminary exposure to reducing LBE leads to intergranular cracks; some of them will propagate during LCF testing, depending locally on the chemical and metallurgical conditions (Figure 7.5.9).

Figure 7.5.9. SEM micrographs of cross-sections of T91 specimens 613 h ageing in reducing LBE ($<10^{-10}$ wt.% oxygen): a) before LCF testing and b) after LCF testing in LBE at 300°C, $\Delta\varepsilon_t$ = 2.2%

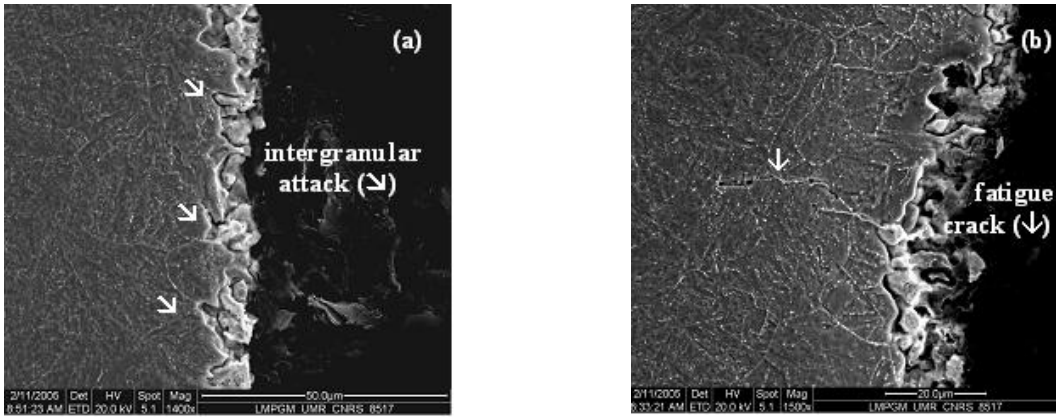

For the T91-LBE couple, the distribution of cracks was analysed by J-B. Vogt, *et al*. [Vogt, 2006], [Verleene, 2006] as function of the imposed strain amplitude in LCF tests in both media (air, LBE) with the following observations:

- In air, the growth of grain-sized cracks is limited by the grain boundaries, which can be overcome after a certain number of cycles. Crack extension therefore occurs by crystallographic growth, which again is limited by other grain boundaries but the crack length attains now three or four grains sizes; longer microcracks can form by coalescence of smaller ones. Finally, only very few of them propagate in a plane perpendicular to the stress axis into the bulk. The role of the microstructure on crack growth in air was already published [Vogt, 1988].
- •In LBE, the author suggests that once a microcrack forms inside a grain, the grain boundary resistance to crystallographic growth vanishes in contact with the liquid metal, allowing for crack extension throughout the neighbouring grains until final rupture.

It remains to explain why and how LBE facilitates the extension of the first crack embryo, and correlatively prevents the initiation of other cracks, at all scales (not only macroscopic, but also microscopic and sub-microscopic). Let us recall:

- that LBE is oxidising in the above-reported studies, except in the conditions of Figure 7.5.9;
- that the mechanism of transport of the embrittling atoms in a crack, at all stages of crack growth, is unknown;

- that the mechanism of oxygen transport in a confined liquid medium like a grain boundary or a crack is unknown;
- that the penetration of LMs at grain boundaries or into cracks has been treated recently by different authors, but that a unique model accounting for all experimental details is still missing.

7.5.8 Low-cycle fatigue behaviour of 316L type stainless steel in contact with lead alloys, in comparison with lithium and sodium

There is an abundant literature on compatibility of 316 type austenitic stainless steels with Pb-17Li and alkali metals like Li and Na. In this paragraph, we have deliberately selected a few papers summarising the information on LCF and FCG of austenitic steels in these media (see Table 7.5.1 in the annex to this chapter).

Once the differences due to the impurity content in the LMs (especially O, C and N), due to the testing procedure including pre-exposure effects, and the characteristics of the material (commercial heat, product form, initial heat treatment) are taken into account, it appears that the fatigue behaviour of austenitic stainless steels in sodium and lithium is superior to that in air [Chopra, 1983], and that the LCF behaviour of 316L is unaffected by contact with Pb-17Li [Benamati, 1994]. It was also reported that the FCG rate for 316LN in sodium is considerably lower than in air, with a threshold stress intensity factor being a function of the stress R-ratio [Mishra, 1997].

Recent results on the fatigue behaviour of 316LN stainless steels in mercury were published at ORNL [Strizak, 2001]. Mercury has no effect on the endurance limit. However, at higher stresses, for fully reversed traction-compression tests (R = -1), mercury reduces the fatigue life by a factor of 2-3 with respect to air. The influence of mercury also appeared to be frequency sensitive with a synergic effect. Fatigue lifetimes in Hg at 0.1 Hz were found to be approximately 70% lower than those at 10 Hz. The role of wetting by mercury on the fatigue life was also emphasised.

Turning now to the low-cycle fatigue behaviour of 316L stainless steel in stagnant LBE, the available data are largely consistent with the above-mentioned results [Kalhhof, 2003]:

- Cyclic softening of 316L, as noted above for MANET II and T91, is found independent of the environment, air or LBE at 260°C.
- At low strain amplitude, ε_{at} = 0.3%, even attaining 0.5%, the fatigue life for 316L in LBE is comparable to that in air;
- At total strain amplitude $\varepsilon_{at} \geq 0.5\%$, a weak influence of LBE was observed.

The only detrimental effect of LBE on LCF of 316L concerns the crack propagation, considered by the authors slightly faster in LBE than in air, at 260°C, for $\Delta\varepsilon_t$ = 0.3%, and 1 Hz cycle frequency (see Figure 7.5.2).

To conclude, as of this date, the influence of LBE on the LCF behaviour of 316L SS can be considered weak.

7.6 Creep properties: Definition and state of the art concerning the austenitic steel of type 316 and the ferritic/martensitic steel of type T91 in contact with lead and LBE

7.6.1 Definition

Creep of materials is associated with time-dependent plasticity under constant stress at elevated temperature, often larger than roughly 0.5 T_m with T_m being the absolute melting temperature. Either constant stress or constant strain rate conditions can be adopted. The micro-mechanisms controlling creep deformation involve dislocation glide and climb and also, at low stresses, diffusion controlled mass transport along grains boundaries.

Classically, the creep rate varies in between 10^{-7} h^{-1} and 10^{-1} h^{-1}, depending on applied stress (from tens to a few hundred of MPa) and temperature. In specific cases, creep tests have been performed on creep machines allowing for creep rates $\dot{\varepsilon}$ as low as 10^{-9} h^{-1}. The creep data include the stress vs. time to rupture, the total elongation vs. time to rupture, the reduction of area vs. time to rupture as function of temperature, and also the evolution of the creep rate as function of temperature, under various applied stresses.

The creep strength is defined in terms of stress versus creep rate and is measured in stress relaxation tests lasting 24 hours.

7.6.2 Creep properties of martensitic and austenitic stainless steels in air or liquid metals other than lead or LBE

There is in the literature a substantial amount of creep data in air, on commercial heats of modified 9Cr-1Mo steels over a wide temperature range, from 425°C to ~700°C. These data were required to establish the effect of a number of metallurgical parameters like heat treatment, cold work, notch sensitivity, thermal ageing and applied stress. Irradiation creep of ferritic/martensitic steels was also thoroughly investigated using different reactors or in laboratory irradiation facilities [Klueh, 2001], [Toloczko, 1996]. The (interrupted) tests are followed by micro-structural investigations.

Today, the tempered martensitic Cr-steels are reputed for their quite stable microstructures and good mechanical properties at elevated temperatures thanks to the pinning of dislocations and lath interfaces by fine precipitates and elements in solid solution (Cr, Mo, C…) [Guttmann, 1997], [Hättestrand, 2001].

The 10^5 hours creep rupture strength of T91 steel at 600°C was measured to be of the order of 100 MPa [Boutard, 2001].

As noted above in Section 7.5 dedicated to fatigue and creep-fatigue behaviour, the creep behaviour of both martensitic and austenitic stainless steels in contact with Pb-17Li, lithium and sodium were studied in parallel, in the framework of the fast breeder reactors and fusion projects. Perhaps it could be an element of information to recall that there is no evidence of a deleterious influence of sodium on the creep properties of type 316 austenitic stainless steels. As concerns the influence of Pb-17Li on the creep properties of martensitic steels, one should refer to the review papers by H.U. Borgstedt and co-workers; once again a slight reduction of creep life was obtained in a number of experimental conditions.

7.6.3 Creep and creep crack growth of both austenitic and ferritic/martensitic steels in lead or LBE

There is almost no information on the creep strength, creep damage and creep crack growth rates of both T91 and 316L in contact with lead or LBE, referring to the available accessible literature. E.E. Glickman was the first to mention a detrimental effect of liquid metals on creep [Glickman, 1976, 1977, 1985, 2000]. At the end of the 70s, the author proposed an explanation, considering that liquid metal accelerated creep (LMAC) is one more manifestation of the Rebinder effect, besides LME. A study of 2004 reporting an LMAC effect on both the T91-lead and the T91-LBE couples is briefly described in Section 7.6.5. At the same period, in Russia, in the context of the BREST-0D-300 reactor system, creep tests were performed on a chromium steel 10Kh9NSMFB (containing 1.2%Si) in flowing liquid lead under 70, 100 MPa between 420 and 550°C, showing an earlier transition into the third stage of creep and a decrease of the duration of the steady creep stage, explained by the authors as a consequence of the lead corrosiveness [Kashtanov, 2004]. More detailed information about the test conditions and composition and structure of the steel/lead interface would be of interest at all stages of the test. This includes easier access to the Russian previous and present literature on structural materials in contact with liquid metals for nuclear applications [Balandin, 1961], [Bryant, 1988].

7.6.4 Liquid metal accelerated creep (LMAC)

An increase in the secondary creep rate, by a factor of 2 to 100, was reported for single and polycrystals of Zn, Cd, Cu, Fe and Fe-Ni alloy, tested under tensile or compressive stress in experiments performed in the former USSR [Glickman, 1976, 1978; Nikitin, 1967]. LMs accelerate, at the same time, creep and the nucleation growth of vacancy voids near the metal surface in traction or compression.

7.6.5 Accelerated plastic strain of T91 steel in contact with lead

Recently, F. Gamaoun, *et al*. [Gamaoun, 2002, 2003, 2004] reported LMAC effects on T91 steel platelets in contact with lead and LBE under OCS, using the two COXCIMEL[13] and FLEXIMEL[14] set-ups for control of the oxygen activity in molten lead and LBE developed by V. Ghetta, *et al*. [Ghetta, 2001, 2002].

The FLEXIMEL specimens are (4 mm × 50 mm × 1 mm) platelets inserted in an alumina specimen holder, which applies a fixed symmetric four-point bending. They can be annealed either in a liquid LM bath under OCS, or in gas atmosphere (air or pure H_2). A constant deflection of 0.2 mm is imposed to the platelets between the central and outer bearings, which corresponds to an initial maximum stress of 135 MPa, about 25% of the yield stress at the imposed temperature of 525°C. During annealing in lead, LBE or in air at elevated temperature, the elastic energy stored is relaxed and activates plastic deformation mechanisms.

The test results are shown in Figures 7.6.1 and 7.6.2. The authors observed the formation of cavities and an acceleration of plastic strain in the T91 steel specimens under fixed four-point bending at 525°C in both reducing (oxygen activity: $a_0 = 2.7\ 10^{-16}$) and oxidising (oxygen activity: $a_0 = 3.1\ 10^{-10}$) lead or LBE, which is never observed at same temperature in air.

[13] COXCIMEL: *in French*, "Corrosion sous OXygène Contrôlé et Interaction avec les MEtaux Liquides", refers to an original oxygen control system (OCS) developed by V. Ghetta, *et al*. [Ghetta, 2001], which permitted to determine the values of the oxygen solubility in lead and LBE over the 250-700°C temperature range, in very good agreement with the results obtained by J.L. Courouau using a CEA made OCS device [Courouau, 2002, 2004].

[14] FLEXIMEL: *in French*, "FLEXion sous OXygène Contrôlé et Interaction avec les MEtaux Liquides", refers to an experimental set-up allowing for four-point bending test under the OCS developed earlier by V. Ghetta [Ghetta, 2002].

Figure 7.6.1. SEM micrographs of the FLEXIMEL specimen central cross-section after 1 month annealing in stagnant liquid lead bath at 525°C under Ln(a_0) = -16 oxygen activity: a) tensile zone; b) compressive zone

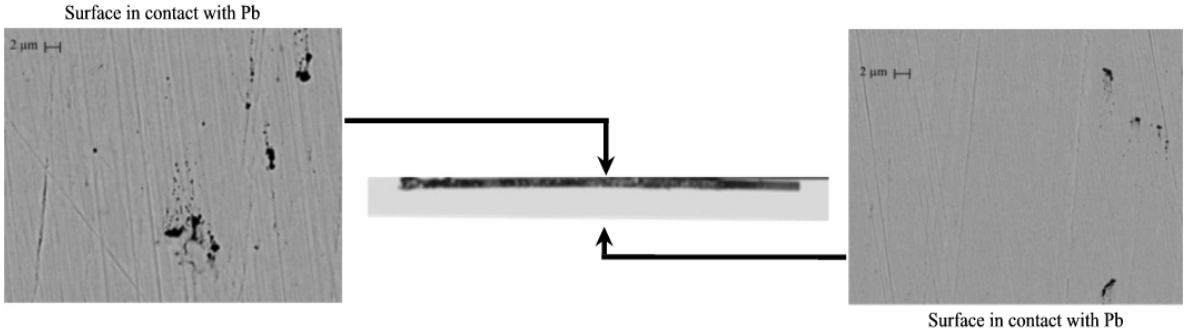

Figure 7.6.2. Volume fraction of cavities in the central cross-section of a FLEXIMEL specimen after 1 month annealing in stagnant liquid lead bath under flowing H_2 at 525 °C (image analysis)

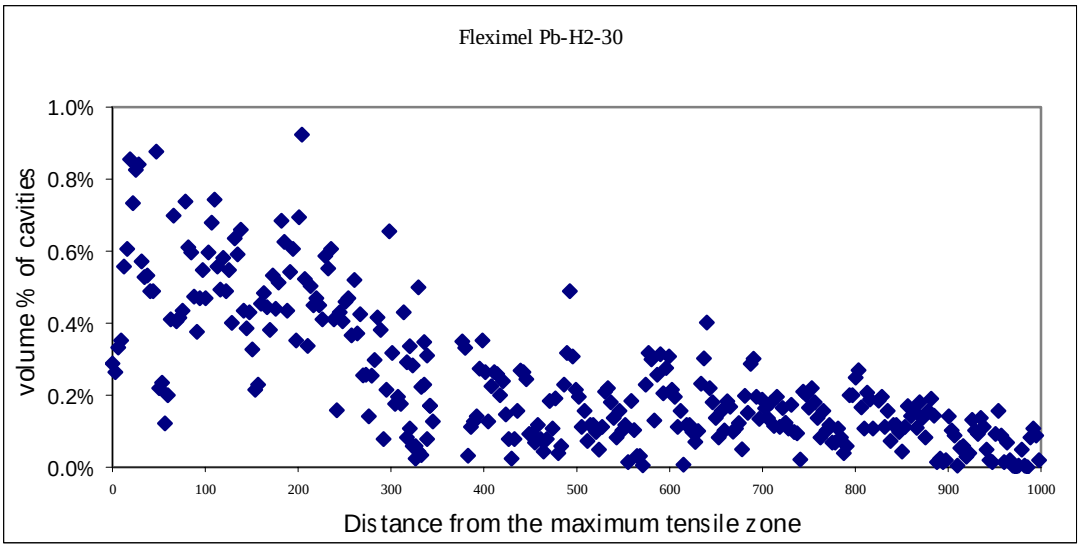

Apparently no such LMAC effect is detected at 380°C, in otherwise identical conditions [Gamaoun, 2003]. The threshold temperature for appearance of an LMAC effect is still missing.

7.6.6 Creep crack growth of T91 and 316L in contact with LBE or lead

There are no data on creep crack growth for T91 or 316L in contact with LBE or lead.

7.7 Fracture mechanics: Case of both austenitic steel of type 316 and ferritic/martensitic steel of type T91 in contact with lead and LBE

There is a large body of literature devoted to the fracture of structural materials, hardened and often embrittled under irradiation, covering a wide range of experimental test conditions. Indeed, this is an information of primary importance, which, for example, allowed for an estimate of the service life of the MEGAPIE target [Dai, 2005].

There is no such information available for structural materials (both T91 and 316L) in contact with HLMs. It is sometimes stated that the ductile to brittle transition temperature, which may increase by approximately one hundred degrees after irradiation, should be only little increased due to contact with HLMs. This is pure conjecture, and must be verified experimentally.

7.8 Recommendations for testing procedures

We begin by listing some of the ASTM standards, which could be useful for mechanical tests in HLMs, in spite of the fact that none of them are valid in such LM environment. We continue with a brief summary of the possible experimental installations, pointing out the drawbacks for each of them. Then we present some recommendations for the mechanical testing procedures, emphasising all that concerns the surface state.

7.8.1 ASTM standards useful for mechanical tests in LBE

Strictly speaking, there is no ASTM standard rigorously applicable in HLM environment. However, we shall recall the ones giving some information useful for our activities.

ASTM E 1457 – 98

Standard test method for measurement of creep crack growth rates in metals.

Aim: Determination of creep crack growth rates in metals at elevated temperature using compact type C(T) specimens subjected to static loading. The crack growth rate da/dt is expressed in terms of the magnitude of a crack tip parameter C*(t). For definitions of C*(T), see Test.

Note that the surface crack length measurement by optical means is not, in principle, considered reliable as a primary but only as an auxiliary method, because of the possibly non-uniform crack extension across the thickness of the specimen.

Table I. Some specifications and conditions of application of ASTM E 1457-98

Applicable	Restricted to materials in which crack growth is accompanied by accumulation of substantial time dependent creep strains at crack tip.
Not applicable	If crack growth controlled by high temperature corrosion. In case of transition creep behaviour leading to transient crack growth behaviour. In case of wide spread creep damage at crack tip.
Specimens	C(T), M(T)[1] *possibly* required: fatigue pre-cracking.
Referenced documents	E139: Test method for conducting creep, creep-rupture and stress-rupture tests of metallic materials. E399[2]:Test method for fracture toughness of metallic materials E616[3]: Terminology related to fracture testing. E647: Test method to measure fatigue crack growth rates.

[1] M(T) = centre cracked tension specimens.
[2] ΔK, the stress intensity factor range, can be calculated using equations in test method E 399.
[3] J-integral = line or surface integral describing the local stress-strain field around the crack front, as described in test method E 616.

Concluding remarks: *Stricto sensu*, the ASTM E1457-98 test is not applicable to quantify creep crack growth rates in case of structural materials in contact with corroding heavy liquid metals like lead and

a fortiori corroding LBE. Nevertheless, the recommendations mentioned in the test method E 1457 will be useful to determine qualitatively the creep crack growth rates of T91 steel wetted/corroded by lead or LBE, under various temperature and loading conditions.

ASTM E 813 – 89 (*discontinued 1998*)

Standard test method for J_{IC}, a measure of fracture toughness.

Aim: Determination of $J_{IC,}$[15] which can be used as an engineering estimate of fracture toughness near the initiation of slow stable crack growth for metallic materials.

Table II. Some specifications and conditions of application of ASTM E 813-89

Applicable	To sufficiently ductile material. Lacking sufficient thickness to be tested for K_{IC} according to test method **E 399**. Displaying ductile slow stable crack growth at test temperature. To evaluate the effects of metallurgical variables, heat treatments and weldments.
Not applicable	In case of predominant environmentally assisted cracking.[4] In case of fast fracture, and especially brittle (cleavage) fracture of steels.
Specimens	Containing notches or flaws, sharpened by fatigue cracks. Recommended: three-point bend specimen SE(B),[1] or C(T) with slow loading rate.
Referenced documents	E 399[2]: Test method for fracture toughness of metallic materials. E 616[3]: Terminology relating to fracture testing. E 1152: Test method for determining J-R curves.

[1] SE(B) = single edge-cracked specimens of length $0.5 \leq a_0/W \leq 0.75$.
[2] ΔK, the stress intensity factor range, can be calculated using equations in test method E 399.
[3] J-integral = line or surface integral describing the local stress-strain field around the crack front, as described in test method E 616. The J_{IC} value is in principle independent of the testing speed in quasi-static regime. Its value becomes a function of testing speed in the dynamic regime.
[4] Environmental attack under sustained stress or cyclic loading can cause crack extension at J values less than J_{IC}.

Concluding remarks: *Stricto sensu*, the ASTM E813-98 test is not applicable to determine the fracture toughness of structural materials in contact with heavy liquid metals like lead or LBE, especially in case wetting could cause sudden brittle failure. Nevertheless, the recommendations mentioned in the test method E 813 will be useful to determine qualitatively the resistance to crack growth of T91 steel wetted/corroded by lead or LBE, under various temperature and loading conditions.

ASTM E 1820 – 99

Standard test method for measurement of fracture toughness, combination of ASTM E 813 for J_{IC} evaluation and ASTM E 1152 for J-R curve evaluation.

Aim: Determination of fracture toughness of metallic materials using the parameters K, J and CTOD (δ). Assuming the presence of a pre-existing sharp fatigue crack, the fracture toughness values identified by this method characterises its resistance to: 1) fracture of a stationary crack; 2) fracture after some stable tearing; 3) stable tearing onset; 4) sustained stable tearing.

Concluding remarks: See those for test method E 813.

[15] J_{IC} designates the line or surface integral characterising the local stress-strain field around the crack tip, near the onset of stable crack growth.

Table III. Some specifications and conditions of application of ASTM E 1820-99

Applicable	"When the material response cannot be anticipated before the test". Useful as a basis for material comparison, selection and quality assurance. Useful as a basis for structural flaw tolerance assessment.
Specimens	C(T), SE(B), DC(T)[1] ; Required: notches sharpened by fatigue cracks
Referenced documents	E 399[2]: Test method for plain-strain fracture toughness of metallic materials. E 813[3]: Test method for J_{1c}, a measure of fracture toughness. E 1152: Test method to determine J-R curves. E 1290: Test method for crack tip opening displacement (CTOD) fracture toughness measurement. E 1737: Test method for J-integral fracture toughness determination. E 1823: Terminology relating to fatigue and fracture testing.

[1] SE(B) = single edge bend; DC(T)= disk-shaped compact.
[2] ΔK, the stress intensity factor range, can be calculated using equations in test method E 399
[3] J-integral = line or surface integral describing the local stress-strain field around the crack front, as described in test method E 616.

ASTM E 1921-05

Standard test method for measurement of reference temperature T_0, which characterises the fracture toughness of a steel that experiences onset of cleavage cracking at elastic, or elastic-plastic KJc instabilities, or both.

Aim: Determination of fracture toughness of metallic materials using the parameter J in the transition temperature region.

Table IV. Some specifications and conditions of application of ASTM E 1921-05

Applicability	To steel that fails by cleavage.
Specimens	C(T), SE(B), DC(T). Required: notches sharpened by fatigue cracks.
Referenced documents	E 399: Test method for plain-strain fracture toughness of metallic materials. E 1823: Terminology relating to fatigue and fracture testing.

7.8.2 Adaptation of experimental installations for HLMs

1) Use an open crucible, containing the test specimen immersed in stagnant LM, which is located within an inert gas cell or glove box. Advantage: inexpensive to build and operate. Drawback: exposure to contaminants…
2) Use a circulating loop; CT and three-point bend specimens can be studied in such installation. The advantage is obvious in case of *in situ* testing; tests are generally conducted *post mortem*; this procedure is convenient provided the tests are conducted at the temperature of exposure to the flowing LM, with layers of liquid metal present on the specimen surface. Otherwise, one should be careful for interpretation of results obtained at room temperature.
3) Use sealed environmental chamber attached to the specimen, that completely surrounds the notch and crack extension plane for compact-type specimens, which contains the LM but does not extend to the region of the loading holes. Advantage: simple and low cost. Drawback: static LM…hence the characteristics of large heat-transport systems (e.g. mass transport due to non-isothermal operation) cannot be studied.
4) Controlled specimen preparation, using surface physics techniques, in order to wet, oxidise, protect or corrode the specimens, particularly notch or pre-cracked area. Advantage: possibility to follow (optically…) the damage evolution, well adapted to understand damage mechanisms. Drawback: impossible to reproduce the conditions of a liquid metal cooling system.

Other additional difficulty in case of conductive liquid metals in contact with conductive structure materials, electric potential methods cannot be adapted. To make a parallel, if one thinks to the electrochemic methods applicable to the study of stress corrosion cracking in aqueous environment, this is again a unique possibility to follow crack propagation that is lost in the case of HLMs like liquid lead or LBE.

For the future, the ultrasonic techniques recently developed to investigate the LM/steel interfaces would be of great interest [Lesueur, 2004].

7.8.3 Recommendations for testing procedures

Are concerned the steel surface and metallurgical preparation prior testing, testing procedure itself with relevant indications possibly given by ASTM standards, and post-test analysis of the specimens. All that concerns the metallurgical preparation prior testing, the heat treatment must be "standardised". We concentrate on the surface preparation conditions and surface state prior and after mechanical testing. Contrary to what is considered mandatory for corrosion studies, OCS is not required for mechanical tests, provided the surface state is followed, using all possible surface analysis methods, over the whole test duration. This includes:

Prior mechanical test

1) Polishing conditions must be made precise: diamond-polishing should be preferred, knowing that electro-polishing is an efficient passivating treatment, which is not the case of manual polishing (SiC or diamond); coarse mechanical grinding should be avoided.
2) General aspect must be made precise: shiny if possible; in case of roughness: the presence of metallurgical defects like inclusions, scratches, presence, distribution and size of superficial pre-cracks (if possible) must be mentioned.
3) Ageing time and conditions (air, cover gas, LBE…) prior testing must be noted:
   - In case of air ageing, it is important to know precisely the ageing time, even if a few hours, since the native oxide on Cr containing steels is evolving very rapidly during the first 24 hours, the first week of ageing, which may have non negligible consequences on the mechanical resistance.
   - In case of direct immersion and ageing in liquid LBE, the oxygen activity in LBE and temperature must be known if possible, if different from that applied during testing.

During mechanical test

Except in some specific cases, in an opaque LM, it is not generally possible to follow the surface state. However, All accessible parameters must be known: temperature, duration of the different test phases, and oxygen content in LM, depending on the test (for slow strain rate tensile test if possible, for creep test and creep crack growth testing…).

During mechanical test, once a crack initiated, it would be important, ideally, to know how LBE fills the crack. It could be of interest to analyse some specimens obtained during interrupted tests. It should be important for creep, fatigue and creep-fatigue testing. This is a hard task, but which could be really helpful in order to interpret the obtained mechanical data, as far as LME or EAC effects are concerned.

Post-test analysis

Surface state analysis is very important for all tests:

1) general aspect including roughness, porosity of surface layers;
2) distribution of cracks (if possible);
3) chemical and (if possible) structural analysis of surface layers (top view and cross-sections).

For Charpy impact testing, this is mandatory, especially if one wants to determine a DBTT shift due to contact with LBE, since we can already infer that the DBTT shift should strongly depend on the contact conditions. Moreover, it could help to quantify the data since the DBTT shift due to LBE is unpredictable, and will be strongly dependent on the contact conditions between the steel and the embrittling species. In case of a wide scattering of data, it could help to determine reliable ones! Moreover, it would help to compare the DBTT shift that could be obtained *in fine* by different laboratories and teams.

In any case, whatever the applied experimental procedure [with tests carried out: 1) in LM; 2) in air after exposure to LM at same temperature; 3) always in air but at room temperature], information on the evolution of fracture toughness or ductile to brittle transition temperature will be of primary importance since there is no data available in the literature, for both T91 and 316L.

For fatigue, creep and tensile tests, post-test surface state analysis is also requested. Analysis of specimens after interrupted tests is requested and could be helpful to improve understanding of LME or EAC.

7.9 Conclusions

The study of the compatibility of structural materials with heavy liquid metals (lead, lead-bismuth eutectic…) represents a non negligible contribution to the international research effort dedicated to the development of accelerator-driven systems and other innovative concepts of LM-cooled fast reactors concepts of Generation IV. It is worth recalling that compatibility means both corrosion and mechanical resistance, possibly in a radiation environment which should be the more representative of the nuclear facilities in project.

If one forgets deliberately the radiation environment, the problem is not so much simplified since the mechanical resistance is largely dependent on the corrosion properties of the system under study. It is worth recalling that the mechanical behaviour of a system will not be fully understood so long as the physicochemical processes occurring in contact with the selected HLM are not known in each experimental situation. They are varied, going from the corrosion-dissolution, corrosion-erosion, or oxide formation at the steel surface, to the formation of surface alloys with the reactive HLM in contact, to the formation of de-alloyed layers (possibly associated with the $\gamma \rightarrow \alpha$ phase transition of austenitic steels in contact with lead alloys) to the reactive or non reactive wetting depending on the miscibility of the solid and liquid phases in contact. In addition, if one recalls that a non-equilibrium steady state is only attainable for a material in contact with a corrosive HLM, one immediately observes that the mechanical resistance may change with the surface state, during ageing. This is certainly the reason why the Russian metallurgists, who can be considered as pioneers in this field, studied the mechanical properties of steels in contact with HLMs, taking two opposite orientations: either the intrinsic mechanical answer was obtained in conditions of direct contact between the two solid and liquid phases, by using the method of the soldering fluxes, or the mechanical answer was

followed in an HLM environment of controlled corrosiveness, thanks to the early development of the oxygen control systems in the former USSR. This orientation was caused by the corrosiveness of lead and lead alloys which may dissolve substantial amounts of oxygen with solubility limits largely varying between 250 and 600°C, i.e. in the temperature range of interest for the nuclear facilities in service or in project.

Another difficulty encountered in this chapter dedicated to the mechanical properties of structural materials in HLMs comes from the variety of the literature sources worldwide (in Russia, Japan, China, Korea…), with no translation, or only partial information available. Let us recall that when the European countries started to work on compatibility of lead and LBE with structural materials in the frame of the ADS project in 1997/1998, the crucial point was the absence of OCS…outside Russia, and the main question how to redevelop this technology. In 2004, the expression for the oxygen solubility limit in lead as function of temperature, proposed by Orlov, is rediscovered and discussed in EU, USA, Japan. In 2006, we are far from this state of the art as concerns the mechanical properties of Cr containing steels in contact with lead and LBE. The Russian expertise in this area is only very partially known.... Apart from the absence of translation of an impressive literature, there is the problem of the steel grades developed in the former USSR, differing from the ones developed outside Russia. One knows that the corrosion properties of a steel is function not only of its major but also largely of the presence of its minor alloying elements. One also knows that the mechanical properties of a given steel grade in a HLM environment will be largely function of its composition, structure and microstructure, which were optimised for a specific application. Consequently, it is a fact that so long as the steel grades, in and outside Russia, will not be compared, not only for their corrosion behaviour but also for they mechanical properties in HLMs, one should be concerned by such a lack of information.

In this chapter, emphasis is put on the austenitic steel of type 316L and on the ferritic/martensitic steel of type T91, which were selected as structural materials for the European ADS project and MEGAPIE target. In such a review, not only the tensile and fatigue properties, but also the creep, the creep-fatigue and fracture properties of both austenitic and ferritic/martensitic steels in contact with lead, lead-bismuth eutectic should have been reported. At the end of this chapter, a certain number of points are noticeable. The study of the tensile properties of T91 in lead and LBE in various experimental conditions revealed that the T91-LBE, and certainly the T91-lead couples are embrittling. However, provided the surface state be protected by an oxide film remaining adherent to the steel surface during long term ageing, the risk of embrittlement should be largely minimised. The T91-LBE couple is also susceptible to EAC, after long-term ageing in reducing LBE. The embrittling character of both the 316L-lead and of the 316L-LBE couples remains to be proved. Fatigue is inherent to any structural component in service. The more significant effects of LBE on the fatigue behaviour of T91 are the following: there is a detrimental effect of LBE on the fatigue crack initiation resistance, vanishing at low strain amplitudes or low stress amplitudes. LBE modifies the mechanism of formation of long fatigue cracks. LBE increases the fatigue crack growth rate. The effect of surface roughness is very important. Corrosion of T91 by LBE, in the dissolution regime, provides defects that are ready to propagate by cyclic loading, provided LBE attains the crack tip. Once a short crack forms in T91 in contact with LBE, it rapidly propagates into the bulk. This entails the need to protect the steel surface. Oxygen in LBE gives rise to an oxide layer that limits the interaction of LBE with short cracks. To the contrary, the low cycle fatigue of 316L stainless steel is only little affected by LBE. Only a weak effect of LBE on the fatigue life was observed, which was not considered as the proof of an embrittling effect. An accelerated plastic strain is observed with T91 in contact with both oxidising and reducing lead or LBE under OCS at the temperature of 525°C. However information is still strongly missing about the creep behaviour of both T91 and 316L in contact with lead or LBE. Likewise, information is completely missing concerning the fracture behaviour of both 316L and T91 in lead and LBE, i.e. the evolution of the ductile to brittle transition temperature, of the fracture

toughness as function of the contact conditions with LBE. The crack growth R resistance curve or the J resistance curves to be determined as functions of the plastic deformation evidenced locally in the crack tip area are also missing.

To terminate this chapter, it is not uninteresting to remark the consensus between all metallurgists confronted to the problem of LME immediately arising when one studies the compatibility of structural materials with HLMs. Today, in absence of an accepted theory of LME, the susceptibility to LME of structural materials being deformed in HLMs is unpredictable. Consequently, to solve practical problems, it is necessary to conduct investigations under conditions imitating or at least approaching the service ones. In all cases, it is recommended to investigate in more details the relationship between the physico-chemical processes occurring at the interface and the deformation and failure of the material, which could be useful for the future development of a physical model of liquid- and solid-metal embrittlement In the future, one should also establish the rules of the origin of cracks and of their development in the presence of liquid media and solid metal films under long static and cyclic loads, and under conditions of mechanical failure to be able to describe properly the cracking process, which is extremely necessary for solutions of practical problems.

This point of view was proposed in the USSR in 1987 by Popovich [Popovich, 1987]. From the point of view of this handbook, it remains valid twenty years later, especially for all that concerns the metallurgical and mechanical factors determining the formation and further evolution of a crack embryo in contact with a liquid metal!

REFERENCES

Abramov, V.Y., S.N. Bozin, O.I. Eliseeva, G.M. Kalinin, V.I. Kalyandruk, E.M. Lyutyi (1994), "Influence of Lead Melt on Plastic Deformation of High-alloyed Heat-resistant Steels", *Materials Science*, 30, pp. 465-469.

Abramov, V.Y., S.N. Bozin, S.V. Evropin, B.S. Rodchenkov, V.N. Leonov, A.I. Filin, V.G. Markov (2004), "Corrosion and Mechanical Properties of BREST-OD-300 Reactor Structural Materials", *Proceedings of the 11th International Conference on Nuclear Engineering (ICONE11 – 36413)*, Tokyo, Japan, 20-23 April 2003, *published in JSME International Journal B* (2003), Vol. 47.

Aiello, A., P. Agostini, G. Benamati, B. Long, G. Scaddozzo (2004), "Mechanical Properties of Martensitic Steels After Exposure to Flowing Liquid Metals", *J. Nuclear Mat.*, 335, 217.

Antipenkov, A., V. Belous, I. Danilov, G. Kalinin, Yu. Makarenkov, G. Markov, V. Rybin, A. Sidorov, G. Shatalov, Yu. Strebkov, V. Vinokurovand, V. Zemlyankin (1991), "Compatibility of Eutectic with Structural Materials", *Fusion Engineering and Design*, 14, pp. 347-351.

ASTM-STP 942 (1988), "Low Cycle Fatigue – Directions for the Future", H.D. Solomon, G.R. Halford, L.R. Kaisand, B.N. Leis (Eds.), ASTM, pp. 329-341.

Auger, T., G. Lorang, S. Guérin, J-L. Pastol, D. Gorse (2004), "Effect of Contact Conditions on Embrittlement of T91 Steel by Lead-bismuth", *J. Nuclear Mat*., 335, pp. 227-231.

Auger, T., G. Lorang (2005), "Liquid Metal Embrittlement Susceptibility of T91 Steel by Lead-bismuth", *Scripta Materialia*, 52, pp. 1323-1328.

Balandin, Yu.F., V.G. Markov (1961), "Structural Materials for Systems with Liquid Metal Coolants", *Sudpromgiz*, Leningrad.

Balandin, Yu.F., I.F. Divisenko (1970), "Strength and Ductility of a Type 12 Khm Heat-resistant Steel in Contact with Liquid Pb-Bi Eutectic", *Fiz. Khim. Mekh. Mater*., 6, pp. 85-89.

Benamati, G., P. Agostini, I. Alessandrini, S. Storai (1994), "Corrosion and Low-cycle Fatigue Properties of AISI 316L in Flowing Pb-17Li", *J. Nuclear Mat*., 212, pp. 1515-1518.

Benamati, G., C. Fazio, I. Ricapito (2002), "Mechanical and Corrosion Behaviour of EUROFER 97 Steel Exposed to Pb-17Li", *J. Nuclear Mat.*, 307-311, pp. 1391-1395.

Bibilashvili, U.K., A.G. Ioltukhovsky, Y.I. Kazennov, M.V. Leont'eva-Smirnova, N.A. Istishov, V.P. Kondrat'ev (1999), "12% Chromium Steels Working Characteristics with Reference to the Conditions of Operating the Core Elements of Reactors Using Lead and Lead-bismuth Coolants", *Proceedings of Heavy Liquid Metal Coolants in Nuclear Technology*, Vol. 2, pp. 737-745, Obninsk.

Bichuya, A.L. (1969), "Effect of Oxide Films on the Corrosion-fatigue Strength of 1Cr18Ni9Ti Steel in Liquid Pb-Bi Eutectic", *Sov. Mater. Sci*., 5, 352-354.

Borgstedt, H.U., M. Grundmann (1986), "The Fracture of Austenitic and Martensitic Steels in Liquid Lithium", *Nuclear Engineering and Design/Fusion*, 3, pp. 273-286.

Borgstedt, H.U., G. Frees, M. Grundmann, Z. Peric (1991), "Corrosion and Mechanical Properties of the Martensitic Steel X18CrMoVNb 12 1 in Flowing Pb-17Li", *Fusion Engineering and Design*, 14, pp. 329-334.

Bryant, K., S. Benerjie (1988), "Embrittlement of Structural Steels and Alloys", *Metallurgiya*, Moscow (Russian translation).

Broc, M., J. Sannier, G. Santarini (1983), "Experimental Studies on the Use of Liquid Lead in a Molten Salt Nuclear Reactor", *Nuclear Technology*, 63, pp. 197-208.

Chatain, D., F. Chabert, V. Ghetta (1993), "New Experimental Setup for Wettability Characterization Under Monitored Oxygen Activity: I. Role of Oxidation State and Defect Concentration on Oxide Wettability by Gold", *J. Am. Ceram. Soc*., 76, pp. 1568-1576.

Chaevskii, M.I., V.I. Likhtman (1962), "The Effect of the Rate of Deformation on the Strength and Plasticity of Carbon Steel in Contact with a Melt of a Low-melting Metal", *Soviet Physics Doklady*, 6, pp. 914-916.

Chaevskii, M.I, A.L. Bichuya (1969), "Eliminating the Weakening Effect of Lead-bismuth Eutectic on Steel by Reducing the Strain Rate", *Sov. Mater. Sci*., 5, pp. 82-84.

Chopra, O.K., D.L. Smith (1983a), "Compatibility of Ferrous Alloys in a Forced Circulation Pb-17Li System", *J. Nuclear Mat.*, 141-143, pp. 566-570.

Chopra, O.K. (1983b), "Effects of Sodium and Lithium Environments on Mechanical Properties of Ferrous Alloys", *J. Nuclear Mat.*, 115, pp. 223-238.

Clegg, R.E. (2001), "A Fluid Flow Based Model to Predict Liquid Metal Induced Embrittlement Crack Propagation Rates", *Eng. Fracture Mechanics*, 68, pp. 1777-1790.

Coen, V., H. Kolbe, L. Orecchia, T. Sasaki (1984), "Stress Corrosion of 1.4914 Steel in Pb-17Li and Liquid Metal Embrittlement (LME) Susceptibility of its Welded Structure", *Proceedings of the 4th International Conf. on Liquid Metal Engineering & Technology*, Vol. 3, 526-1-10, SFEN, Avignon.

Courouau, J-L., P. Deloffre, R. Adriano (2002), "Oxygen Control in Lead-bismuth Eutectic: First Validation of Electrochemical Oxygen Sensors in Static Conditions", *J. Phys. IV*, 12, Pr8-141-153.

Courouau, J-L. (2004), "Electrochemical Oxygen Sensors for On-line Monitoring in Lead-bismuth Alloys: Status of Development", *J. Nuclear Mat.*, 335, pp. 254-259.

Dai, Y., C. Fazio, D. Gorse, F. Gröschel, J. Henry, A. Terlain, J-B. Vogt, T. Auger, A. Gessi (2006), "Summary of the Preliminary Assessment of the T91 Window Performance in the MEGAPIE Conditions", *Proceedings of the International Conference on Accelerator Applications*, Venise, Sept. 2005, forthcoming in *Nuclear Instruments and Methods A*.

Dai, Y., B. Long, F. Gröschel (2006), "Slow Strain Rate Tensile Tests on T91 in Static Lead-Bismuth Eutectic", forthcoming in *Proceedings of IWSMT7*, in a special issue of *J. Nuclear Mat.*

Dmukhovs'ka, I.H., V.V. Popovich (1993), "Influence of Stress Concentrators on the Temperature Dependence of the Liquid Metal Embrittlement of Armco Iron", *Materials Science*, Vol. 29, pp. 501-506.

Dmukhovs'ka, I.H. (1993), "Embrittlement of Armco Iron by Indium at High Temperatures", *Materials Science*, Vol. 29, pp. 596-599.

Dmukhovs'ka, I.H., V.V. Popovich (1995), "Effect of Lithium-lead Eutectic and Hydrogen on the Fatigue Behavior of some Austenitic Alloys", *Materials Science*, 31, pp. 99-104.

Ebrill N., Y. Durandet, L. Strezov (2000), "Dynamic Reactive Wetting and its Role in Hot Dip Coating of Steel Sheet with an Al-Zn-Si Alloy", *Metallurgical and Mater. Trans.*, 31B, 1069.

Espié, L., B. Drevet, N. Eustathopoulos (1994), "Experimental Study of the Influence of Interfacial Energies and Reactivity on Wetting in Metal/oxide Systems", *Metallurgical and Materials Trans.*, 25A, 599-605.

Fazio, C., I. Ricapito, G. Scaddozzo, G. Benamati (2003), "Corrosion Behavior of Steels and Refractory Metals and Tensile Features of Steels Exposed to Flowing PbBi in the LECOR Loop", *J. Nuclear Mat.*, 318, pp. 325-332.

Funaki, S. (Nippon Steel Corp., Japan) (1993), "Environment Embrittlement Evaluation of Metals", Jpn. Kokai Tokkyo Koho, patent written in Japanese, Application: JP 92-80793 19920402. Priority: CAN 120:83053 AN 1994:83053.

Gamaoun, F., M. Dupeux, V. Ghetta, J-L. Pastol, C. Leroux, S. Guérin, D. Gorse (2002), "Influence of Long Term Exposure to Molten Lead on the Microstructure & Mechanical Behavior of T91 Steel", *J. Phys. IV*, 12, Pr8-191-202.

Gamaoun, F. (2003), "Effet de maintiens de longue durée en bain de plomb ou d'eutectique plomb-bismuth liquide sur un acier martensitique à 9%Cr", PhD Thesis, *Institut National Polytechnique de Grenoble*.

Gamaoun, F., M. Dupeux, V. Ghetta, D. Gorse (2004), "Cavity Formation and Accelerated Plastic Strain in T91 Steel in Contact with Liquid Lead", *Scripta Materialia*, 50, 619.

Ghetta,V., F. Gamaoun, J. Fouletier, M. Henault, A. Le Moulec (2001), "Experimental Setup for Steel Corrosion Characterization in Lead Bath", *J. Nuclear Mat.*, 296, pp. 295-300.

Ghetta, V., J. Fouletier, M. Henault, A. Le Moulec (2002), "Control and Monitoring of Oxygen Content in Molten Metals. Applications to Lead and Lead-bismuth Melts", *J. Phys IV*, Vol. 12, Pr8-123-140.

Glasbrenner, H., F. Gröschel, T. Kirchner (2003), "Tensile Tests on MANET II Steel in Circulating Pb-Bi Eutectic", *J. Nuclear Mat.*, 318, pp. 333-338.

Glasbrenner, H., F. Gröschel (2004), "Bending Tests on T91 Steel in Pb-Bi Eutectic, Bi and Pb-Li Eutectic", *J. Nuclear Mat.*, 335, pp. 239-243.

de Gennes, P-G., F. Brochard-Wiart, D. Quéré (2002), "Gouttes, bulles, perles et ondes", Belin (Ed.), Paris.

Glickman, E.E., Yu.V. Goryunov, V.M. Denim, K.Y. Sarychev (1976), "Kinetics and Mechanism of Copper Fracture During Deformation in Surface-active Baths", *Sov. Phys. Journal*, 19, 844-849.

Glickman, E.E., Yu.V. Goryunov (1978), "Mechanisms of Embrittlement by Liquid Metals and Other Manifestations of the Rebinder Effect in Metal Systems", *Fiz. Khim. Mek. Mater*, 14, pp. 20-30.

Glickman, E.E., Yu.V. Goryunov, V.M. Denim (1985), "The Effect of Intercrystalline Internal Absorption of Bismuth on the Intergranular Fracture of Copper in Liquid Bismuth and the Mechanism of Liquid Metal Embrittlement", *Phys. Chem. Mech. Surf*., 2, pp. 3041-3052.

Glickman, E.E. (2000), "Mechanism of Liquid Metal Embrittlement by Simple Experiments: From Atomistics to Life-time", in *Multiscale Phenomena in Plasticity*, J. Lepinoux, *et al.* (Eds.), *Kluwer Academic Publishers* (Dordrecht, The Netherlands), pp. 383-401.

Gordon, P., H.H. An (1982), "The Mechanisms of Crack Initiation and Crack Propagation in Metal-induced Embrittlement of Metals" *Metal. Trans.*, 13A, 457.

Gorse, D. (2000), "Stress Corrosion Cracking: An Electrochemist Point of View" in *Multiscale Phenomena in Plasticity*, J. Lepinoux, *et al.* (Eds.), Kluwer Academic Publishers (Dordrecht, The Netherlands), pp. 425-439.

Gorse-Pomonti, D., V. Russier (2006), "Liquid Metals for Nuclear Applications", *Journal of Non-crystalline Solids*, forthcoming.

Gorynin, I.V., G.P. Karzov, V.G. Markov, V.S. Lavrukhin, V.A. Yakovlev (1999), "Structural Materials for Power Plants with Heavy Metals as Coolants", *Proceedings of the Conference on Heavy Liquid Metal Coolants in Nuclear Technology*, Obninsk, B.F. Gromov (Ed.), Vol. 1, pp. 120-132.

Gorynin, I.V., G.P. Karzov, V.G. Markov, V.A. Yakovlev (2000), "Structural Materials for Atomic Reactors with Liquid Metal Heat-transfer Agents in the Form of Lead or Lead-bismuth Alloy", *Metal Science and Heat Treatment*, Vol. 41, pp. 384-388.

Goryunov, Yu.V., G.I. Den'shchikova, L.S. Soldatchenkova, B.D. Summ (1978), "The Intermittent Growth of Cracks in Single Crystals of Zinc During Strain at a Contact with Mercury and Gallium", *Sov. Phys. Dokl*., 23, 683-684.

Griffith, A.A. (1920), *Phil. Trans. Roy. Soc*., A 221, 163.

Gromov, B.F., Yu.S. Belomitcev, E.I. Yefimov, M.P. Leonchuk, P.N. Martinov, Yu.I. Orlov, D.V. Pankratov, Yu.G. Pashkin, G.I. Toshinsky, V.V. Chekunov, B.A. Shmatko, V.V. Stepanov (1997), "Use of Lead-bismuth Coolant in Nuclear Reactors and Accelerator-driven Systems", *Nuclear Engineering and Design*, 173, 207.

Guérin, S., J-L. Pastol, C. Leroux, D. Gorse (2003), "Synergy Effect of LBE and Hydrogenated Helium on Resistance to LME of T91 Steel Grade", *J. Nuclear Mat.*, 318, pp. 339-347.

Guttmann, M (1997), "Metallurgy, Properties and Ageing Behaviour of High-Cr Steels for Potential Use in Hybrid Nuclear Reactors", *GEDEON Workshop on Materials for Hybrid Systems,* Paris, 24 September 1997.

Halford, G.R. (1997), "Creep-fatigue Interaction, Heat Resistant Materials", *ASM International 1997*, pp. 499-517.

Handbook of Chemistry and Physics, 46th Edition, R.C. Weast, S.M. Selby, C.D. Hodgman (Eds.), The Chemical Rubber Co., Cleveland, 1965-1966.

Hättestrand, M., H-O. Andrén (2001), "Influence of Strain on Precipitation Reactions During Creep of an Advanced 9% Chromium Steel", *Acta Materialia*, 49, pp. 2123-2128.

Huthmann, H., G. Menken, H.U. Borgstedt, H. Tas (1980), "Influence of Flowing Sodium on the Creep Rupture and Fatigue Behaviour of Type 304 SS at 550°C", *Proceedings of the 2nd International Conference on Liquid Metal Technology in Energy Production*, Richland, Washington, 20-24 April, pp. 19-33.

Ina, K., H. Koizumi (2004), "Penetration of Liquid Metals into Solid Metals and Liquid Metal Embrittlement", *Mater. Sci. Eng*., A 387-389, pp. 390-394.

De Jonghe, V., D. Chatain (1995), "Experimental Study of Wetting Hysteresis on Surfaces with Controlled Geometrical and/or Chemical Defects", *Acta Mater*., 43, 1505-1515.

Joseph, B., M. Picat, F. Barbier (1999), "Liquid Metal Embrittlement: A State-of-the-art Appraisal", *Eur. Phys. J. AP*., 5, pp. 19-31.

Kalkhof, D., M. Grosse (2003), "Influence of PbBi Environment on the Low-cycle Fatigue Behavior of SNS Target Container Materials", *J. Nuclear Mat.*, 318, pp. 143-150.

Kamdar, M.H. (1973), "Embrittlement by Liquid Metals", *Prog. Mater. Sci*., 15, pp. 289-372.

Kanetani, K., Inoue, H. (Nippon Steel Corp., Japan) (1992), "Steels Resistant to Brittle Fracture in Molten Lead", Jpn. Kokai Tokkyo Koho, patent written in Japanese, Application: JP 90-280039 19901018. Priority: CAN 117:237822 AN 1992:637822.

Kano, S., T. Maruyama, T. Ito, Y. Wada, I. Nihei, M. Usami, H. Tanabe, Y. Himeno (PNC-OEC, Japan) (1987), "In-air Mechanical Properties and Sodium Compatibility of Mod.9Cr-1Mo Steel for Large Scale Fast Breeder Reactor", 536, pp. 1-10.

Kashtanov, A.D., V.S. Lavrukhin, V.G. Markov, V.A. Yakovlev, S.N. Bozin, V.N. Leonov, B.S. Rodchenkov, A.I. Filin (2004), "Corrosion-mechanical Strength of Structural Materials in Contact with Liquid Lead", *Atomic Energy*, 97, pp. 538-542.

Klueh R.L., D.R. Harries (2001), "High-chromium Ferritic and Martensitic Steels for Nuclear Applications", *ASTM stock number MONO3*, pp. 113-121.

Kurata, Y., T. Takizuka, T. Osugi, H. Takano (2002), "The Accelerator Driven Strategy in Japan", *J. Nuclear Mat*., 301, pp. 1-7.

Kurata, Y., private communication.

Leger, L., F.J. Joanny (1992), "Liquid Spreading", *Rep. Prog. Phys*., pp. 431-486.

Legris, A., G. Nicaise, J-B. Vogt, J. Foct, D. Gorse, D. Vançon (2000), "Embrittlement of a Martensitic Steel by Liquid Lead", *Scripta Mater.*, 43, pp. 997-1001.

Legris, A., G. Nicaise, J-B. Vogt, J. Foct (2002), "Liquid Metal Embrittlement of the Martensitic Steel T91: Influence of the Chemical Composition of the Liquid Metal; Experiments and Electronic Structure Calculations", *J. Nuclear Mat*., 301, pp. 70-76.

Lesueur, C., D. Chatain, C. Bergman, P. Gas, F. Baque (2002), "Analysis of the Stability of Native Oxide Films at Liquid Lead/Metal Surfaces", *J. Phys IV*, Vol. 12, Pr8-155.

Lesueur, C. (2004), "Contribution à l'étude de la propagation des ultrasons à une interface liquide – solide composite", PhD thesis from *L'université d'Aix – Marseille III*.

Likhtman, V.I., P.A. Rebinder, G.V. Karpenko (1954), "Influence of Surface-Active Media on Deformation of Metals", *Akad. Nauk SSSR*, Moscow (in Russian).

Likhtman, V.I., E.D. Shchukin (1958), "Physico-chemical Phenomena in the Deformation of Metals", *Usp. Fiz. Nauk*, 66, pp. 213-245.

Likhtman, V.I., E.D. Shchukin, P.A. Rebinder (1962), "The Physico-chemical Mechanics of Metals", *Izd. Akad. Nauk SSSR*, Moscow.

Loewen, Eric P., Akira Thomas Tokuhiro (2003), "Status of Research and Development of the Lead-alloy-cooled Fast Reactor", *J. Nuclear Science and Technology*, 40, pp. 614-627.

Mae, T., S. Hori (1991), "Liquid-metal Embrittlement of Aluminium by Several Eutectic Alloys Containing Zinc", *J. Mater. Sci*., 26, pp. 479-483.

Maitre, A., J-M. Fiorani, J-J. Kuntz, J-C. Gachon (2002), "Preliminary Study of some Parts of the Quinary System Bi-Fe-Hg-O-Pb", *J. Phys IV*, Vol. 12, Pr8-163-174.

Maitre, A., M. François, J-C. Gachon (2004), "Experimental Study of the Bi_2O_3-Fe_2O_3 Pseudo-binary System", *J. Phase Equilibria and Diffusion*, 25, pp. 59-67.

Maitre, A. (2005), "Transformations de phases dans quelques systèmes réactifs métalliques et céramiques: aspects thermodynamiques et cinétiques", *Habilitation à Diriger les Recherches de l'Université Henri Poincaré, Nancy I*, 24 January 2005.

Manly, W.D., A. Brasunas (1954) "Interim Report on Static Liquid-metal Corrosion", report from ORNL, Metallurgy Division.

Medina-Almazan, L., J-C. Rouchaud, T. Auger, D. Gorse, "Wetting of Iron-base Alloys by Mercury at Room Temperature", submitted to *J. Nuclear Mat.*

Medina-Almazan, L., D. Gorse, T. Auger (2006), "Embrittlement of Structural Materials like 316L and T91 by Mercury at Room Temperature", submitted to *Acta Materialia*.

Mishra, M.P., C.C. Packiaraj, S.K. Ray, S.L. Mannan, H.U. Borgstedt, "Influence of Sodium Environment and Load Ratio (r) on Fatigue Crack Growth Behaviour of a Type 316LN Stainless Steel at 813 K", *Int. J. Pres. Ves. & Piping*, 70, pp. 77-82.

Naidich, Ju.V. (1981), "The Wettability of Solids by Liquid Metals", *Progress in Surface and Membrane Science*, Vol. 14, pp. 353-484.

Nakae, H., H. Fujii, K. Sato (1992), "Reactive Wetting of Ceramics by Liquid Metals", *Materials Transactions JIM*, 33, pp. 400-406.

Nicaise, G., A. Legris, J-B. Vogt, J. Foct (2001), "Embrittlement of the Martensitic Steel T91 Tested in Liquid Lead", *J. Nuclear Mat.*, 296, 256-264.

Nicholas, M.G., C.F. Old (1979), "Review Liquid Metal Embrittlement", *J. Mater. Sci.*, 14, 1-18.

Nicholas, M.G., C.F. Old, B.C. Edwards (1981), "A Summary of the Literature Describing Liquid Metal Embrittlement", Materials Development and Metallurgy Division, AERE Harwell, *AERE – 9199* (Revised).

Nicholas, M.G. (1982), "A Survey of Literature on Liquid Metal Embrittlement of Metals and Alloys", in *Embrittlement by Liquid and Solid Metals*, M.H. Kamdar (Ed.), St. Louis, *TMS-AIME*, pp. 27-50.

Nifenecker, H., O. Meplan, S. David (2003), "Accelerator Driven Subcritical Reactors", R.R. Betts, W. Greiner (Eds.), Institute of Physics Publishing, Bristol and Philadelphia, ISBN 0 7503 0743 9.

Nikitin V.I. (1967), "Physicochemical Phenomena in the Interaction of Liquid and Solid Metals", *Atomizdat*, Moscow (in Russian).

Nikolaev, V.A., Yu.A. Utkin (1979), "High-temperature Radiation Embrittlement of Austenitic Steel with an Increased Content of Low-melting Impurities", *Izvestiya Akademii Nauk SSSR, Metally* (1), 171-5 (in Russian).

Nikolin, E.S., G.V. Karpenko (1968), "Effect of Liquid Low-melting Metals on the Fatigue Strength of Carbon Steel in Relation to the Stress Frequency", *Sov. Mater. Sci.*, 4, pp. 15-17.

Novakovic, R., E. Ricci, D. Giuranno, F. Gnecco (2002), "Surface Properties of Bi-Pb Liquid Alloys", *Surface Sci.*, 515, pp. 377-389.

Passerone, A., E. Ricci (1998), "High Temperature Tensiometry", in *Drops and Bubbles in Interfacial Research*, D. Möbius and R. Miller (Eds.), Elsevier, Amsterdam, pp. 475-524.

Pastol, J-L., S. Guérin, S.B. Goryachev, D. Gorse, F. Gamaoun, M. Dupeux, V. Ghetta (2002), "Resistance to Corrosion and Embrittlement of T91 Steel in Stagnant Pb-Bi of Eutectic Composition", *J. Phys. IV*, 12, Pr8-203-216.

Pokrovskii, N.L., P.P. Pugachevich, N.A. Golubev (1969), *Russian J. Phys. Chem.*, 43, 1212.

Popovich,V.V., I.G. Dmukhovskaya (1978), "Rebinder Effect in the Fracture of Armco Iron in Liquid Metals", *Sov. Mater. Sci.*, 14, pp. 365-370.

Popovich, V.V. (1979), "Mechanisms of Liquid Metal Embrittlement", *Sov. Mater. Sci.*, 15, pp. 438-445.

Popovich, V.V., I.G. Dmukhovskaya (1983), "Liquid Metal Embrittlement of Deformable Metals", Preprint N°69, Karpenko Physico-mechanical Institute, Ukrainian Academy of Sciences, L'viv.

Popovich, V.V., I.G. Dmukhovskaya (1987), "The Embrittlement of Metals and Alloys Being Deformed in Contact with Low-melting Alloys (A Review of the Foreign Literature)", *Fiz. Khim. Mekh. Mater*., 23, N°6, 3.

Potak, Y.M., I.M. Shchlegakov (1955a), *Zhur. Tech. Fiz*., 25, 897.

Potak, Y.M. (1955b), "The Brittle Failure of Steels and Steel Parts", *Oborongiz* (in Russian).

Protsenko, P., N. Eustathopoulos (2005), "Surface and Grain Boundary Wetting of Fe-based Solids by Molten Pb and Pb-Bi Eutectic", *J. Mater. Sci*., 40, 2383-2387.

Rabkin, E. (2000), "Grain Boundary Embrittlement by Liquid Metals", in *Multiscale Phenomena in Plasticity*, J. Lepinoux, *et al.* (Eds.), Kluwer Academic Publishers (Dordrecht, The Netherlands), pp. 403-413.

Rebinder, P.A. (1928), "Investigation of the Influence of the Surface Energy of a Crystal on its Mechanical Properties when the Surface Tension of its Faces is Lowered by the Introduction of Surface-active Substances into the Working Medium", *Proceedings of the 6th Conference of Russian Physicists*, compendium of lectures, *Gosizdat*, Moscow, pp. 29-30 (in Russian).

Rebinder, P.A., E.D. Shchukin (1972), "Surface Phenomena in Solids in the Processes of Their Deformation and Failure", *Usp. Fiz. Nauk*, 108, pp. 3-42.

Rebinder, P.A., E.D. Shchukin (1972), *Progress in Surface Science*, Vol. 3, N°2, SG. Davison (Ed.) Pergamon Press, Oxford, p. 97.

Robertson, W.M. (1966), "Propagation of a Crack Filled with Liquid Metal", *Trans. Met. Soc. AIME*, 236, pp. 1478-1482.

Rostoker, W., J.M. McCaughey, H. Markus (1960), "Embrittlement by Liquid Metals", *Reinhold Publishing Corporation*, New York.

Rubbia, C., J-R. Rubio, S. Buono, F. Carminati (1995), *Conceptual Design of a Fast Neutron Operated High Power Energy Amplifier*, CERN/AT/95-44(ET), 29 September 1995.

Saiz, E., A.P. Tomsia, R.M. Cannon (1998), "Ridging Effects on Wetting and Spreading of Liquid on Solids", *Acta Mater*, 46, pp. 2349-2361.

Saiz, E., R.M. Cannon, A.P. Tomsia (2000), "Reactive Spreading: Adsorption, Ridging and Compound Formation", *Acta Mater*, 48, pp. 4449-4462.

Sample, T., H. Kolbe (2000), "Liquid Metal Embrittlement (LME) Susceptibility of the 8-9% Cr Martensitic Steels F82H-mod., OPTIFER IVb and Their Simulated Welded Structures in Liquid Pb-17Li", *J. Nuclear Mat.*, 283-287, pp. 1336-1340.

Sannier, J., G. Santarini (1982), "Etude de la corrosion de deux aciers ferritiques par le plomb liquide circulant dans un thermosiphon; recherché d'un modèle", *J. Nuclear Mat.*, 107, pp. 196-217.

Santarini, G., private communication.

Sapundjiev, D., A. Al Mazouzi, S. Van Dyck (2006), "Effects of Liquid Lead Bismuth Eutectic on the Mechanical Properties of A316L and T91 Materials", forthcoming in *Proceedings of EUROCORR 2005*, Lisbon.

Sapundjiev, D., J. Van den Bosch, A. Al Mazouzi (2006), forthcoming in *Proceedings of EUROCORR 2005*, Lisbon.

Sasa, T., H. Oigawa, K. Tsujimoto, K. Nishihara, K. Kikuchi, Yu. Kurata, S. Saito, M. Futakawa, M. Umeno, N. Ouchi, Ya. Arai, K. Minato, H. Takano (2004), "Research and Development on Accelerator-driven Transmutation at JAERI", *Nuclear Engineering and Design*, 230, pp. 209-222.

Shchukin, E.D. (1977), "Environmentally Induced Lowering of Surface Energy and the Mechanical Behavior of Solids", in *Surface Effects in Crystal Plasticity*, R. Latanision, J. Fourie (Eds.), *NATO ASI Series E 317*, Nordhoff, Leyden, pp. 701-736.

Shchukin, E.D. (1999), "Physical-chemical Mechanics in the Studies of P.A. Rehbinder and his School", *Colloids and Surfaces A*, 149, pp. 529-537.

Soldatchenkova, L.S., Yu.V. Goryunov, G.I. Den'shchikova, Z.M. Polukarova, B.D. Summ, E.D. Shchukin (1972), "Effect of an Artificial Defect in a Layer Near the Surface on the Ductility of Zinc Single Crystals in the Presence of Mercury", *Soviet Physics Doklady*, 17, pp. 253-256.

Solonin, M.I., A.G. Ioltukhovskii, Yu.K. Bibilashvili, M.V. Leont'eva-Smirnova, E.A. Medvedeva, N.M. Mitrofanova, Y.P. Budanov, V.M. Chernov, A.V. Tselishchev (2001), "Problems in the Development and Modification of Stainless Steels for Components of Cores of Fast Neutron Nuclear Reactors and a Fusion Reactor", *Fizika i Khimiya Obrabotki Materialov*, 5, pp. 5-13 (in Russian).

Stoloff, N.S. (1982), "Metal Induced Embrittlement – A Historical Perspective", in *Embrittlement by Liquid and Solid Metals*", M.H. Kamdar (Ed.), USA.

Strizak, J.P., J.R. Distefano, P.K. Liaw, H. Tian (2001), "The Effect of Mercury on the Fatigue Behavior of 316 LN Stainless Steel", *J. Nuclear Mat.*, 296, pp. 225-230.

Strizak, J.P., L.K. Mansur (2003), "The Effect of Mean Stress on the Fatigue Behavior of 316LN Stainless Steel in Air and Mercury", *J. Nuclear Mat.*, 318, pp. 151-156.

Svoboda, J., V. Sklenicka (1990), "Fractographic Study of Creep Cavitation in Nickel", *Scripta Metallurgica et Materialia*, 24, pp. 779-782.

Tanaka, M., H. Fukunaga (1969), "Fatigue Strength of Mild Steel, 13 Cr Steel and 18 Cr-8 Ni Steel Subjected to Elevated Temperatures and to Contact with Liquid Pb and Sn", *J. Soc. Material Sci. Jpn.*, 18, 186.

Tian, H., P.K. Liaw, J.P. Strizak, L.K. Mansur (2003), "Effects of Mercury on Fatigue Behavior of Type 316LN Stainless Steel: Application in the Spallation Neutron Source", *J. Nuclear Mat.*, 318, pp. 157-166.

Toloczko, M.B., F.A. Garner (1996), "Radiation Creep, Related to Void Swelling, is Apparently Independent of the Crystal Structure (b.c.c or f.c.c) in Iron-base Alloys", *J. Nuclear Mat*, 233, 289.

Verleene, A., J-B. Vogt, I. Serre, A. Legris (2006), "Low Cycle Fatigue Behaviour of T91 Martensitic Steel at 300°C in Air and Liquid Lead Bismuth Eutectic", submitted to *Int. J. Fatigue*.

Vogt, J-B., G. Degallaix, J. Foct (1988), "Cyclic Mechanical Behavior and Microstructure of a 12Cr-Mo-V Martensitic Stainless Steel", *Fatigue Fract. Eng. Mater. Struct*., 11, pp. 435-446.

Vogt, J-B., G. Nicaise, A. Legris, J. Foct (2002), "The Risk of Liquid Metal Embrittlement of the Z10CDNbV 9-1 Martensitic Steel", *J. Phys. IV*, Vol. 12, Pr8-217-225.

Vogt, J-B., A. Verleene, I. Serre, A. Legris (2004), "Mechanical Behaviour of the T91 Martensitic Steel Under Monotonic and Cyclic Loadings in Liquid Metals", *J. Nuclear Mat.*, 335, 222-226.

Vogt, J-B., A. Verleene, I. Serre, F. Balbaud-Célérier, A. Terlain (2006), "Coupling Effects Between Corrosion and Fatigue in Liquid Pb-Bi of T91 Martensitic Steel", to be published in *Proceedings of EUROCORR 2005*, Lisbon.

Warke, W.R., K.L. Johnson, N.N. Breyer (1970), "Liquid Metal Embrittlement of Steel by Lead and Lead Alloys", in *Corrosion by Liquid Metals*, J.E. Draley, J.R. Weeks (Eds.), Plenum Press, pp. 417-439.

Westwood, A.R.C., M.H. Kamdar (1963), "Concerning Liquid Metal Embrittlement, Particularly of Zinc Monocrystals by Mercury", *Phil. Mag*., 8, pp. 787-803.

Wolski, K., V. Laporte, N. Marie, M. Biscondi (2002), "Liquid Metal Embrittlement Studies on Model Systems with Respect to the Spallation Target Technology: The Importance of Nanometer-thick Films", *J. Phys IV*, Pr8-249-261.

Yachmenyov, G.S., A.Ye. Rusanov, B.F. Gromov, Yu.S. Belomytsev, N.S. Skvortsov, A.P. Demishonkov (1999), "The Problems of Structural Materials Corrosion in Lead-bismuth Coolants", *Proceedings of the Conference on Heavy Liquid Metal Coolants in Nuclear Technology*, Obninsk, B.F. Gromov (Ed.), Vol. 1, pp. 133-140.

Yoshida, H., T. Shige, M. Hasegawa, M. Enoeda, Y. Naruse (1992), *Preliminary Test of Liquid Metal Embrittlement in Liquid LiPb and Stainless-steel Systems*, Report *JAERI-M-92-066*, Order N°Des93753130.

Young, T. (1805), *Phil. Trans. Soc. London*, 95, 65.

Chapter 7 Annex

Table 7.4.1. Tensile behaviour of smooth and notched specimens of T91 in HLMs, as function of specimen preparation

Material	T_{test} (°C)	Specimen preparation and heat treatment	Environmental testing conditions	Strain rate	Mechanical data *(see definitions below)*	Remarks	Ref.
T91	20	Smooth cylindrical specimen: 20 mm gauge length 4 mm diameter Normalised at 1050°C (1 h) Tempered at 750°C (1 h)	Air	4. 10^{-3} s^{-1}	$\sigma_{0.2}$ = 500 MPa σ_{TS} = 650 MPa A(%) = 25	• Ductile fracture surface.	[Verleene, 2006]
T91	300		Air	4. 10^{-3} s^{-1}	$\sigma_{0.2}$ = 450 MPa σ_{TS} = 570 MPa A(%) = 20	• No pre-wetting procedure. • No embrittlement of T91 by Pb under air. • Ductile fracture surface.	
T91	300		Lead under air (no OCS)	4. 10^{-3} s^{-1}	$\sigma_{0.2}$ = 440 MPa σ_{TS} = 550 MPa A(%) = 19		
T91	350	Smooth cylindrical specimen: 20 mm gauge length 4 mm diameter Electro-polished Normalised at 1050°C (1 h) tempered at 750°C (1 h)	Air	10^{-4} s^{-1}	$\sigma_{0.2}$ = 350 MPa σ_{TS} = 520 MPa A(%) = 22	• No pre-wetting procedure. • No embrittlement of T91 by Pb under air. • Ductile fracture surface.	[Legris, 2000]
T91	350		Lead under air (no OCS)	10^{-4} s^{-1}	$\sigma_{0.2}$ = 350 MPa σ_{TS} = 520 MPa A(%) = 22		
T91	350	Same as above, except tempering at 500°C (1 h)	Air	10^{-4} s^{-1}	$\sigma_{0.2}$ = 900 MPa σ_{TS} = 1250 MPa A(%) = 15	• No pre-wetting procedure. • Same conclusions as above. • Sole effect of hardening heat treatment: reduction of elongation to rupture. • The fracture remains fully ductile.	[Legris, 2000]
T91	350		Lead under air (no OCS)	10^{-4} s^{-1}	$\sigma_{0.2}$ = 900 MPa σ_{TS} = 1250 MPa A(%) = 15		
T91	350	Notched specimen: notch of 0.5 mm depth and 0.25 mm root radius 20 mm gauge length 4 mm diameter Electro-polished Normalised at 1050°C (1 h) Tempered at 750°C (1 h)	air	2 µm/s	–	• Same as above. • Sole effect of notch: reduction of elongation to fracture. • Ductile fracture surface.	[Legris, 2000]
T91	350		Lead under air (no OCS)	2 µm/s	–		
T91	350	Notched specimen: as described above Normalised at 1050°C (1 h) Tempered at 500°C (1 h)	Air	2 µm/s		• Ductile fracture in air.	[Legris, 2000]
T91	350		Lead under air (no OCS)	2 µm/s		• Brittle (transgranular) facture of hardened T91(by tempering at 500°C) in Pb, in spite of the presence of an oxide film on T91, confirmed by SEM.	

Table 7.4.1. Tensile behaviour of smooth and notched specimens of T91 in HLMs, as function of specimen preparation (*cont.*)

Material	T_{test} (°C)	Specimen preparation and heat treatment	Environmental testing conditions	Strain rate	Mechanical data *(see definitions below)*	Remarks	Ref.
T91	20	Notched specimen: notch of 0.5 mm depth and 0.20 mm root radius 20 mm gauge length 4 mm diameter Normalised at 1050°C (1 h) Tempered at 500°C (1 h)	Air	2 μm/s		• The fracture surface of notched and hardened specimens tested *in air and in Hg at 20*°C is brittle, showing a transgranular fracture in both cases.	[Nicaise, 2001]
T91	20		Hg under air (no OCS)	2 μm/s			
T91	260		Air	2 μm/s		• Ductile fracture in air. • Brittle transgranular fracture of notched and hardened specimens at 260°C tested in LBE or in Sn.	[Nicaise, 2001] [Legris, 2002]
T91	260		LBE under air (no OCS)	2 μm/s			
T91	260		Sn under air (no OCS)	2 μm/s			
T91	350	Notched specimen: notch of 0.5 mm depth and 0.20 mm root radius 20 mm gauge length 4 mm diameter Normalised at 1050°C (1 h) Tempered at 500°C (1 h)	air	2 μm/s	$E_{fracture}$ = 4 J	• For notched and hardened specimens of T91 in contact with Pb in air, there is a ductility trough extending from 350 to 425°C for a displacement velocity of 2 μm/s. • *We shall see below that the ductility trough is function of the strain rate.*	[Vogt, 2002]
T91	350		Lead under air (no OCS)	2 μm/s	$E_{fracture}$ = 1.2 J		
T91	375		Lead under air (no OCS)	2 μm/s	$E_{fracture}$ = 1.2 J		
T91	400		Lead under air (no OCS)	2 μm/s	$E_{fracture}$ = 1.6 J		
T91	425		Lead under air (no OCS)	2 μm/s	$E_{fracture}$ = 3 J		
T91	450		Lead under air (no OCS)	2 μm/s	$E_{fracture}$ = 3.5 J		
T91	450		Air	2 μm/s	$E_{fracture}$ = 3.6 J		

$E_{fracture}$: area under the load versus cross head-displacement curve.

Table 7.4.2. Tensile behaviour of notched specimens of T91 in LBE under vacuum or hydrogenated helium

Material	T_{test} (°C)	Specimen preparation and heat treatment	Environmental testing conditions	Strain rate	Mechanical data *(see definitions below)*	Remarks	Ref.
T91	300	15 mm gauge length 4 mm diameter Diamond polished	Vacuum	$1.7\ 10^{-5}$ $3.0\ 10^{-4}$ $6.7 10^{-3}$	A^* = 135, E_{crack} = 3.3 J, UTS = 1000 A^* = 152, E_{crack} = 3.8 J, UTS = 1000 A^* = 162, E_{crack} = 4.1 J, UTS = 1000		[Guerin, 2003]
T91	350	Notched specimen: V-shaped 60° notch of 0.6 mm depth and 0.25 mm root radius Normalised at 1050°C (1 h) Tempered at 750°C (1 h)	Vacuum	$1.7\ 10^{-5}$ $6.7 10^{-5}$ $6.7 10^{-4}$ $6.7 10^{-3}$	A^* = 128, E_{crack} = 3.2 J, UTS = 1010 A^* = 150 ,E_{crack} = 3.6 J, UTS = 970 A^* = 153, E_{crack} = 3.8 J, UTS = 970 A^* = 141, E_{crack} = 3.4 J, UTS = 970		
T91	350		LBE under vacuum	$1.7\ 10^{-5}$ $6.7 10^{-5}$ $6.7 10^{-4}$ $6.7 10^{-3}$	A^* = 142, E_{crack} = 3.45 J, UTS = 990 A^* = 147, E_{crack} = 3.55 J, UTS = 985 A^* = 143, E_{crack} = 3.5 J, UTS = 965 A^* = 149, E_{crack} = 3.6 J, UTS = 845	• No direct contact between T91 and LBE under present vacuum conditions. • Correlatively there is no observable degradation of the tensile behaviour.	[Guerin, 2003]
T91	300	15 mm gauge length 4 mm diameter Diamond polished	Stagnant LBE under He + 4%H_2	$1.7\ 10^{-5}$ $6.7 10^{-5}$ $6.7 10^{-4}$ $6.7 10^{-3}$	A^* = 120, E_{crack} = 2.7 J, UTS = 945 A^* = 124, E_{crack} = 2.8 J, UTS = 935 A^* = 134, E_{crack} = 3.2 J, UTS = 940 A^* = 154, E_{crack} = 3.4 J, UTS = 880	• The degradation of the mechanical properties depends on the deformation rate against oxidation rate. • The ductility trough, visible on the plot of energy to rupture vs. strain rate is pronounced at 350°C. • At 300°C the minimum ductility is just attained at $1.7\ 10^{-5}$ mm s^{-1}.	[Guerin, 2003]
T91	350	Notched specimen: V-shaped 60° notch of 0.6 mm depth and 0.25 mm root radius		$1.7\ 10^{-5}$ $6.7 10^{-5}$ $6.7 10^{-4}$ $6.7 10^{-3}$	A^* = 132, E_{crack} = 3.0 J, UTS = 900 A^* = 120, E_{crack} = 2.5 J, UTS = 900 A^* = 116, E_{crack} = 2.6 J, UTS = 880 A^* = 140, E_{crack} = 3.0 J, UTS = 870		
T91	400	Normalised at 1050°C (1 h) Tempered at 750°C (1 h)		$1.7\ 10^{-5}$ $6.7 10^{-5}$ $6.7 10^{-4}$ $6.7 10^{-3}$	A^* = 148, E_{crack} = 3.1 J, UTS = 840 A^* = 148, E_{crack} = 3.3 J, UTS = 885 A^* = 116, E_{crack} = 2.4 J, UTS = 870 A^* = 126, E_{crack} = 2.8 J, UTS = 890		

A^* = Maximum cross-head displacement divided by initial notch length (in %).
E_{crack} = area under the load versus cross head-displacement curve (J).
UTS = maximum load divided by the initial notched section (2.8 mm diameter) (MPa).

Table 7.4.3. Tensile behaviour of smooth or rough T91 steel specimens in oxygen saturated LBE

Material	T (°C)	Specimen preparation and heat treatment	Environmental testing conditions	Strain rate	Mechanical data	Remarks	Ref.
T91	200	Cylindrical smooth specimen: 15 mm gauge length 4 mm diameter Diamond polishing Normalised at 1050°C (1 h) Tempered at 750°C (1 h)	Vacuum	$1.7\ 10^{-3}$	$\sigma_{0.2}$ = 540 MPa σ_{TS} = 675 MPa A(%) = 22 ± 1	• On smooth oxidised specimens of T91, LBE has no detrimental influence on the tensile behaviour at 300°C. • See [Legris, 2000].	[Pastol, 2002]
T91	200		Oxygen saturated LBE under vacuum	$1.7\ 10^{-3}$	$\sigma_{0.2}$ = 540 MPa σ_{TS} = 675 MPa A(%) = 23 ± 1		
T91	300			$3.3\ 10^{-4}$	$\sigma_{0.2}$ = 540 MPa σ_{TS} = 650 MPa A(%) = 20 ± 1		
T91	350			$1.7\ 10^{-2}$	$\sigma_{0.2}$ = 515 MPa σ_{TS} = 610 MPa A(%) = 20 ± 1		
T91	300	Flat specimen: $5 \times 1.5 \times 0.75$ mm^3 in gauge section Prepared by EDM cutting + electropolishing + mechanical polishing	Oxygen saturated LBE	10^{-5}	$\sigma_{0.2,300}$ = 420 MPa $\sigma_{TS,300}$ = 550 MPa $\sigma_{crack,300}$ ~ 400 MPa	• Electro-polishing not only removes the flaws produced as a result of EDM cutting but also passivates efficiently the T91 steel specimens. • Consequently electropolishing may prevent a possible embrittling effect of LBE.	[Dai, 2006]
T91	375			10^{-5}	$\sigma_{0.2,375}$ = 400 MPa $\sigma_{TS,375}$ = 550 MPa $\sigma_{crack,375}$ ~ 350 MPa		
316L	200	Supplied by SIDERO STAAL (heat 744060) solution annealed + some cold work 12 mm gage length 2.40 mm diameter	Air reference	$5\ 10^{-6}$	$\sigma_{0.2}$ = 510 MPa σ_{TS} = 550 ± 10 MPa $\sigma_{crack,}$ ~ 340 ± 10 MPa A(%) = 22 ± 1	• The authors hypothesis is that an intimate SM/LM contact is obtained thanks to the cracks forming spontaneously in the "brittle interfacial oxide" as a result of the conditioning system in autoclave. • Slow strain rate tensile behaviour of 316L at 200°C is unmodified as a result of exposure to LBE, oxygenated or not, in present experimental conditions, according to the authors.	[Sapundjiev, 2006]
316L	200		Specimen in autoclave with gas conditioning system: LBE under Ar + 5%H_2 bubbling (4 h)	$5\ 10^{-6}$	$\sigma_{0.2}$ = 550 MPa σ_{TS} = 580 ± 10 MPa σ_{crack} ~ 340 ± 10 MPa A(%) = 22 ± 2		
316L	200		As above + final conditioning to obtain 10^{-8} wt.%. Oxygen dissolved in LBE	$5\ 10^{-6}$	$\sigma_{0.2}$ = 550 MPa σ_{TS} = 580 ± 10 MPa σ_{crack} ~ 340 ± 10 MPa A(%) = 21 ± 2		

Table 7.4.3. Tensile behaviour of smooth or rough T91 steel specimens in oxygen saturated LBE (*cont.*)

Material	T (°C)	Specimen preparation and heat treatment	Environmental testing conditions	Strain rate (s^{-1})	Mechanical data	Remarks	Ref.
T91	200	Supplied by UGINE (heat 36224) Normalised at 1040°C (1 h) Tempered at 760°C (1 h) 10 mm gage length 2.45 mm diameter	Air reference	$5\ 10^{-6}$	$\sigma_{0.2}$ = 470 MPa σ_{TS} = 610 MPa A(%) = 21 ± 1	• SSRT behaviour of T91 at 200°C is unmodified due to exposure to LBE, oxygenated or not, in present experimental conditions, according to the authors. • The authors suggested that the auto-repair of the cracked oxide film could explain the results, even at 200°C. • The authors confirmed their findings under controlled reducing environment. • Comparable result were found for T91 in LBE at 250°C (see above).	[Sapundjiev, 2006]
T91	200		LBE under Ar + 5%H_2 bubbling (4 h)	$5\ 10^{-6}$	$\sigma_{0.2}$ = 470 MPa σ_{TS} = 600 MPa A(%) = 22 ± 1		
T91	200		As above + final conditioning to obtain 10^{-8} wt.% Oxygen dissolved in LBE	$5\ 10^{-6}$	$\sigma_{0.2}$ = 470 MPa σ_{TS} = 600 MPa A(%) = 20 ± 1		
T91	245	Normalised at 1040°C (1 h) Tempered at 760°C (1 h) 10 mm gage length 2.45 mm diameter	Ar + 5%H_2	$5\ 10^{-6}$	$\sigma_{0.2}$ = 460 MPa σ_{TS} = 600 MPa A(%) = 21 ± 1		[Sapundjiev, 2006]
T91	245			10^{-5}	$\sigma_{0.2}$ = 440 MPa σ_{TS} = 520 MPa A(%) = 21 ± 1		
T91	245			$5\ 10^{-5}$	$\sigma_{0.2}$ = 440 MPa σ_{TS} = 520 MPa A(%) = 21 ± 1		
T91	245			10^{-4}	$\sigma_{0.2}$ = 440 MPa σ_{TS} = 520 MPa A(%) = 21 ± 1		
T91	245			10^{-3}	$\sigma_{0.2}$ = 440 MPa σ_{TS} = 520 MPa A(%) = 23 ± 1		

Table 7.4.3. Tensile behaviour of smooth or rough T91 steel specimens in oxygen saturated LBE (*cont.*)

Material	T (°C)	Specimen preparation and heat treatment	Environmental testing conditions	Strain rate (s^{-1})	Mechanical data	Remarks	Ref.
T91	245	Normalised at 1040°C (1 h) Tempered at 760°C (1 h) 10 mm gage length 2.45 mm diameter	LBE under Ar + 5%H_2	10^{-5}	$\sigma_{0.2}$ = 490 MPa σ_{TS} = 630 MPa A(%) = 18 ± 1	• Coarse mechanical grinding. • No significant effect of strain rate on tensile properties of T91 in LBE at 245°C. • This result could be explained by the surface state, its roughness not allowing for intimate contact with the LM and hindering its possibly detrimental effect on the mechanical behaviour.	[Sapundjiev, 2006]
T91	245			$5\ 10^{-5}$	$\sigma_{0.2}$ = 500 MPa σ_{TS} = 630 MPa A(%) = 18 ± 1		
T91	245			10^{-4}	$\sigma_{0.2}$ = 490 MPa σ_{TS} = 630 MPa A(%) = 19 ± 1		
T91	245			$3\ 10^{-4}$	$\sigma_{0.2}$ = 535 MPa σ_{TS} = 630 MPa A(%) = 17 ± 1		
T91	450	Normalised at 1040°C (1 h) Tempered at 760°C (1 h) 10 mm gage length 2.45 mm diameter	LBE under Ar + 5%H_2	10^{-6}	$\sigma_{0.2}$ = 400 MPa σ_{TS} = 455 MPa A(%) = 25 ± 1	• Slight effect of strain rate observed in LBE at 450°C. • *The main question remains in all cases: how to be sure that the initial cracks are filled by the liquid metal when no LM effect is detected, since post-mortem chemical analysis of the cracked zone is the only possible verification method?*	[Sapundjiev, 2006]
T91	450			$5\ 10^{-6}$	$\sigma_{0.2}$ = 405 MPa σ_{TS} = 460 MPa A(%) = 26 ± 1		
T91	450			10^{-5}	$\sigma_{0.2}$ = 395 MPa σ_{TS} = 465 MPa A(%) = 28 ± 1		
T91	450			$5\ 10^{-5}$	$\sigma_{0.2}$ = 400 MPa σ_{TS} = 480 MPa A(%) = 30 ± 1		
T91	450			10^{-4}	$\sigma_{0.2}$ = 410 MPa σ_{TS} = 490 MPa A(%) = 27 ± 1		
T91	450			10^{-3}	$\sigma_{0.2}$ = 415 MPa σ_{TS} = 500 MPa A(%) = 20 ± 1		

Table 7.4.4. Tensile behaviour of T91 in oxygen saturated LBE, in the presence of a random distribution of flaws in the specimens

Material	$T_{tensile}$ (°C)	Specimen preparation and heat treatment	Environmental testing conditions	Strain rate (s^{-1})	Mechanical data	Remarks	Ref.
T91	250	Flat specimen: $5 \times 1.5 \times 0.75$ mm^3 in gauge section Prepared by EDM cutting + mechanical polishing	Oxygen-saturated LBE at 300°C	10^{-5}	$\sigma_{0.2,250}$ = 450 MPa $\sigma_{TS,250}$ = 580 MPa $\sigma_{crack,250}$ = 525 MPa	• The distribution of cracks due to EDM cutting justifies the tensile behaviour. • The filling of these cracks with LBE, competing with the oxide film formation on crack walls and at crack tip explains the spread in the stress versus elongation curves as function of temperature and exposure time in LBE. • There is no pronounced temperature effect on crack propagation. Same for ageing in LBE. • At such slow strain rate (10^{-5}), oxygen diffusion in cracks is not controlling the cracking process. Passivation of cracks may occur. • Crack propagation occurs apparently at random. • The distribution of cracks, due to EDM cutting and the stress-strain state over the gage length of the specimens are undetermined. • To explain why the "LBE embrittling effect" is not always observable, one should know the distribution of cracks and which ones are filled with LBE, which can only be determined *post-mortem*. • *Fracture surface*: found brittle, when T91 is put into contact with LBE.	[Dai, 2006]
T91	275			10^{-5}	$\sigma_{0.2,275}$ = 420 MPa $\sigma_{TS,275}$ = 570 MPa $350 \leq \sigma_{crack,275} \leq 420$ MPa		
T91	300			10^{-5}	$\sigma_{0.2,300}$ = 450 MPa $\sigma_{TS,300}$ = 580 MPa $420 \leq \sigma_{crack,300} \leq 525$ MPa		
T91	325			10^{-5}	$\sigma_{0.2,325}$ = 450 MPa $\sigma_{TS,325}$ = 560 MPa $475 \leq \sigma_{crack,325} \leq 540$ MPa		
T91	350			10^{-5}	$\sigma_{0.2,350}$ = 430 MPa $\sigma_{TS,350}$ = 570 MPa $400 \leq \sigma_{crack,350} \leq 550$ MPa		
T91	375			10^{-5}	$\sigma_{0.2,375}$ = 400 MPa $\sigma_{TS,375}$ = 550 MPa $360 \leq \sigma_{crack,375} \leq 520$ MPa		
T91	400			10^{-5}	$\sigma_{0.2,400}$ = 430 MPa $\sigma_{TS,400}$ = 530 MPa $300 \leq \sigma_{crack,400} \leq 400$ MPa		
T91	425			10^{-5}	$\sigma_{0.2,425}$ = 400 MPa $\sigma_{TS,425}$ = 500 MPa $300 \leq \sigma_{crack,425} \leq 400$ MPa		

Table 7.4.5. Tensile behaviour of T91 as a function of preliminary corrosion test conditions

Material	T (°C)	Specimen preparation and heat treatment	Preliminary corrosion test conditions	Tensile test conditions	Strain rate (s^{-1})	Tensile properties	Remarks	Ref.
MANET II	180	Flat tensile specimen: geometry adapted for LiSoR test section: 1 mm thickness, 20 mm gauge length, 5 mm width and 35 mm between shoulders Normalised at 1075°C (30 min) Tempered at 750°C (2 h)	As received	Under argon	10^{-4}	$\sigma_{0.2,180}$ = 580 MPa $\sigma_{TS,180}$ = 700 MPa	• Loss of ductility at 250 and 300°C in LBE. • Mixed fracture surface: some flat areas and others showing dimples. • These results could be surprising, considering that LBE is oxygen saturated in LiSoR. • However, flaws (residual cracks) appearing during the preparation of the LiSoR tensile specimens are not excluded, which could explain the overall mechanical behaviour.	[Glasbrenner, 2003]
MANET II	200				10^{-4}	$\sigma_{0.2,200}$ = 560 MPa $\sigma_{TS,200}$ = 660 MPa		
MANET II	250				10^{-4}	$\sigma_{0.2,250}$ = 580 MPa $\sigma_{TS,250}$ = 670 MPa		
MANET II	180		2 hours exposure in LiSoR loop at tensile test temperature	Under flowing LBE (LiSoR loop)	10^{-4}	$\sigma_{0.2,180}$ = 580 MPa $\sigma_{TS,180}$ = 670 MPa		
MANET II	200				10^{-4}	$\sigma_{0.2,200}$ = 550 MPa $\sigma_{TS,200}$ = 660 MPa		
MANET II	250				10^{-4}	$\sigma_{0.2,250}$ = 560 MPa $\sigma_{TS,250}$ = 660 MPa		
MANET II	300				10^{-4}	$\sigma_{0.2,300}$ = 540 MPa $\sigma_{TS,300}$ = 600 MPa		
T91	400	Cylindrical specimen: 15 mm gauge length 3 mm diameter Normalised at 1040°C (1 h) Tempered at 760°C (1 h)	As received	Under argon	$3.\ 10^{-3}$	$\sigma_{0.2}$ =535 ± 42 MPa σ_{TS} =645 ± 26 MPa A(%) = 22 ± 1 RAZ(%) = 72 ± 2	• No clear effect of pre-exposure to LBE on yield stress and ultimate tensile stress, as already mentioned in LME review papers, except for the elongation to rupture (A) and reduction of area (RAZ). • A loss of ductility is observed at the periphery of the fracture surface, which exhibits a flat morphology.	[Fazio, 2003] [Aiello, 2004]
T91	400		1500 hours in LECOR loop at 400°C	Under argon	$3.\ 10^{-3}$	$\sigma_{0.2}$ = 535 ± 10MPa σ_{TS} = 640 ±14 MPa A(%) = 18 ± 1 RAZ(%) = 42 ± 8		
T91	400		4500 hours in LECOR loop at 400°C	Under argon	$3.\ 10^{-3}$	$\sigma_{0.2}$ =515 ± 7 MPa σ_{TS} =625 ± 15 MPa A(%) = 16 ± 1 RAZ(%) = 32 ± 12		[Aiello, 2004]
T91	450	Normalised at 1040°C (1 h) Tempered at 760°C (1 h) 10 mm gage length 2.45 mm diameter	No pre-exposure to LBE	Stagnant LBE under Ar + 5%H_2,	$5.\ 10^{-5}$	$\sigma_{0.2}$ = 430 MPa σ_{TS} = 450 MPa $\sigma_{fracture}$ = 250 MPa	• Possible but not clear effect of pre-exposure to LBE at 450°C. • Fracture surface aspect unknown.	[Sapundjiev, 2006]
T91	450		4000 hours in stagnant LBE at 450°C	Stagnant LBE under Ar + 5%H_2,	$5.\ 10^{-5}$	$\sigma_{0.2}$ = 400 MPa σ_{TS} = 470 MPa $\sigma_{fracture}$ = 210 Mpa		

Table 7.4.5. Tensile behaviour of T91 as a function of preliminary corrosion test conditions (*cont.*)

Material	T (°C)	Specimen preparation and heat treatment	Preliminary corrosion test conditions	Tensile test conditions	Strain rate (s^{-1})	Tensile properties	Remarks	Ref.
T91	380	Cylindrical smooth specimen: 15 mm gauge length 4 mm diameter Normalised at 1050°C (1 h) Tempered at 750°C (1 h)	1 month exposure to LBE under OCS in reducing conditions: $3.5\ 10^{-11}$ O_2 in COXCIMEL device [Ghetta, 2001, 2002] + relaxation test at 494 MPa under He	Under He	$4.5\ 10^{-5}$	$\sigma_{0.2}$ = 500 MPa σ_{TS} = 560 MPa A(%) = 20	• Cavitation effects in T91, as a result of prior ageing in COXCIMEL at 525°C, do not affect significantly the tensile behaviour at 380°C.	[Gamaoun, 2003, 2004]
T91	380				$4.5\ 10^{-5}$	$\sigma_{0.2}$ = 500 MPa σ_{TS} = 550 MPa A(%) = 19.3		
T91	380		1 month exposure to LBE under OCS in reducing conditions: $3.5\ 10^{-11}$ O_2 in COXCIMEL device [Ghetta, 2001, 2002] + relaxation test at 494 MPa in LBE under He	Stagnant LBE under He	$4.5\ 10^{-5}$	$\sigma_{0.2}$ = 500 MPa σ_{TS} = 550 MPa A(%) = 18	• Specimens coated by LBE (coating possibly favoured by the presence of zinc traces), in which case brittle fracture is observed.	
T91	380				$4.5\ 10^{-5}$	$\sigma_{0.2}$ = 500 MPa σ_{TS} = 530 MPa A(%) = 5		

Table 7.4.6. Tensile behaviour of T91, in air, at room temperature, after exposure to lead or LBE

Material	T (°C)	Specimen preparation and heat treatment	Preliminary corrosion test conditions	Tensile test conditions	Strain rate (s^{-1})	Tensile properties	Remarks	Ref.
T91	T_{room}	Cylindrical smooth specimen: 15 mm gauge length 4 mm diameter Normalised at 1050°C (1 h) Tempered at 750°C (1 h)	As received	Air	$4.5\ 10^{-5}$	$\sigma_{0.2\ ,room}$ = 460 MPa $\sigma_{TS,\ room}$ = 760 MPa A(%) = 27.3	• No effect of preliminary exposure of tensile specimen for 1 month or six months in COXCIMEL device under OCS in reducing conditions when the specimens are tensile tested at room temperature. • This result contrasts markedly with the ones obtained using four-point bending tests carried out in LBE under OCS at high temperature (500-525°C)	[Gamaoun, 2003]
T91	T_{room}		1 month exposure to LBE under OCS in reducing conditions: $3.5\ 10^{-11}$ O_2 in COXCIMEL device	Air	$4.5\ 10^{-5}$	$\sigma_{0.2\ ,room}$ = 460 MPa $\sigma_{TS,\ room}$ = 760 MPa A(%) = 29.8		
T91	T_{room}		As received	Air	$1.7\ 10^{-3}$	$\sigma_{0.2}$ = 565 MPa σ_{TS} = 730 MPa A(%) = 26 ± 1	Reference	[Pastol, 2002]
T91	T_{room}		12 h exposure to LBE under He-4%H_2 (no OCS) at 150°C	Air	$1.7\ 10^{-3}$	$\sigma_{0.2}$ = 565 MPa σ_{TS} = 730 MPa A(%) = 26 ± 1	*Surface state*: Passive.	
T91	T_{room}		12 h exposure to LBE under He-4%H_2 (no OCS) at 300°C	Air	$1.7\ 10^{-3}$	$\sigma_{0.2}$ = 565 MPa σ_{TS} = 730 MPa A(%) = 26 ± 1	*Surface state*: roughened by corrosion at sub-micrometer scale.	
T91	T_{room}		12 h exposure to LBE under He-4%H_2 (no OCS) at 600°C	Air	$1.7\ 10^{-3}$	$\sigma_{0.2}$ = 565 MPa σ_{TS} = 700 MPa A(%) = 26 ± 1	*Surface state*: partial wetting.	
T91	T_{room}		12 h exposure to LBE under He-4%H_2 (no OCS) at 650°C	Air	$1.7\ 10^{-3}$	$\sigma_{0.2}$ = 565 MPa σ_{TS} = 700 MPa A(%) = 26 ± 1	*Surface state*: partially and locally wetted by LBE and locally corroded. *Preliminary conclusion*: partial pre-wetting and pre-corrosion of the T91 steel surface by LBE does not cause any degradation of the tensile behaviour of T91 *at room temperature.*	

Table 7.4.7. Tensile behaviour of T91 in conditions of direct contact with Pb-Bi

Material	T (°C)	Specimen and heat treatment	Specimen preparation	Strain rate (s^{-1})	Mechanical data	Remarks	Ref.
T91	350	Cylindrical smooth specimen Normalised at 1050°C Tempered at 750°C; 15 mm gauge length 4 mm diameter	Diamond polishing to 1 μm, tested in air	10^{-5}	$\sigma_{0.2}$ = 380 MPa σ_{TS} = 550 MPa $\sigma_{fracture}$ = 400 MPa A(%) = 23	• The size of the reservoir of Pb-Bi determines the overall tensile behaviour of T91 at 350°C. • This explains the slight degradation of the parameters derived from the tensile tests in the case of the present Pb-Bi deposit, by comparison with reference tests in air. • Brittle fracture surface at the specimen periphery, over the whole cracked areas attained by LBE in present conditions (temperature, surface state and stress-strain state of the cracked zones)	[Auger, 2004, 2005]
T91	350		Diamond polishing to 1 μm + removal of native oxide by krypton ion sputtering + deposit of Pb-Bi layers (few hundreds of nm) onto the steel surface by PVD under UHV	10^{-5}	$\sigma_{0.2}$ = 380 MPa σ_{TS} = 530 MPa $\sigma_{fracture}$ = 400 MPa A(%) = 20		

Table 7.4.8. Embrittlement of martensitic steels in contact with other liquid metals or alloys: lithium and lead-lithium

Material	T_{test} (°C)	Specimen preparation and heat treatment	Environmental testing conditions	Strain rate (s^{-1})	Mechanical data *(see definitions below)*	Remarks	Ref.
1.4914	250	Cylindrical smooth specimen: 30 mm gauge length 3 mm diameter Normalised at 1050°C (30 min) Tempered at 700°C (120 min)	Air	$2.78\ 10^{-2}$ (50 mm/min) $5.56\ 10^{-4}$ (1 mm/min)	$\sigma_{0.2}$ = 590-620 MPa σ_{TS} = 680 MPa RAZ(%) = 68	• No effect if exposure to lithium is followed by tensile test in air. See [Aiello, 2004]. • Corrosive attack caused by pre-exposure to lithium. • The so-formed cracks enlarge during tensile test in air, with no consequence on bulk properties.	[Borgstedt, 1986]
1.4914	250		Pre-exposure to lithium for 1000 h at 550°C prior tensile test in air	$5.56\ 10^{-4}$ (1 mm/min)	RAZ(%) = 65		
1.4914	200 & 250		Lithium: purified to avoid variations of reactivity: < 5 ppm wt. carbon < 200 ppm wt. nitrogen *O and H contents undetermined*		$\sigma_{0.2}$ = 540-590 MPa σ_{TS} = 650 MPa	• Embrittling effect of lithium at 200 or 250°C, with and without pre-exposure to lithium. • Influence of surface quality produced by machining emphasised: – machining marks↔formation of minimum notches inducing an additional stress on the surface. – these notches act as incipient cracks that will propagate under the influence of stress and liquid metal.	[Borgstedt, 1986]
				$2.78\ 10^{-2}$ (50 mm/min)	RAZ(%) = 49 (250°C) RAZ(%) = 43 (200°C)		
				$5.56\ 10^{-4}$ (1 mm/min)	RAZ(%) = 44 (250°C) RAZ(%) = 33 (200°C)		
1.4914	200 & 250		Exposure to lithium for 1000 h at 550°C prior tensile test in lithium	$5.56\ 10^{-4}$ (1 mm/min)	RAZ(%) = 33	• Mixed fracture mode consisting of brittle inter-crystalline cleavage fracture and ductile shear fracture with flat and distorted dimples.	

Table 7.4.8. Embrittlement of martensitic steels in contact with other liquid metals or alloys: lithium and lead-lithium *(cont.)*

Material	T_{test} (°C)	Specimen preparation and heat treatment	Environmental testing conditions	Strain rate (s^{-1})	Mechanical data	Remarks	Ref.
HT9	273 to 454	Cylindrical smooth specimen: 10.2 mm gauge length 2.54 mm diameter Normalised at 1050°C (30 min) Tempered at 700°C (120 min)	Exposure to Pb-17Li for 18 h at 427°C to obtain "complete wetting" prior tensile test in Pb-17%Li *(< 10 ppm wt. nitrogen 22 ppm wt. hydrogen)*	5.10^{-6} 10^{-3} 10^{-2}	$400 \leq \sigma_{0.2,air} \leq 500$ $490 \leq \sigma_{0.2,PbLi} \leq 560$ $600 \leq \sigma_{TS,air} \leq 660$ $600 \leq \sigma_{TS,PbLi} \leq 750$ $50 < RAZ(\%) < 80$	• Dissolution rate of HT9 and 9Cr-1Mo steel in Pb-17Li ~2 to 5 times lower than for 316L: $0.4 \leq$ dissolution rate ≤ 9 mg/m^2 × h. • No effect of Pb-17Li on tensile properties of HT9. • No visible corrosion effects or surface cracks on gauge surface. • Ductile dimpled fracture in all cases.	[Chopra, 1986]
F82H-mod	250	15 mm gauge length 3 mm diameter Normalised at 1040°C (30 min) Tempered at 750°C (1 h)	For reference specimens tested in vacuum: additional heat treatment at 500°C for 15 h in vacuum	$1.1\ 10^{-4}$ 0.1 mm/min	$\sigma_{0.2}$ = σ_{TS} = 559 MPa A(%) = 15	• No embrittling effect of Pb-17Li on F82H-mod and OPTIFER IVb in present testing conditions: tensile behaviour unaffected with respect to air reference and (fully dimpled) fracture surface. • Assuming complete pre-wetting, this supposes that Pb-17Li was directly adherent on to the steel surface. • *De facto*, there is no indication about the polishing treatment, and the presence of a superficial oxide cannot be excluded. • However, when one simulates an HAZ (heat-affected zone) with these materials, an embrittling effect is seen at 250°C whereas the ductility is recovered at 400°C in otherwise identical conditions. • A(%) = plastic strain at rupture.	[Sample, 2000]
F82H-mod	400			$1.1\ 10^{-4}$	$\sigma_{0.2}$ = σ_{TS} = 502 MPa A(%) = 13.2		
F82H-mod	250		Pre-wetting achieved by heating specimens in Pb-17Li at 500°C for 15 h in argon-filled glove box Prior tensile test in Pb-17Li *(semi-industrial production, described in [Coen, 1984])*	$1.1\ 10^{-4}$	$\sigma_{0.2}$ = σ_{TS} = 546 MPa A(%) =14.7		
F82H-mod	400			$1.1\ 10^{-4}$	$\sigma_{0.2}$ = σ_{TS} = 488 MPa A(%) = 15		
OPTIFER IVb	250	15 mm gauge length 3 mm diameter Normalised at 950°C (30 min) Tempered at 730°C (3 h)	For reference specimens tested in vacuum: additional heat treatment at 500°C for 15 h in vacuum	$1.1\ 10^{-4}$	$\sigma_{0.2}$ = σ_{TS} = 569 MPa A(%) = 16.6		
OPTIFER IVb	400			$1.1\ 10^{-4}$	$\sigma_{0.2}$ = σ_{TS} = 500 MPa A(%) = 13.9		
OPTIFER IVb	250		Pre-wetting achieved by heating specimens in Pb-17Li at 500°C for 15 h in argon-filled glove box Prior tensile test in Pb-17Li	$1.1\ 10^{-4}$	$\sigma_{0.2}$ = σ_{TS} = 540 MPa A(%) = 17.1		
OPTIFER IVb	400			$1.1\ 10^{-4}$	$\sigma_{0.2}$ = σ_{TS} = 497 MPa A(%) = 18.2		

Table 7.4.8. Embrittlement of martensitic steels in contact with other liquid metals or alloys: lithium and lead-lithium *(cont.)*

Material	T_{test} (°C)	Specimen preparation and heat treatment	Environmental testing conditions	Strain rate (s^{-1})	Mechanical data	Remarks	Ref.
EUROFER 97	480	Not reported	Reference	$3\ 10^{-3}$ 2 mm/min	$\sigma_{0.2}$ = 425 MPa σ_{TS} = 480 MPa A(%) = 80	• Un-corroded reference.	[Benamati, 2002]
EUROFER 97	480	Not reported	1500 hours in LIFUS II loop* at 480°C Prior tensile test under argon *(without cleaning the specimens)*	$3\ 10^{-3}$	$\sigma_{0.2}$ = 415 MPa σ_{TS} = 460 MPa A(%) = 80	• Corrosive attack in "semi-stagnant" Pb-17Li. • (10^{-2} m/s) at 480°C in LIFUS loop: 40 μm/year. • The samples extracted from the test section of the loop after 1500 h being covered by Pb-17Li, the authors assumed that wetting occurred during this period of exposure.	
EUROFER 97	480	Not reported	3000 hours in LIFUS II loop at 480°C Prior tensile test under argon *(without cleaning the specimens)*	$3\ 10^{-3}$	$\sigma_{0.2}$ = 400 MPa σ_{TS} = 440 MPa A(%) = 80	• The tensile behaviour of EUROFER 97 is unaffected by long-term exposure to Pb-17Li in LIFUS II loop, in spite of the corrosive attack. • This behaviour contrasts markedly with that of T91 after long-term exposure to Pb-55Bi in LECOR loop, in which case the fracture surface after 1500 or even 4500 h of corrosion exhibits a mixed fracture surface (brittle at the periphery, ductile at the centre).	
EUROFER 97	480	Not reported	4500 hours in LIFUS II loop at 480°C Prior tensile test under argon	$3\ 10^{-3}$	$\sigma_{0.2}$ = =400 MPa σ_{TS} = 446 MPa A(%) = 80		

Table 7.4.10. Brief survey of the Russian literature

Material	T_{test} (°C)	Specimen preparation and heat treatment	Environmental testing conditions	Strain rate, traverse rate	Mechanical data	Remarks	Ref.
Armco iron (0.37%C)	200 to 600	Cylindrical smooth specimen of 9 mm diameter Annealed at 1100°C (2 h) Grain size: 35 μm	Exposure to molten Cd, Ga, Bi, Pb, Sn, LBE and Bi-Cd eutectic Gauge portion of specimens pre-tinned using the method of soldering fluxes Tensile test in LM under vacuum (10^{-2} Pa of residual pressure) in the 200-600°C range	5%/min	–	• Efficient wetting obtained by pre-tinning, "even by such media as liquid lead and bismuth" *sic* • Adsorption-induced facilitation of plastic flow leads to strain-hardening, and takes place in an earlier deformation stage in contact with LM than in vacuum, which promotes localisation of the plastic deformation and a change in the rupture mechanism, and may result in LME effects. • Elongation to rupture reduced for Cd, Bi, Pb, Sn, Pb-Bi and Bi-Cd Eutectics, between 225 and 425°C. • Interpretation of results based on Rebinder effect. • Maximum effect of environment at ~350°C. • Complete recovery of plasticity at 450-500°C. • No effect of Ga on tensile behaviour, tentatively explained by the formation of solid solutions and intermetallics, which prevents the formation of cracks in regions of pronounced plastic deformation. • This is not a general rule, after the authors.	[Popovich, 1978]
			Specimens coated with Ga, Pb, Bi, and LBE (as above) *Tested in air*	5%/min	–	• Unsuccessful tests: specimens de-wetted due to interfacial oxidation caused by atmospheric oxygen diffusing throughout the metal films.	[Popovich, 1978]
			Specimens coated with Sn and Cd (as above) *Tested in air*	5%/min	–	• The plasticity of the specimens coated with tin and cadmium were found identical in air and vacuum.	

Table 7.4.10. Brief survey of the Russian literature (*cont.*)

Material	T_{test} (°C)	Specimen preparation and heat treatment	Environmental testing conditions	Mechanical testing conditions	Remarks	Ref.
20Kh13 steel	450	Hardened state see Ref. 44 in [Popovich, 1979]	Vacuum Pb-Sn eutectic at 450°C	Fatigue testing	• Long-term fatigue strength of 20Kh13 steel reduced in contact with Pb-Sn eutectic. • Stress cannot exceed 80 kgf/mm^2.	[Popovich, 1979]
Carbon steel Steel St. 45	25; 250; 400	Specimens annealed to produce a pearlito-ferritic structure 7.52 cm diameter "Class 9" surface finish Smooth specimens V-shape circular groove 0.5 mm deep Occluded notch angle: 50° Notch root radius: 0.03 mm	Air	Fatigue testing in rotation bending at stress-reversal frequency of 25, 80 and 160 cps	• Fatigue strength of smooth carbon steel specimens in liquid tin and tin-lead eutectic is higher than in air at same temperature, with no effect of stress reversal frequency. • Endurance in Pb-Sn eutectic at 250°C much higher than in air; same for tin at 400°C, with an effect of frequency on notched specimens. • *Hypothesis*: Superficial intermetallics ($FeSn_2$…) give rise to high compressive stresses that increase the steel endurance.	[Nikolin, 1968]
	250		Pb-Sn eutectic at 250°C			
	400		Tin at 400°C			
Steel-20	400	40 mm gauge length and 10 mm diameter Used as delivered	Air reference	10 mm/min 0.055 mm/min	• Embrittlement of the steel at "high" deformation rate (10 mm/min), in contact with the melts. • Plasticity recovered at "slow" deformation rate (0.055 mm/min). • *Hypothesis*: Plasticising effect of surface active melt for a certain combination of temperature and deformation rate.	[Chaeveskii, 1962]
			Pre-tinned specimen tested in Pb-Sn eutectic	10 mm/min 0.055 mm/min		
			Pre-tinned specimen tested in LBE	10 mm/min 0.055 mm/min		
1Cr18Ni9Ti steel	500	–	*Un-tinned* specimens fatigue tested *in stagnant/ flowing LBE at 500°C*	*Fatigue testing conditions not reported*	• Pre-tinning with LBE (coated with LBE) using the more suitable soldering flux, prior testing. • Sharp reduction in fatigue strength of pre-tinned specimens at 500°C, by comparison with un-tinned specimens, tested either in stagnant & flowing LBE, or in air.	[Bichuya, 1969]
1Cr18Ni9Ti steel	500	–	Specimens pre-tinned with LBE, then fatigue tested *in LBE at 500°C*			
1Cr18Ni9Ti steel	600	–	Specimens pre-tinned with LBE, then fatigue tested *in air at 600°C*		• Reduction of the oxygen partial pressure leads to the formation of a protective, stable $FeCr_2O_4$ oxide onto the steel surface at 600°C, which explains the steel strength and its endurance limit by inhibiting the potential damage due to LBE. • $FeCr_2O_4$ films are not destroyed by flowing LBE. • Otherwise, in case of formation of brittle oxides, reduction in fatigue strength of both tinned and un-tinned specimens occurs, due to LBE at 600°C in the low endurance range (up to 2 10^7 cycles).	
1Cr18Ni9Ti steel	600	–	Specimens pre-tinned with LBE, then tested *under pure argon at 600°C*			
1Cr18Ni9Ti steel	600	–	Specimens pre-tinned with LBE, then tested *in stagnant or flowing LBE at 600°C*			
1Cr18Ni9Ti steel	600	–	*Un-tinned* specimens tested *in LBE at 600°C*			

Table 7.4.10. Brief survey of the Russian literature (*cont.*)

Material	T (°C)	Specimen preparation and heat treatment	Environmental testing conditions	Mechanical testing conditions and results		Remarks	Ref.
12KhM pearlitic steel	200 to 600	Cylindrical specimens of 20 mm gauge length and 4 mm diameter Prepared from forged 15 mm diameter rods Normalised at 990°C and tempered at 710°C Surface preparation: cleaning in benzene, polishing with emery paper, cleaning in benzene	Air reference Specimen pre-tinned with LBE using the method of soldering fluxes (containing zinc chloride and 7% ammonia chloride) Then held 30 min at the test temperature in ampoule filled with LBE (LM surface in contact with air)	Tensile test (uniaxial tension) at 6.25%/min		• Influence of LBE on mechanical behaviour maximised on pre-tinned specimens. • Maximum reduction of ductility at 400°C independently of the surface preparation (mechanical polishing or pre-tinning). • No corrosion by LBE.	[Balandin, 1970]
12KhM pearlitic steel	500	As above	Pre-tinned with LBE + 0.5 h exposure to LBE under air at 500°C Prior testing in LBE at 500°C	6.25%/min	$\sigma_{0.2}$ = 35 kg/mm^2 σ_{TS} = 48.7 kg/mm^2 A(%) = 12%	• No effect of holding time in oxygen-saturated LBE, from 0.5 h to 25 hours, on the tensile behaviour of 12KhM steel at same temperature. • *Hypothesis*: Formation of an interfacial oxide film, which hinders wetting and prevents any embrittling effect.	[Balandin, 1970]
	500		Pre-tinned with LBE + 2.5 h exposure to LBE under air at 500°C Prior testing in LBE at 500°C	6.25%/min	$\sigma_{0.2}$ = 33.6 kg/mm^2 σ_{TS} = 43.8 kg/mm^2 A(%) = 25.2%		
	500		Pre-tinned with LBE + 5.0 h exposure to LBE under air at 500°C Prior testing in LBE at 500°C	6.25%/min	$\sigma_{0.2}$ = 34 kg/mm^2 σ_{TS} = 45.3 kg/mm^2 A(%) = 21.6%		
	500		Pre-tinned with LBE + 10 h exposure to LBE under air at 500°C Prior testing in LBE at 500°C	6.25%/min	$\sigma_{0.2}$ = 33.4 kg/mm^2 σ_{TS} = 43.9 kg/mm^2 A(%) = 21.9%		
	500		Pre-tinned with LBE + 25 h exposure to LBE under air at 500°C Prior testing in LBE at 500°C	6.25%/min	$\sigma_{0.2}$ = 32.5 kg/mm^2 σ_{TS} = 43.3 kg/mm^2 A(%) = 21.7%		

Table 7.4.10. Brief survey of the Russian literature (*cont.*)

Material	T (°C)	Specimen preparation and heat treatment	Environmental testing conditions	Mechanical testing conditions and results		Remarks	Ref.
12KhM pearlitic steel	500	Cylindrical specimens of 20 mm gauge length and 4 mm diameter Prepared from forged 15 mm diameter rods Normalised at 990°C and tempered at 710°C Surface preparation: cleaning in benzene, polishing with emery paper, cleaning in benzene	Pre-tinning with LBE + 2.5 h exposure to LBE under air Tested after cleaning and re-tinning with LBE	6.25%/min	$\sigma_{0.2}$ = 34 kg/mm^2 σ_{TS} = 44.7 kg/mm^2 A(%) = 10.7%	• Pre-tinning is considered as "a unique procedure" allowing for the establishment of an intimate contact between steel and LBE, since the steel will always be oxidised in oxygen-saturated LBE and neither Pb nor Bi wet oxides of steel constituents. • Re-tinning with LBE after exposure to oxygen-saturated LBE for durations going from 2.5 h to 25 restores the embrittling effect of LBE. • Drawback of pre-tinning: due to the well-known detrimental effect of zinc, which was tested and found negligible by the authors of this work. • However, with increasing tensile strain, cracks can form in the surface oxide and permit contact with the steel surface. In such case, the embrittling effect of the LM would be just delayed (an argument already considered in SCC). • Pre-tinning remains the best way to force the steel/LM contact, provided there is no loss of this contact due to a growing oxide at the SM/SL interface, for example caused by inward penetration of oxygen species throughout the metal layers … • *Postulat*: The ductility of steels could be reduced at temperatures > 500°C if no formation of an oxide film takes place on the surface of specimens already wetted by LBE.	[Balandin, 1970]
	500		Pre-tinning with LBE + 5.0 h exposure |to LBE under air Tested after cleaning and re-tinning with LBE	6.25%/min	$\sigma_{0.2}$ = 34.1 kg/mm^2 σ_{TS} = 43.9 kg/mm^2 A(%) = 11%		
	500		Pre-tinning with LBE + 25 h exposure to LBE under air Tested after cleaning and re-tinning with LBE	6.25%/min	$\sigma_{0.2}$ = 33.8 kg/mm^2 σ_{TS} = 43.7 kg/mm^2 A(%) = 10.8%		[Balandin, 1970]

Table 7.4.10. Brief survey of the Russian literature (*cont.*)

Material	T (°C)	Specimen preparation and heat treatment	Environmental testing conditions	Mechanical testing conditions and results		Remarks	Ref.
St 50 steel	400	Hollow cylindrical specimens (D/d = 16/10) provided with screwed-on jacket	Hollow and ext. jacket filled with LBE Pre-tinning before testing in LBE	Strain rates: 0.05%/min 31.8%/min	Cyclic deformation in torsion	• Efficient wetting obtained by pre-tinning. • Strain-hardening during the first two cycles followed by continuous decrease in strength until fracture at 31.8%/min strain rate. • Plasticising effect of LBE is suggested at slow strain rate (0.05%/min.).	[Chaevskii, 1969]
04X16H11M3T austenitic steel	350	Cylindrical specimens of 5 mm diameter	Air reference	1.1 10^{-4} s^{-1} 0.1 mm/min	$\sigma_{0.2}$ = 158 MPa σ_{TS} = 474 MPa A(%) = 42.7 RAZ(%) = 72.5 $\sigma_{fracture}$ = 1789	• No effect of Pb-17Li on 04X16H11M3T in present testing conditions: tensile behaviour of specimens pre-tinned with Pb-17Li unaffected with respect to air reference (cf. [Chopra, 1986]).	[Antipenkov, 1991]
04X16H11M3T austenitic steel	350	Cylindrical specimens of 5 mm diameter	Specimens cleaned with zinc chloride Pre-tinned with Pb-17Li Prior tensile testing	1.1 10^{-4} s^{-1}	$\sigma_{0.2}$ = 241 MPa σ_{TS} = 471 MPa A(%) = 49.3 RAZ(%) = 66.3 $\sigma_{fracture}$ = 1193	• Corrosion behaviour: the 04X16H11M3T austenitic steel under stress (at ~ $\sigma_{0.2}$) in flowing Pb-17Li at 0.5 m/s at 500°C exhibits a weight loss × 2, with respect to the unstressed state.	
08Kh16N11S3MB austenitic chromium-nickel steel	300 to 700	Flat specimen of 10 mm length and 1 × 3 mm working cross-section Austenitised at 1050°C (0.5 h)	Reference specimen (without coating) Tensile tested under same conditions	8. 10^{-4} s^{-1}		• No embrittling effect of lead on the 08Kh16N11S3MB austenitic steel in the considered temperatures range and deformation rates. • Slight influence of lead, tending to decrease very slightly the strength and ductility of pre-tinned austenitic steel in the 300-450°C range. • Plasticising effect of the lead melt in the 400-500°C range. • No effect of lead at T > 500°C.	[Abramov, 1994]
			Pre-tinning under argon → coating by a thin Pb layer at 350°C Followed by tensile testing	8. 10^{-4} s^{-1}			

Table 7.4.10. Brief survey of the Russian literature (*cont.*)

Material	T (°C)	Specimen preparation and heat treatment	Environmental testing conditions	Strain rate	Remarks	Ref.
Kh12MVSFBR ferritic/martensitic steel	300 to 700	Flat specimen of 10 mm length and 1 × 3 mm working cross-section Heat treatment: TT-1: Hardening from 1050°C + tempering at 750°C (1 h) (5-10% δ ferrite + martensite)	Reference specimen Tensile tested under same conditions	8. 10^{-4} s^{-1}	• Strength of reference and tinned specimens decreases with increasing test temperature, whereas the plasticity increases with T_{test}. • Liquid Pb hardens the Kh12MVSFBR martensitic steel when heat-treated in mode TT-1. • Effect of Pb increases at T ≥ 400°C (TT-1 case). • Plasticity of specimens in contact with molten lead is lower than that of original specimens in the 300-500°C range: – maximum decrease of plasticity at 450°C: $K_\delta = \delta^{Pb}/\delta^c = 0.5$ with δ^{Pb} and δ^c being respectively the specific elongation of the pre-tinned and reference specimens; – plasticity recovered at T ≥ 600°C.	[Abramov, 1994]
Kh12MVSFBR ferritic/martensitic steel	300 to 700		Pre-tinning under argon → coating by a thin Pb layer (at 350°C) Followed by tensile testing	8. 10^{-4} s^{-1}		
Kh12MVSFBR ferritic/martensitic steel	300 to 700	Flat specimen of 10 mm length and 1 x 3 mm working cross-section Heat treatment: TT-2: Hardening from 1100°C	Reference specimen Tensile tested under same conditions	8. 10^{-4} s^{-1}	• Heat treatment TT-2 leads to a significant increase in strength: $\sigma_{0.2} \geq 1100$ MPa at 300°C.	[Abramov, 1994]
			Pre-tinning under argon → coating by a thin Pb layer (at 350°C) Followed by tensile testing		• TT-2 heat treatment yields to a noticeable decrease in the plasticity of tinned specimens and to a broadening of the ductility trough, going from 350 to 600°C. • Maximum decrease of plasticity at 450°C: $K_\delta = \delta^{Pb}/\delta^c = 0.2$. • Plasticity recovered at 700°C. • For pre-tinned specimens: (at an embrittling temperature) well visible cracks, filled with Lead, propagate, at least initially, in the direction normal to the loading axis. • Crack propagation is spasmodic (see [Soldatchenkova, 1972]). • LME effects are typical of Cr steels, and become more pronounced in the hardened martensite phase. • LME effects can be moderated by tempering at high temperature and formation of δ ferrite.	

Table 7.4.10. Brief survey of the Russian literature (*cont.*)

Material	T (°C)	Specimen preparation and heat treatment	Environmental testing conditions	Strain rate	Remarks	Ref.
Armco iron (0.037 wt.% C)		Cylindrical specimen of 9 mm diameter Stress concentrators with 0.75 mm depth notched with a polishing wheel (60° angle and 0.1 mm curvature radius) Annealing & grain size: 500°C (1 h) → 26 μm 1100°C (2 h) → 80 μm 1250°C (5 h) → 110 μm	Under vacuum ($1.3\ 10^{-3}$ Pa)	$8.3\ 10^{-4}\ s^{-1}$	• From 100 to 350°C, σ_{TS} of smooth specimens increases due to Dynamic Strain Ageing (DSA).	[Dmukhovs'ka, 1993a]
			Pre-tinning with Pb-Bi followed by tensile testing in Pb-Bi under vacuum	$8.3\ 10^{-4}\ s^{-1}$	• Significant LME effect on specimens with stress concentrators: considerable decrease in strength for T ≥ 250°C in both LMs (In, LBE). • Decrease in strength (σ_{TS}) begins at temperatures < T_m of indium, whereas, for LBE, no embrittling effect is observed below 200°C, i.e. well above T_m of LBE. • *Suggestion*: Tendency to LME is a consequence of strained state and testing conditions, the temperature of the melt being only one factor among the others.	
			Pre-tinning with indium followed by tensile testing in indium under vacuum	$8.3\ 10^{-4}\ s^{-1}$		
Armco iron (0.037 wt.% C)		Square cross-section of 6 × 6 mm (obtained by polishing the lateral surfaces of the cylindrical specimens) Annealed at 1100°C (2 h) Average grain size ~ 80 μm	Under vacuum	$8.3\ 10^{-4}\ s^{-1}$	• For specimens with square cross-sections (where faces play the role of stress concentrators), the tensile behaviour is intermediate between the one obtained with "plain" specimens and the other one obtained on specimens with stress concentrators. • *1st conclusion*: The temperature range of LME may depend on the shape of the specimens. • *2nd conclusion*: Specimens tested with stress concentrators reveal that the higher the level of embrittlement, the lower the temperature of its initiation; this result is consistent with modelling taking into account the influence of the adsorbing medium on plastic deformation in surface layers [Dmukhovs'ka, 1982].	[Dmukhovs'ka, 1993a]
			Pre-tinning with indium followed by tensile testing in indium under vacuum	$8.3\ 10^{-4}\ s^{-1}$		

[Dmukhovs'ka, 1982] Dmukhovs'ka, I.H., V.V. Popovich (1982), "Phenomenological Models for Embrittlement of Metals in Adsorbing Liquid Metal Media", *Fiz. Khim. Mech. Mater*., Vol. 6, 5-13.

Table 7.4.10. Brief survey of the Russian literature (*cont.*)

Material	T (°C)	Specimen preparation and heat treatment	Environmental testing conditions	Mechanical testing conditions and results		Remarks	Ref.
Armco iron	700 to 1000	Hollow cylindrical specimens of 9 mm external diameter and 4 mm internal diameter	Indium (self fluxing medium at HT)	Tensile test at $8.3\ 10^{-4} s^{-1}$	–	• Indium embrittles Armco iron in the 850-950°C temperature range. • LME is caused by an indium-induced decrease in flow stress, which localises strain in the α phase and initiates its premature cracking. • Indium corrodes Armco iron. • Fracture surface of embrittled specimens is microscopically flat. • It is proved that corrosion is not responsible for high temperature LME.	Dmukhovs'ka, 1993, b]
1Cr-1.5Si-0.5Mo steel	400	*No indication on specimen preparation*	No coating Air reference		$\sigma_{0.2}$ = 265 MPa σ_{TS} = 480 MPa A(%) = 23 RA(%) = 63	• Austenitic Si steels are not susceptible to embrittlement by liquid lead. • Nickel-plating leads to the greatest reduction of plasticity, due to the removal of the natural oxidation film. • Nikel-plating is more efficient than the method of soldering fluxes to reduce the mechanical strength of steels in contact with liquid metals. • Oxidation, as always reported, suppresses the reduction in strength due to absorption of metal species. • Similarly, pre-oxidation of 1Cr-1.5Si-Mo steel suppresses the effect of environment on its fatigue life at 400°C in Pb-Bi, found equal to that in air, whereas it is significantly reduced without pre-oxidation treatment, under the same conditions.	[Gorynin, 1999]
	400		Ni coating Air environment		$\sigma_{0.2}$ = – σ_{TS} = 500 MPa A(%) = – RA(%) = 63		
	400		Without coating Un-wetted surface tested in Pb-Bi		$\sigma_{0.2}$ = σ_{TS} = 500 MPa A(%) = – RA(%) = 46		
	400		Surface wetted by soldering Tested in Pb-Bi		$\sigma_{0.2}$ = σ_{TS} = 451 MPa A(%) = 20 RA(%) = 38		
	400		Ni coating Tested in Pb-Bi		$\sigma_{0.2}$ = 274 MPa σ_{TS} = 480 MPa A(%) = 13 RA(%) = 16		
	400		Surface oxidation Prior testing in Pb-Bi		$\sigma_{0.2}$ = 225 MPa σ_{TS} = 451 MPa A(%) = 23 RA(%) = 58		

Table 7.4.11. Chemical compositions of the above mentioned steels (wt.%, balance Fe)

	Cr	W	Ni	Mn	V	Nb	Mo	Ta	Ti	Al	Cu	As	Sn	C	N	P	S	B	Si	Ref.
T91	8.26		0.13	0.38	0.2	0.08	0.95			0.024	0.08	0.02	0.008	0.105	0.055	0.009	0.003		0.43	[*]
MANET	10.37	–	0.657	0.76	0.21	0.16	0.5B	–	–	0.007	0.01	–	–	0.10	0.032	0.004	0.005	0.0075	0.18	[Glasbrenner, 2003]
1.4914	10.6		0.82	0.54	0.24	0.19	0.49			0.05	0.01			0.172		0.005	0.005	0.002	0.34	[Borgstedt, 1986]
HT9	11.8	0.52	0.51	0.50	0.33	–	1.03	–	–	–	–	–	–	0.21	–	–	–	–	0.21	[Chopra, 1986]
F82H-mod	7.66	2.0		0.16	0.16	–		0.02						0.09	0.005				0.11	[Sample, 2000]
OPTFER IVb	8.3	1.4		0.34	0.22	–		0.06						0.12	0.03					[Sample, 2000]
EUROFER 97	8.8	1.15		0.44	0.2	0.002	0.003							0.10	–				0.05	[Benamati, 2002]
04X16H11M3T	15.79	0.1	0.6	1.3	–	–	2.18		0.32	–	–			0.04	–	0.012	0.015	–	0.54	[Antipenkov, 1991]

[*] = [Legris, 2000, 2002], [Nicaise, 2001], [Vogt, 2002], [Pastol, 2002], [Gamaoun, 2002, 2003], [Guerin, 2003], [Auger, 2004, 2005], [Verleene, 2006].

Table 7.5.1. Fatigue behaviour of martensitic and austenitic steels in heavy liquid metals

Material	T_{test} (°C)	Specimen preparation and heat treatment	Environmental testing conditions	Mechanical testing conditions	Results and Remarks	Ref.
MANET	550	Heat treatment: 950-980°C (2 h) 1075°C (30 min) then 750°C (2 h) Hourglass shape specimen: 8.8 mm min diameter 21 mm gauge length	Under argon	Strain control: Strain amplitude range from 0.006 to 0.0125	• LCF tests in Pb-17Li gives a longer fatigue life than in gaseous environment.	[Borgstedt, 1991]
MANET	550		Stagnant Pb-17Li (provided by Metallgesellschaft A.G., Frankfurt)			
MANET	550		1000 h pre-exposure to Pb-17Li		• Prolonged preliminary contact with Pb-17Li reduces this beneficial effect. • However, LCF life of pre-corroded specimens still longer than that of reference specimens under gas. • Wetting by LM is apparently a prerequisite to detect its influence on fatigue.	
*316L	450	Hourglass shape specimen: 10 mm gauge length Surface finish: total roughness of 1.5 to 2 μm	Under argon with 5-10 ppm O_2 and 10-15 vl.ppm H_2O	Strain control: Average strain = 0.05 superimposed to strain cycle $0.008 \leq \Delta\varepsilon_t \leq 0.016$ $5\ 10^{-5} \leq \dot{\varepsilon} \leq 1.07\ 10^{-4}$ Cycle frequency: 0.0033 Hz Non-fully-reversed triangular wave form	• *Under argon*: Numerous finger-like cracks, some of which propagate deeply in 316L. • Transgranular crack propagation.	[Benamati, 1994]
*316L	450		30 hours pre-exposure to Pb-17Li to wet the specimen Prior LCF test at a flow velocity of 0.01 m/s in the LIFUS II loop		• Tensile strain limit slightly higher than compressive strain limit in order to enhance the corrosive effect on crack tip generated by fatigue. • ASTM E606 standard. • *In Pb-17Li*: Few broad cracks propagating transgranularly, characterised by a rounded tip. • Consistent with the absence of LM penetration at grain boundaries observed during corrosion tests. • *LCF behaviour*: Generally improved in Pb-17Li with respect to air or cover gas.	

* Composition and microstructure in: G. Benamati, S. Storai, I. Alessandrini, P. Agostini, *Low Cycle Corrosion Fatigue of AISI 316L*, ENEA Report, NT Fus. Bra Isp 34 (1993).

Table 7.5.1. Fatigue behaviour of martensitic and austenitic steels in heavy liquid metals (*cont.*)

Material	T_{test} (°C)	Specimen preparation and heat treatment	Environmental testing conditions	Mechanical testing conditions	Results and remarks	Ref.
Type 316	593	*For specimen preparation, see Refs. [25-32] of O.K. Chopra, J. Nuclear Mat., 115, 223 (1983).*	Pre-exposure (for 1500 h…) to sodium of controlled purity (0.4 ppm carbon) Between 550 and 700°C or thermal ageing for long duration	*For mechanical testing conditions, see Refs. [25-32] of O.K. Chopra, J.N..M.., 115, 223 (1983) [Chopra, 1983]*	• *Fatigue behaviour* in sodium superior to that in air, environmental effects being negligible in low oxygen containing sodium (≤ 3 ppm), with a steel surface considered absolutely free from corrosion products. • *Fatigue life* increased of ~ 4 to 10, for $\Delta\varepsilon = 1\%$ in Na, compared to air. • Differences among data assumed to come from the heat of material, product form and heat treatment.	[Chopra, 1983]
316LN	540	Cut from a 40 mm thick plate in the as-received state (solution annealed) with the rolling direction parallel to the chevron-notch (T-L orientation) 12.5 mm thick compact tensile specimen	Air	Under load control (ASTM E-647) using a sine wave form at 5 Hz To simulate service type loading: R = 0.6, 0.8	• Fatigue crack growth rate in sodium and argon at 540°C considerably lower than in oxidising air environment at same temperature. • Strong R-dependence of ΔK_{th} in air and sodium: ΔK_{th} decreasing with increasing R: – from 6 MPa√m for R = 0.6 to .4 MPa√m for R = 0.8; – same for air or argon cover gas.	[Mishra, 1997]
316LN	540		Argon			
316LN	540		Designed chamber to allow for continuous flow of LM around CT specimen. Flowing sodium continuously purified: ≤ 2 ppm oxygen; carbon and nitrogen activities also controlled			
316LN	540					
316LN	Room T	Uniform gauge fatigue specimen machined parallel to the primary rolling direction of the 25 mm thick plate used 12.7 mm gauge length 5.08 mm diameter *Polishing conditions missing*	Air	R = -1 Cycle frequency: 0.2-0.5 Hz	• *Fatigue endurance limit*, in air, decreases from 240 MPa at R = -1, to 170 MPa for R = 0.1. • Same for Hg. • *Fatigue life* reduced in Hg compared to air, the effect being amplified with decreasing cycle frequency from 10 Hz to 0.1 Hz. This effect nearly disappears at high frequency (700 Hz, R = 0.1, temperature control for CF in air). • *Wetting and LME*: From the observation that Hg is adherent onto the fracture surface and not on the gauge length, it is conjectured that Hg plays a role on crack propagation, by accelerating the crack propagation rate, but not at the stage of crack initiation.	[Strizak, 2001]
316LN	Room T		Air	R = 0.1 (tensile mean stress) Cycle frequency: 0.1, 1, 10 Hz		
316LN	Room T		Hg	R = -1 Cycle frequency: 0.2 to 0.5 Hz		
316LN	Room T		Hg	R = 0.1 (tensile mean stress) Cycle frequency: 0.1, 1.0, 10 Hz		

Table 7.5.1. Fatigue behaviour of martensitic and austenitic steels in heavy liquid metals (*cont.*)

Material	T_{test} (°C)	Specimen preparation and heat treatment	Environmental testing conditions	Mechanical testing conditions	Results and remarks	Ref.
316L	Room T	Cylindrical specimen: fabricated using "low stress grinding and polishing" treatment 40 mm gauge length 10 mm diameter Tested in as-received state	Air	Total strain amplitude control: $0.3\% \le \varepsilon_{ta} \le 1\%$ $R_\varepsilon = -1$, triangular waveform Frequency: 1 Hz for all tests	• *Fatigue life* of 316L rather comparable in air and LBE at low strain amplitude (0.3%), even for $\Delta\varepsilon$ attaining 1%. • *Cyclic softening*: For 316L and MANET II independent of environment, air or LBE, under present experimental conditions. • *Crack propagation*: Slightly faster in LBE than in air for 316L, under present conditions ($\Delta\varepsilon$ = 0.3%, 1 Hz, 260°C). • $\varepsilon_{at,air,260°C} = 6.86\ N^{-0.30}$, $\varepsilon_{at,LBE,260°C} = 3.90\ N^{-0.25}$.	[Kalkhof, 2003]
316L	260		Air			
316L	260		Stagnant LBE	Total strain amplitude control: $0.3\% \le \varepsilon_{ta} \le 0.6\%$ $R_\varepsilon = -1$, triangular waveform Frequency: 1 Hz for all tests $(5\ 10^{-5} \le \dot{\varepsilon} \le 1.07\ 10^{-4})$		
MANET II	260		Air	Total strain amplitude control: $0.3\% \le \varepsilon_{ta} \le 1\%$ R = -1, triangular wave form Cycle frequency: 0.1 Hz	• *Fatigue life*: longer for 316L than for MANET II. • Fatigue life of MANET II clearly reduced in LBE: – reduced of ~2, for $\Delta\varepsilon$ = 0.3% at 1 Hz; – reduced of ~7, for $\Delta\varepsilon$ = 0.3% at 0.1 Hz; (*Reduction amplified with decreasing cycle frequency.*) – with a large scatter in the number of cycles for crack initiation. • *Crack propagation*: very fast in LBE compared to air for MANET II, in present conditions ($\Delta\varepsilon$ = 0.3%, 1 Hz, 260°C); it is suggested that wetting of crack walls results in an additional tensile stress during crack closure, hindering crack tip blunting. *Main hypothesis: wetting of crack walls by LBE!* • $\varepsilon_{at,air,260°C} = 5.12N^{-0.30}$, $\varepsilon_{at,LBE,260°C} = 2.66N^{-0.25}$	[Kalkhof, 2003]
MANET II	260		Stagnant LBE	Total strain amplitude control: $0.3\% \le \varepsilon_{ta} \le 1\%$ $R_\varepsilon = -1$, triangular waveform Frequency: 1 Hz for all tests; 0.1 Hz for tests conducted at ε_{ta} = 0.3 and 0.4%		
T91	300	Cylindrical specimen: 10 mm gauge length 10 mm diameter Electropolished Austenitised: 1050°C (1 h) Tempered: 750°C (1 h)	Air	Total strain range control: $0.36\% \le \varepsilon_{ta} \le 2.4\%$ $R_\varepsilon = -1$, symmetrical triangular waveform Constant strain rate: $\dot{\varepsilon} = 4\ 10^{-3}\ s^{-1}$ 0.08 Hz ≤ frequency ≤ 0.55 Hz	• *Cyclic softening*: for T91, independent of environment, air or LBE. Hypothesis: LBE affects surf., not bulk properties. • *Fatigue life* of T91 reduced in LBE, compared to air: – reduced of ~2, for $\Delta\varepsilon_\tau$ = 2.2% at 0.33 Hz. • *Fatigue crack initiation*: low density of short cracks in LBE, compared to air. • *Fatigue crack propagation*: very fast in LBE, compared to air.	[Vogt, 2004, 2006], [Verleene, 2006]
T91	300		Stagnant LBE under air			

Table 7.5.2. Fatigue and creep fatigue behaviour of austenitic and martensitic steels in lead alloys

Material	T_{test} (°C)	Specimen preparation and heat treatment	Environmental testing conditions	Mechanical testing conditions	Results and remarks	Ref.
T91	300	Cylindrical specimen: 10 mm gauge length 10 mm diameter Electropolished Austenitised at 1050°C (1 h) tempered at 750°C (1 h)	Air	Symmetrical triangular wave form (R = -1)	• Stress response to strain cycling for all tests, unmodified by hold time, in air or in LBE • *Fatigue life:* – reduced for T91 in LBE by introduction of 10 min hold time for $0.4\% \leq \Delta\varepsilon_t \leq 2.5\%$; – unmodified in air in similar conditions.	[Vogt, 2006]
T91	300		Air	Trapezoidal wave form (10 min. hold time in tension) Two tests with $\Delta\varepsilon_t$ = 2.5, 1.6%		
T91	300		Stagnant LBE (no OCS)	Symmetrical triangular wave form (R = -1)		
T91	300			Trapezoidal wave form 10 min hold time in tension		
T91	300	Four-point bent specimens: 10 mm × 10 mm × 55 mm	Air	Specific device, using pre-cracked specimens Load ratio R = 0.5 cycle frequency: 5 Hz	• *Fatigue crack growth*: faster in LBE than in air; in agreement with the results of Kalkhof & Grosse (2003).	[Vogt, 2006]
T91	300		Stagnant LBE (no OCS)			
T91	300	Cylindrical specimen: 10 mm gauge length 10 mm diameter Electropolished Austenitised at 1050°C (1 h) tempered at 750°C (1 h)	613 hours pre-exposure to LBE at 600°C under reducing conditions prior to fatigue testing at 300°C in LBE under air	Symmetrical triangular wave form (R = -1) $\dot{\varepsilon} = 4\ 10^{-3}\ s^{-1}$ $\Delta\varepsilon_t$ = 0.6, 1.6, 2.2% Cycle frequency: 0.09, 0.125, 0.33 Hz	• *Fatigue life*: – reduced by preliminary corrosion in reducing LBE for 600 h; – only slightly enhanced by preliminary oxidation in oxygen-saturated LBE for 600 h, compared to LCF directly conducted in LBE under air.	[Vogt, 2006]
T91	300		502 hours pre-exposure to LBE at 470°C in oxygen saturation conditions prior to fatigue testing at 300°C in LBE under air			
0.4Kh16N11M3T	80, 250, 350	Specimens made by stamping sheet materials; then polished over the surfaces and along the contour Working part: 15 mm in length & 1.5 × 5 mm cross-section Blanks austenitised at 1050°C (1 h)	Specimens covered with Pb-17Li melt in a pressure chamber prior fatigue testing in Pb-17Li under cover gas	Symmetric pure bending, total strain amplitude ≤ 3% Low-cycle tests: cycle frequency: 0.5 Hz High-cycle test: cycle frequency: 8.3 Hz	• *Fatigue life* of austenitic 0.4Kh16N11M3T and 03Kh20N45M4BCh alloys reduced by contact with Pb-17Li under low-cycle loading at 250 and 350°C. • This effect increases with increasing $\Delta\varepsilon_t$. • The amplitude of total deformation, $\Delta\varepsilon_t$ (in %), at the fatigue limit, is decreased due to contact with Pb-17Li (base: 10^7 cycles).	[Dmukhovs'ka, 1995]
03Kh20N45M4BCh						

Table 7.5.3. Chemical compositions of the above mentioned steels (wt.%, balance Fe)

	Cr	W	Ni	Mo	Mn	Si	V	Nb	Ta	Al	Ti	Cu	Co	As	Sn	C	N	P	S	B	Ref.
MANET	10.6		0.87	0.77	0.82	0.37	0.22	0.16		0.054		0.015	0.01			0.13	0.020	0.005	0.04	0.0085	[Borgstedt, 1991]
316L																					[Chopra, 1983]
316LN	17.34		12.5	2.40		0.32		0.042	0.042		0.008	0.12	0.03			0.02	0.08	0.02	0.0006	0.0014	[Mishra, 1997]
316LN[a]	16.31		10.2	2.07	1.75	0.39						0.23	0.16			0.009	0.11	0.029	0.002		[Strizak, 2001]
MANET II	10.50		0.644	0.55	0.927	0.263					0.001		0.006			0.08		0.007	0.005		[Kalkhof, 2003]
316L	17.2		12.6	2.60	1.67	0.370					0.003		0.35			0.02		0.024	0.003		[Kalkhof, 2003]
T91[b]	8.8		0.17	1.00	0.38	0.41	0.25	0.07								0.11					[Vogt, 2004]
T91[c]	8.5		0.12	0.95	0.47	0.22	0.21	0.06								0.10					[Vogt, 2004]
04Kh16N11M3T	15.8		11.7	2.4	1.5	0.54				0.03	0.34	0.2				0.04		0.008	0.008		[Dmukhovs'ka, 1995]
03Kh20N45M4BCh	19.0		45.6	3.8	0.6	0.26	0.75	0.85		0.12	0.003	0.08					0.18 N_2	0.01	0.0004		[Dmukhovs'ka, 1995]

[a] 316LN supplied by Jessop Steel Company, heat 18474 type 316 LN.
[b] T91 supplied by Creusot-Loire Industrie.
[c] T91 supplied by Ascometal.